# Developments in the Centroid Phase Space Formulation of Quantum Statistical Mechanics

by

Lindsay A. Orr

A thesis
presented to the University of Waterloo
in fulfillment of the
thesis requirement for the degree of
Master of Science
in
Chemistry

Waterloo, Ontario, Canada, 2015

I hereby declare that I am the sole author of this thesis. This is a true copy of the thesis, including any required final revisions, as accepted by my examiners.

I understand that my thesis may be made electronically available to the public.

# Abstract

The centroid formalism provides a phase space representation of quantum statistical mechanics based on the Feynman path integral. Real time quantum correlation functions can be exactly calculated using the centroid formalism, though this requires diagonalizing the system Hamiltonian which is intractable for large collections of molecules. A computational method for computing real time correlation functions called centroid molecular dynamics (CMD) has been formulated to circumvent this issue though the results are approximations. The centroid formalism had previously only been able to treat systems moving in Euclidean space. This is insufficient to capture rotational motion and intramolecular torsions, which may be viewed as motion in a constrained subspace of the Euclidean space. Herein we present a method for incorporating this type of motion into the centroid formalism and test the validity by examining the motion of a particle on a ring. Past work has also seen the centroid formalism extended to pairs of particles obeying Bose-Einstein and Fermi-Dirac statistics by way of a projection operator. In this work we examine the case where this projection operator projects onto an individual quantum state. This will allow the centroid formalism, and hence CMD, to be extended to microcanonical ensembles. Results are shown for the quantum harmonic oscillator, quartic well system and double well system.

# Acknowledgements

I am very thankful for my supervisor Pierre-Nicholas Roy for his continued encouragement and enthusiasm. I would also like to thank the other members of my committee, Scott Hopkins and Marcel Nooijen, for taking the time to critique this work.

Thank you to previous group members professors Grégoire Guillon and Tao Zeng, for their assistance with this work during my first term with the group. And to the rest of the Theoretical Chemistry group, thank you for listening to my rants about my work and for all the help during the past two years. I am especially indebted to Prateek Goel for introducing me to this field.

To my good friends Emma and Cary, thank you for the love and support!

To my evil twin,
Our constant childhood competition has brought me to this point.
Thank you Nate.

# Table of Contents

# List of Figures

## List of Abbreviations

| | |
|---|---|
| CMD | Centroid Molecular Dynamics |
| POR | Particle on a Ring |
| POS | Particle on a Sphere |
| QDO | Quasi-Density Operator |
| QHO | Quantum Harmonic Oscillator |
| RPMD | Ring Polymer Molecular Dynamics |
| SA-CMD | Symmetry-Adapted Centroid Molecular Dynamics |
| SP-CMD | State-Projected Centroid Molecular Dynamics |
| TDSE | Time Dependent Schrödinger Equation |
| TISE | Time Independent Schrödinger Equation |

## List of Symbols

| | |
|---|---|
| $A := B$ | Definition |
| $A \equiv B$ | Equivalence |
| $A \approx B$ | "Weakly" equal |
| $A \propto B$ | Proportional |
| $[\hat{A}, \hat{B}]$ | Commutator |
| $\{\hat{A}, \hat{B}\}$ | Anti-commutator |
| $[A, B]_P$ | Poisson bracket |
| $[A, B]_D$ | Dirac bracket |
| $ad_A(B)$ | Adjoint representation of Lie algebra |

# Chapter 1

# Introduction

One of the central problems in chemical physics is determining the equilibrium and dynamical properties of systems of atoms or molecules. Directly solving for the properties of a system using a quantum mechanical treatment with operators is in general intractable since the computational resources grow exponentially with every additional degree of freedom. Since this is the regime of chemical physics, alternate formulations must be employed. One such approach for studying finite temperature properties of large systems is the Feynman path integral formulation of quantum mechanics [1]. The method under study in this thesis is based on the path integral formalism which uses the centroids of the path integral [2–4] to define a phase space distribution for the system. This method allows us to practically compute approximations of quantum time correlation functions of dynamical variables using the centroid molecular dynamics (CMD) approximation [5, 6] and the very closely related ring polymer molecular dynamics (RPMD) method [7–9]. These are currently two of the most popular molecular dynamic methods based on the path integral, and allow for the efficient simulation of the time evolution of systems composed of large numbers of particles given as real time correlation functions. Correlation functions have connections to various time dependent properties of physical systems including spectra, transport properties, and chemical kinetics [10]. However only CMD can be connected with the operator formulation of quantum mechanics, being a semi-classical approximation to the exact quantum dynamics of the true centroid dynamics [11]. The CMD method has modeled the transport properties of para-hydrogen [12, 13] and ortho-deuterium [14] clusters. It has also accurately predicted the infrared spectrum of liquid water [15, 16]. In comparison to CMD, no connection with the operator formulation of quantum dynamics has yet been demonstrated for RPMD, and so it must be classified as an ad-hoc method or algorithm. Despite this, RPMD has managed to accurately model chemcial reaction rates [17, 18]. The method can also be used to model very large chemical systems, and has been succesfully applied to the dynamics of enzyme catalysis [19].

Thus far the centroid formalism has only been formulated for systems undergoing motion in Cartesian space and cannot fully capture the motion on constrained surfaces. Being able to extend the formalism to motion on these sorts of spaces, which include circles and spheres, would allow for the CMD method to be applied to the study of rotations or torsions. It is the main goal of this thesis to present a means of extending the centroid formalism to these sorts of spaces. In the latter half of this thesis we will examine the centroid formalism in the case where we project the system onto a single state. The content of this thesis is mostly theoretical in scope with some numerical results presented as validation of the new formalisms.

## 1.1 Path integral quantum mechanics

In quantum mechanics the operator which governs the time evolution of a physical system is a hermitian operator known as the Hamiltonian, $\hat{H}$. In the Schrödinger picture of quantum mechanics it is the state vector, $|\psi\rangle$, which undergoes time evolution by way of the time dependant Schrödinger equation (TDSE)

$$i\hbar\frac{\partial}{\partial t}|\psi\rangle = \hat{H}|\psi\rangle \tag{1.1.1}$$

where $\hbar$ is the reduced Planck's constant. For the derivation of the path integral presented here the Hamiltonian is explicitly time independent and in separable form and is therefore a sum of momentum and position dependent components

$$\hat{H} = T(\hat{p}) + V(\hat{q}) \tag{1.1.2}$$

where $T(\hat{p}) = \hat{p}^2/2m$ is the kinetic energy operator and $V(\hat{q})$ is the potential energy operator. $\hat{p}$ and $\hat{q}$ are the momentum and position operators, respectively. It is assumed that these operators both possess instantaneous eigenstates

$$\hat{q}|q\rangle = q|q\rangle \qquad \hat{p}|p\rangle = p|p\rangle \tag{1.1.3}$$

which independently form continuous complete orthonormal bases for the Hilbert space. The eigenvectors are also assumed to have the following inner products

$$\langle q_a|q_b\rangle = \delta(q_a - q_b) \qquad \langle p_a|p_b\rangle = \delta(p_a - p_b) \tag{1.1.4}$$

where $\delta(x)$ is the Dirac delta distribution, hereafter referred to as the delta function. Since both sets of eigenstates form complete bases for the Hilbert space, the identity operator may be written as

$$\mathbb{1} = \int_{-\infty}^{\infty} dq\,|q\rangle\langle q| \tag{1.1.5}$$

$$\mathbb{1} = \int_{-\infty}^{\infty} dp\,|p\rangle\langle p| \tag{1.1.6}$$

where we have integrals because the spectral range of the position and momentum operators are the real numbers and hence continuous; this is referred to as the resolution of the identity. The position and momentum operators are non-commuting and obey the so-called canonical commutation relation

$$[\hat{q}, \hat{p}] = i\hbar \tag{1.1.7}$$

where $[\hat{A}, \hat{B}] = \hat{A}\hat{B} - \hat{B}\hat{A}$ is the commutator. As a result of this, the inner product of the position and momentum eigenvectors is

$$\langle q|p\rangle = \frac{1}{\sqrt{2\pi\hbar}}e^{ipq/\hbar} \tag{1.1.8}$$

Now that the necessary mathematical background has been established, we can proceed to the motivation for the path integral formulation. In the Schrödinger picture, assuming that Hamiltonian is time independent, the TDSE may be solved to give the time evolved state vector

$$|\psi, t\rangle = e^{-i\hat{H}t/\hbar}|\psi\rangle \tag{1.1.9}$$

where to practically solve the time evolution operator, $\exp(-i\hat{H}t/\hbar)$, one would have to solve the time independent Schrödinger equation (TISE)

$$\hat{H}\,|\chi_n\rangle = E_n\,|\chi_n\rangle \tag{1.1.10}$$

where $\{|\chi_n\rangle\}$ are the set of eigenvectors of the Hamiltonian with associated eigenvalues $\{E_n\}$, which are also referred to as eigenenergies; here $n$ can take on discrete values. The eigenvectors of the Hamiltonian also form a complete orthonormal basis for the Hilbert space, and in the case where the eigenstates form a discrete set have a resolution of the identity of the form

$$\mathbb{1} = \sum_n |\chi_n\rangle\,\langle\chi_n| \tag{1.1.11}$$

where we have a sum rather than an integral because the infinite set $\{n\}$ is discrete and therefore countable. Using (1.1.9) the time evolution from one state at time $t_a$, $|\psi, t_a\rangle$, to another state at a later time $t_b$, $|\psi, t_b\rangle$, is given by the unitary transformation

$$\langle\psi, t_b| = \hat{U}(t_b, t_a)\,|\psi, t_a\rangle = e^{-i\hat{H}(t_b - t_a)\hbar}\,|\psi, t_a\rangle \tag{1.1.12}$$

The probability of transitioning to some other arbitrary state at this time, $|\phi, t_b\rangle$, is then given by the inner product

$$\langle\phi, t_b|\hat{U}(t_b, t_a)|\psi, t_a\rangle = \langle\phi, t_b|e^{-i\hat{H}(t_b - t_a)\hbar}|\psi, t_a\rangle \tag{1.1.13}$$

Naturally, one can insert sets of resolutions of the identity using the position eigenstates, see (1.1.5), between the state vectors and the time evolution operator to obtain

$$\langle\phi, t_b|\psi, t_a\rangle = \int_{-\infty}^{\infty}\int_{-\infty}^{\infty} dq_a dq_b\ \langle\phi, t_b|q_b\rangle\,\langle q_b|e^{-i\hat{H}(t_b - t_a)/\hbar}|q_a\rangle\,\langle q_a|\psi, t_a\rangle \tag{1.1.14}$$

$$= \int_{-\infty}^{\infty}\int_{-\infty}^{\infty} dq_a dq_b\,\phi^*(q_b, t_b)\psi(q_a, t_a)\,\langle q_b, t_b|q_a, t_a\rangle \tag{1.1.15}$$

where $\langle q|\psi, t\rangle$ represents the projection of the state vector onto the position basis, which is equivalent to the wave function $\psi(q, t)$ which assumed to be known. The inner product of the time evolved position eigenstates,

$$\langle q_b, t_b|q_a, t_a\rangle = \langle q_b|e^{-i\hat{H}(t_b - t_a)/\hbar}|q_a\rangle \tag{1.1.16}$$

is called the transition amplitude, and it is solving this quantity that is the goal of the path integral formulation of quantum mechanics. We begin by splitting the time evolution operator into a product of exponentials using the Lie-Trotter product formula

$$e^{t(\hat{A}+\hat{B})} = \lim_{N\to\infty}\left[e^{t\hat{A}/N}e^{t\hat{B}/N}\right]^N \tag{1.1.17}$$

where $t$ is any complex number and where the infinite dimensional operators $\hat{A}$ and $\hat{B}$ are Hermitian.[1] The evolution operator is thusly split into an infinite number of *time slices*

$$e^{-i\hat{H}(t_b - t_a)/\hbar} = \lim_{N\to\infty}\left[e^{-i\epsilon T(\hat{p})/\hbar}e^{-i\epsilon V(\hat{q})/\hbar}\right]^N \tag{1.1.18}$$

[1]The product formula has been shown to hold for all finite dimensional matrices by Sophus Lie. Trotter gave the original proof for infinite dimensional unbounded self-adjoint (also known as Hermitian) operators, and it has been shown to hold for bounded operators. It is not yet known to be true for all infinite dimensional operators, and does not appear to have been proven for all the types of operators which will appear in later sections, though we will wave our hands and ignore this technical problem when continuing to use this result.

where $\epsilon = (t_b - t_a)/N$. We insert the completeness relation (1.1.5) between each time slice and (1.1.6) between the exponential of the kinetic and potential operator within each time slice to retrieve

$$\begin{aligned}\langle q_{k+1}|e^{-i\epsilon T(\hat{p})/\hbar}e^{-i\epsilon V(\hat{q})/\hbar}|q_k\rangle &= \int_{-\infty}^{\infty} dp_k\ \langle q_{k+1}|e^{-i\epsilon T(\hat{p})/\hbar}|p_k\rangle\,\langle p_k|e^{-i\epsilon V(\hat{q})/\hbar}|q_k\rangle \\ &= \int_{-\infty}^{\infty} dp_k\, e^{-i\epsilon(T(p_k)+V(q_k))/\hbar}\,\langle q_{k+1}|p_k\rangle\,\langle p_k|q_k\rangle \\ &= \frac{1}{2\pi\hbar}\int_{-\infty}^{\infty} dp_k\, e^{-i(\epsilon\mathcal{H}(p_k,q_k)-p_k(q_{k+1}-q_k))/\hbar} \end{aligned} \tag{1.1.19}$$

where (1.1.8) was used to get the final result. Since we are assuming that $q_k$ is the position coordinate value associated with the state at time $t_k$ we can use the definition of the derivative to write

$$\lim_{\epsilon\to 0}\frac{q_{k+1}-q_k}{\epsilon} \equiv \lim_{\epsilon\to 0}\frac{q_k(t_{k+1})-q_k(t_k)}{\epsilon} = \frac{dq_k}{dt} = \dot{q}_k \tag{1.1.20}$$

Combining all the time slices, and remembering to include the integrations over $dq_k$, the transition amplitude may now be written as

$$\langle q_b, t_b|q_a, t_a\rangle = \lim_{N\to\infty}\int dq_1\ldots dq_{N-1}dp_0\ldots dp_{N-1}\prod_{k=1}^{N-1}\frac{1}{2\pi\hbar}e^{-i\epsilon(\mathcal{H}(p_k,q_k)-p_k\dot{q}_k)/\hbar} \tag{1.1.21}$$

where we have made the replacements $q_b = q_N$ and $q_a = q_0$. The product of exponentials may be combined into a sum in one exponential since there is no longer any worry about operator ordering

$$\begin{aligned}\lim_{N\to\infty}\prod_{k=1}^{N-1}\exp\left(-\frac{i}{\hbar}\epsilon\left[\mathcal{H}(p_k,q_k)-p_k\dot{q}_k\right]\right) &= \exp\left(\lim_{N\to\infty}\frac{i}{\hbar}\epsilon\sum_{k=0}^{N-1}\left[p_k\dot{q}_k-\mathcal{H}(p_k,q_k)\right]\right) \\ &= \exp\left(\frac{i}{\hbar}\int_{t_a}^{t_b}dt\left[p\dot{q}-\mathcal{H}(p,q)\right]\right)\end{aligned} \tag{1.1.22}$$

Equation (1.1.22) follows due to the fact that the infinite limit of the sum here is indeed a Riemann sum and so may be replaced by an integral. We may now define "measures" for the path integration over the position and momentum variables

$$\mathcal{D}q = \lim_{N\to\infty}\prod_{k=1}^{N-1}dq_k \qquad \mathcal{D}p = \lim_{N\to\infty}\frac{1}{(2\pi\hbar)^N}\prod_{k=0}^{N-1}dp_k \tag{1.1.23}$$

Finally, the transition amplitude may be written in the path integral formulation as a functional integral

$$\begin{aligned}\langle q_b, t_b|q_a, t_a\rangle &= \int_{q(t_a)=q_a}^{q(t_b)=q_b}\mathcal{D}q\,\mathcal{D}p\ \exp\left(m\frac{i}{\hbar}\int_{t_a}^{t_b}dt[p\dot{q}-\mathcal{H}(p,q)]\right) \\ &= \int_{q(t_a)=q_a}^{q(t_b)=q_b}\mathcal{D}q\,\mathcal{D}p\ \exp(iS[t]/\hbar)\end{aligned} \tag{1.1.24}$$

where the identification has been made that

$$\mathcal{L} \equiv p\dot{q} - H(p,q) \tag{1.1.25}$$

is the Lagrangian, written here as a Legendre transform of the Hamiltonian, and hence its time integral is the real time action

$$S[t] = \int_{t_a}^{t_b} dt\, \mathcal{L}(q(t), \dot{q}(t)) = \int_{t_a}^{t_b} dt\, (p\dot{q} - \mathcal{H}(p, q)) \tag{1.1.26}$$

The operator Hamiltonian has disappeared in (1.1.24) and has been replaced by an analogous classical-like Hamiltonian composed of *symbols*

$$\hat{H}(\hat{p}, \hat{q}) = T(\hat{p}) + V(\hat{q}) \quad \rightarrow \quad \mathcal{H}(p, q) = T(p) + V(q) \tag{1.1.27}$$

Classical symbols always commute so there is no need to worry about non-commutativity of operators in the final path integral. It is trivial to extend this result to multiple Euclidean dimensions using Cartesian coordinates since the position and momentum operators along the different axes will commute. We say the Hamiltonian is classical like, since there may be additional terms which appear in the Hamiltonian when expressed in other coordinate systems [20] so the path integral Hamiltonian is not guaranteed to be equivalent to the Hamiltonian for the analogous classical system. We also note that while this derivation using the Trotter factorization holds in the case of a separable Hamiltonian, if there are terms coupling position and momentum then a different approach may be required.

## 1.2 Quantum statistical mechanics

Given that the number of possible states of a collection, or ensemble, of subsystems grows exponentially with increasing degrees of freedom, when considering large systems it is impossible to treat each subsystem independently due to current limitations in computational and analytic methods. Instead it is practical to only treat the system as a whole and through this treatment derive statistical averages of the ensemble's physical properties; the physical theory behind this treatment is known as quantum statistical mechanics. Here, the focus is on a collection of subsystems which is in thermal equilibrium and therefore has a constant temperature $T$, along with a fixed volume and number of constituent systems; this is referred to as a canonical ensemble. By further assuming that the subsystems in the ensemble are noninteracting then the state of each subsystem is independent of all others and will follow the same statistics as the entire canonical ensemble. The statistical distribution of the possible energy states that the subsystems may inhabit is known as the Boltzmann distribution, and all systems considered hereafter are assumed to follow this distribution. One of the most important quantities associated with a canonical ensemble is the partition function, $Z$, which is defined as the following operator trace in quantum statistical mechanics

$$Z = \mathrm{Tr}\left[e^{-\beta\hat{H}}\right] \tag{1.2.1}$$

where $\beta = 1/k_B T$ is known a the thermodynamic beta, $k_B$ is Boltzmann's constant, and $T$ is the temperature given in Kelvin. Each system in the ensemble is assumed to have the same Hamiltonian, $\hat{H}$. $Z$ will converge to a finite value except in the infinite temperature case, $\beta \to 0$, where it diverges to positive infinity. The partition function acts as a normalizing factor for the Boltzmann distribution and can be used to generate the system's Helmholtz free energy, average energy, heat capacity and entropy. The operator $\exp(-\beta\hat{H})$ therefore acts as the generator of the Boltzmann distribution. The expectation value for an arbitrary measurement of the ensemble associated with the operator $\hat{A}$ may be calculated by using

$$\langle\hat{A}\rangle = \frac{1}{Z}\mathrm{Tr}\left[e^{-\beta\hat{H}}\hat{A}\right] \tag{1.2.2}$$

where, as previously stated, $Z$ acts a normalizing factor. This formula applies to both quantum and classical systems, but under the assumption that the system is purely classical the partition function may be represented as a $2N$ dimensional integral over the system's phase space

$$Z = \frac{1}{h^N} \int dq_1 \dots dq_N \, dp_1 \dots dp_N \, e^{-\beta \mathcal{H}(q_1,\dots,q_N,p_1,\dots,p_N)} \tag{1.2.3}$$

where $h$ is the Plank constant and the operator Hamiltonian has been replaced by the classical symbol Hamiltonian. Similarly, the statistical average of some property represented by the symbol $A$ is given by

$$\langle A \rangle = \frac{1}{Z h^N} \int dq_1 \dots dq_N \, dp_1 \dots dp_N \, e^{-\beta \mathcal{H}} A \tag{1.2.4}$$

Returning to the quantum case, the trace may be performed by taking a set of states which forms a complete orthonormal basis for the Hilbert space of $\hat{H}$ and taking the inner product with $\exp(-\beta \hat{H})$. If the set of basis states, denoted by $\{|n\rangle\}$, is discrete and thus the notational parameter $n$ takes discrete values the trace takes the form of a sum over the set of inner products

$$Z = \sum_n \langle n | e^{-\beta \hat{H}} | n \rangle \tag{1.2.5}$$

but if the set is continuous, and so the parameter $n$ is uncountable, the trace takes the form of an integral

$$Z = \int \langle n | e^{-\beta \hat{H}} | n \rangle \, dn \tag{1.2.6}$$

To represent the partition function using path integrals we use the set of position eigenstates, $\{|q\rangle, q \in \mathbb{R}\}$, which as previously stated forms a continuous basis. The partition function may then be represented as an integral over all of position space

$$Z = \int_{-\infty}^{\infty} \langle q_a | e^{-\beta \hat{H}} | q_a \rangle \, dq_a \tag{1.2.7}$$

Noting that the integrand is similar to the real time transition amplitude in equation (1.1.16) where the initial and final positions are the same and where the elapsed time is an imaginary value, $t_b - t_a = -i\hbar\beta$, we can replace $\exp(-\beta \hat{H})$ with the path integral from equation (1.1.24)

$$Z = \int_{-\infty}^{\infty} dq_a \int_{q(0)=q_a}^{q(\beta\hbar)=q_a} \mathcal{D}q \, \mathcal{D}p \, \exp\left( -\frac{1}{\hbar} \int_0^{\beta\hbar} d\tau \, \left[ \mathcal{H}(\sqrt{}, \Pi) - ip\dot{q} \right] \right) \tag{1.2.8}$$

$$= \int_{-\infty}^{\infty} dq_a \int_{q(0)=q_a}^{q(\beta\hbar)=q_a} \mathcal{D}q \, \mathcal{D}p \, \exp\left(-S[\tau]/\hbar\right) \tag{1.2.9}$$

where $\tau = it$ is the imaginary time variable and $S[\tau]$ is the imaginary time action; all time derivatives and integrals are now with respect to $\tau$ and the path integral is said to have undergone a Wick rotation.

## 1.3 Centroid formulation of quantum statistical mechanics

### 1.3.1 Static centroid symbols

The *centroid* is conceptually defined as the mean of an imaginary time thermal path in the path integral; these thermal paths are closed since the partition function is defined using a trace. The

use of centroids to calculate statistical quantities from the path integral formulation of the partition function was first proposed by Feynman so as to "save effort and increase our accuracy" [1, pp. 279]. The formal definition of the centroid for some operator $\hat{A}$ with corresponding path integral symbol $A$ is

$$A_0 = \frac{1}{\beta\hbar}\int_0^{\beta\hbar} d\tau\, A(\tau) \tag{1.3.1}$$

where the use of $A(\tau)$ indicates that $A$ has a functional dependence on the imaginary time variables, as is the case for the action. This is then used to construct a constraint in the path integral through the use of the delta function, which is inserted into the integrand. The result is no longer the partition function but a density function for the associated centroid variable, which will be denoted by $A_c$,

$$\rho_c(A_c) = \int_{-\infty}^{\infty} dq_a \int_{q(0)=q_a}^{q(\beta\hbar)=q_a} \mathcal{D}q\,\mathcal{D}p\,\delta(A_c - A_0)\,\exp(-S[\tau]/\hbar) \tag{1.3.2}$$

$$= \frac{1}{\sqrt{2\pi}}\int_{-\infty}^{\infty} d\xi\, e^{-i\xi A_c}\int_{-\infty}^{\infty} dq_a \int_{q(0)=q_a}^{q(\beta\hbar)=q_a} \mathcal{D}q\,\mathcal{D}p\,\exp\left(-\frac{1}{\hbar}\int_0^{\beta\hbar} d\tau\left[\mathcal{H}(p,q) - ip\dot{q} - i\frac{\xi}{\beta}A\right]\right) \tag{1.3.3}$$

where the following Fourier representation of the delta function has been used

$$\delta(x) = \frac{1}{\sqrt{2pi}}\int_{-\infty}^{\infty} e^{-i\omega x} d\omega \tag{1.3.4}$$

Specifically it is the position and momentum variables which are constrained to their thermal path centroids and this is what we will assume for the remainder of the work. In Cartesian coordinates, the centroid distribution is then

$$\rho_c(q_c, p_c) = \int \mathcal{D}q\,\mathcal{D}p\,\delta(q_c - q_0)\,\delta(p_c - p_0)e^{-S[\tau]/\hbar} \tag{1.3.5}$$

$$= \frac{\hbar}{2\pi}\int_{-\infty}^{\infty}\int_{-\infty}^{\infty} d\xi\, d\eta e^{-i\xi q_c}e^{-i\eta p_c}\,\mathrm{Tr}\left[e^{-\beta\hat{H}+i\xi\hat{q}+i\eta\hat{p}}\right] \tag{1.3.6}$$

To obtain (1.3.6) the derivation detailed in sections 1.1 and 1.2 is performed in reverse, where the momentum centroid is paired with the kinetic term and the position centroid is paired with the potential term, the identity operators are removed and finally the Lie-Trotter product formula is reversed to obtain the operator trace. Since the kinetic terms in the path integral are quadratic in the momentum symbols the integrals over the momentum are Gaussian integrals and may be evaluated under the assumption that the potential is position dependent only. The centroid density then becomes separable in the position and momentum centroid variables

$$\rho_c(q_c, p_c) = e^{-\beta p_c^2/2m}\rho_c(q_c) \tag{1.3.7}$$

where the position centroid density is defined using (1.3.2). The density is uniquely defined for each system through the potential term; to date only the quantum harmonic oscillator (QHO) can be formulated exactly. Also note that the centroid density has no regions of negative density and so is a positive semidefinite function (that is $\rho_c(q_c, p_c) \geq 0, \forall q_c, p_c \in \mathbb{R}$). We can now write the quantum partition function in a classical like manner as an integral over the entire centroid phase space

$$Z = \iint \frac{dq_c\, dp_c}{2\pi\hbar}\rho_c(q_c, p_c) \tag{1.3.8}$$

Jang and Voth noted [21] that information about the system has been lost through the use of the trace and thus the centroid density is insufficient to reproduce statistical averages for observables of the system. This led to the definition of a density operator for the centroid phase space as the untraced centroid density,

$$\hat{\delta}_c(q_c,p_c) = \frac{\hbar}{2\pi\rho_c(q_c,p_c)}\int_{-\infty}^{\infty}\int_{-\infty}^{\infty} d\xi\, d\eta\, e^{-i\xi q_c}e^{-i\eta p_c}\, e^{-\beta\hat{H}+i\xi\hat{q}+i\eta\hat{p}} := \hat{\varphi}_c(q_c,p_c)/\rho_c(q_c,p_c) \quad (1.3.9)$$

For notation sake we define the *effective centroid Hamiltonian* as

$$\hat{H}'(\xi,\eta) := \hat{H} - \frac{i}{\beta}\xi\hat{q} - \frac{i}{\beta}\eta\hat{p} \quad (1.3.10)$$

The operator $\hat{\delta}_c(q_c,p_c)$ is of unit trace since the centroid density acts as normalizing factor. We can define an associated symbol in the centroid phase space for any static operator $\hat{A}$ by tracing

$$A_c(q_c,p_c) := \mathrm{Tr}\Big[\hat{\delta}_c(q_c,p_c)\hat{A}\Big] \quad (1.3.11)$$

Note that while the centroid density has no negative regions, the same cannot be said in general for the phase space distribution $A_c(q_c,p_c)$ so it is not a probability distribution. $\hat{\delta}_c(q_c,p_c)$ is therefore not a true density operator and so will be called the *quasi-density operator* (QDO) and so $\hat{\varphi}_c(q_c,p_c)$ from (1.3.9) will then be called the unnormalized QDO; the centroid density may therefore be defined as the trace of the unnormalized QDO

$$\rho_c(q_c,p_c) = \mathrm{Tr}[\hat{\varphi}_c(q_c,p_c)] \quad (1.3.12)$$

The expectation value for the operator $\hat{A}$ is now defined in a classical-like manner as the space space average of the associated centroid symbol

$$\langle A_c\rangle_c := \frac{1}{Z}\iint \frac{dq_c\,dp_c}{2\pi\hbar}\rho_c(q_c,p_c)A_c \quad (1.3.13)$$

$$= \frac{1}{Z}\mathrm{Tr}\left[\iint \frac{dq_c\,dp_c}{2\pi\hbar}\hat{\varphi}_c(q_c,p_c)\hat{A}\right] \quad (1.3.14)$$

$$= \frac{1}{Z}\mathrm{Tr}\Big[e^{-\beta\hat{H}}\hat{A}\Big] \equiv \langle\hat{A}\rangle \quad (1.3.15)$$

It is useful to define the centroid symbol corresponding to the Hamiltonian of the system

$$H_c := \mathrm{Tr}\Big[\hat{\delta}_c(q_c,p_c)\hat{H}\Big] = T_c + V_c \quad (1.3.16)$$

where $T_c$ and $V_c$ are the centroid symbols corresponding to $T(\hat{p})$ and $V(\hat{q})$, respectively. The centroid phase space average of $H_c$ is defined to be the average energy of the ensemble. It is also possible to show[2] that the centroid symbols for the position and momentum operators are

$$q_c = \mathrm{Tr}\Big[\hat{\delta}_c(q_c,p_c)\hat{q}\Big] \quad (1.3.17)$$

$$p_c = \mathrm{Tr}\Big[\hat{\delta}_c(q_c,p_c)\hat{p}\Big] \quad (1.3.18)$$

It then follows using the linearity of the trace that for an operator which is linear in position and momentum, $\hat{B} = B_0\hat{I} + B_1\hat{q} + B_2\hat{p}$, the centroid symbol is then

$$B_c \equiv B_0 + B_1 q_c + B_2 p_c = \mathrm{Tr}\Big[\hat{\delta}_c(q_c,p_c)\hat{B}\Big] \quad (1.3.19)$$

[2]Refer to A.1

It is important to note that this is not true for any other operator, so for example

$$(q^2)_c = \mathrm{Tr}\Big[\hat{\delta}_c(q_c, p_c)\hat{q}^2\Big] \neq (q_c)^2 \tag{1.3.20}$$

In the case of other distributions, such as the Wigner distribution, this leads to the generalization of the usual notion of a product for distributions in the phase space. The centroid symbol for the operator $\hat{q}^2$ is therefore defined as the *phase space product* of the centroid distribution for $\hat{q}$, that is

$$(q^2)_c \equiv q_c \star q_c \tag{1.3.21}$$

where $\cdot \star \cdot$ is the phase space product, also referred to as a star product or $\star$-product. Past attempts to find an expression for this star product have been unsuccessful [22], so for now the phase space distribution for nonlinear operators must be independently computed.

### 1.3.2 Dynamic centroid symbols

The usefulness of the centroid method comes from the ability to define dynamic centroid symbols which contain information about the statistical fluctuations undergone by observables of the Boltzmann ensemble. We first define a time evolving operator using the definition from the Heisenberg picture of quantum mechanics

$$\hat{A}(t) := e^{i\hat{H}t/\hbar}\hat{A}e^{-i\hat{H}t/\hbar} \tag{1.3.22}$$

The definition of time dependent centroid variables is then as follows

$$A_c(t; q_c, p_c) := \mathrm{Tr}\Big[\hat{\delta}_c(q_c, p_c)\hat{A}(t)\Big] \equiv \mathrm{Tr}\Big[\hat{\delta}_c(t; q_c, p_c)\hat{A}\Big] \tag{1.3.23}$$

where we can define a time dependent QDO

$$\hat{\delta}_c(t; q_c, p_c) = e^{-i\hat{H}t/\hbar}\hat{\delta}_c(q_c, p_c)e^{i\hat{H}t/\hbar} \tag{1.3.24}$$

and so view the QDO as undergoing time evolution according to Liouville's theorem. The QDO is then an object which creates a dynamical centroid symbol corresponding to a stationary observable. Due to cyclicality of the trace the centroid density corresponding to the time dependent QDO remains independent of time. The reason to adopt this viewpoint is that the Boltzmann distribution is inherently stationary, that is the ensemble average of dynamic observables is independent of time

$$\langle\hat{A}(t)\rangle := \mathrm{Tr}\Big[e^{-\beta\hat{H}}e^{i\hat{H}t/\hbar}\hat{A}e^{-i\hat{H}/\hbar}\Big] = \mathrm{Tr}\Big[e^{-\beta\hat{H}}\hat{A}\Big] \equiv \langle\hat{A}\rangle \tag{1.3.25}$$

So viewing the QDO as being time dependent allows for the interpretation of the centroid QDO as containing all of the non stationary fluctuations in the canonical ensemble. It follows from equations (1.3.25) and (1.3.15) that the centroid phase space average for the static and dynamic centroid symbols corresponding to $\hat{A}$ are identical

$$\frac{1}{Z}\iint \frac{dq_c\, dp_c}{2\pi\hbar}\rho_c(q_c, p_c)A_c(q_c, p_c) = \frac{1}{Z}\iint \frac{dq_c\, dp_c}{2\pi\hbar}\rho_c(q_c, p_c)A_c(t; q_c, p_c) \tag{1.3.26}$$

While the phase space average over all the trajectories of the centroid variable $A_c(t)$ is a stationary quantity, the individual trajectories based on different starting conditions in phase space are non

stationary. The time evolution of the QDO, being a phase space distribution function, is given by the quantum Liouville equation

$$\frac{d}{dt}\hat{\delta}_c(t;q_c,p_c) = \frac{1}{i\hbar}[\hat{H},\hat{\delta}_c(t;q_c,p_c)] \tag{1.3.27}$$

The time evolution of the centroid symbol $A_c(t)$ is therefore

$$\frac{d}{dt}A_c(t;q_c,p_c) = \mathrm{Tr}\left[\frac{d}{dt}\hat{\delta}_c(t;q_c,p_c)\hat{A}\right] \tag{1.3.28}$$

$$= \mathrm{Tr}\left[\frac{1}{i\hbar}[\hat{H},\hat{\delta}_c(t;q_c,p_c)]\hat{A}\right] \tag{1.3.29}$$

$$= \mathrm{Tr}\left[\hat{\delta}_c(t;q_c,p_c)\frac{i}{\hbar}[\hat{H},\hat{A}]\right] \tag{1.3.30}$$

where we notice that

$$\frac{d}{dt}\hat{A}(t) = \frac{i}{\hbar}[\hat{H},\hat{A}] \tag{1.3.31}$$

is the Heisenberg equation of motion for an operator defined by (1.3.22). Using (1.3.30) and the following equations of motion

$$\frac{d}{dt}\hat{q}(t) = \frac{i}{\hbar}[\hat{H},\hat{q}] = \frac{\hat{p}}{m}\frac{d}{dt}\hat{p}(t) = \frac{i}{\hbar}[\hat{H},\hat{p}] \tag{1.3.32}$$

we are able to write the dynamics of the position and momentum centroid symbols using Hamilton's equations

$$\frac{d}{dt}q_c(t;q_c,p_c) = \frac{p_c(t;q_c,p_c)}{m} \tag{1.3.33}$$

$$\frac{d}{dt}p_c(t;q_c,p_c) = F_c(t;q_c,p_c) \tag{1.3.34}$$

where $F_c(t;q_c,p_c)$ is the dynamic centroid symbol corresponding to the quantum force operator, defined as

$$\hat{F} := \frac{d}{dt}\hat{p} = \frac{i}{\hbar}[V(\hat{q}),\hat{p}] \tag{1.3.35}$$

Since the momentum operator will commute with the kinetic portion of the Hamiltonian, only the potential determines the force, as expected. It must be emphasized that the statistical fluctuations obtained from the dynamical equations (1.3.33) and (1.3.34) are exact quantum dynamics; the method which approximately solves of these Heisenberg equations is called centroid molecular dynamics (CMD).

### 1.3.3 Centroid Molecular Dynamics

The first step in making the CMD approximation is removing the explicit time dependence in the centroid symbols and instead treats them as parametric functions of the time dependent symbols $q_c(t)$ and $p_c(t)$. This is done by writing the QDO as follows

$$\hat{\delta}_c(t;q_c,p_c) = \hat{\delta}_c(q_c(t),p_c(t)) \tag{1.3.36}$$

where the time evolution of $q_c(t)$ and $p_c(t)$ will be determined by solving the Heisenberg equations of motion. The dynamic centroid symbols defined so far are explicitly time dependent quantities

and exhibit the non-locality inherent to quantum mechanics. This means that even for closed trajectories in the centroid phase space the centroid distributions for the operators will be different at the exact same point in phase space at a later time. CMD has destroyed this non-locality and so the results will only be approximate as the dynamic force symbol is now equivalent to the static force symbol. The static force symbol may be written as [21]

$$F_c = -\frac{\partial}{\partial q_c} V_{cm}(q_c) = -\frac{1}{\beta} \ln\left[\rho_c(q_c)\right] \tag{1.3.37}$$

where $V_{cm}(q_c)$ is a potential of mean force and is not equal to the centroid symbol for the potential operator, $V_c$. The force is only position dependent due to separability of the momentum and position components of the centroid distribution as seen in (1.3.7). Although the force symbol no longer contains all the necessary information regarding its time evolution, it is still possible to recover the exact quantum dynamics. This would require us to include an additional equation of motion for the force symbol

$$\frac{d}{dt} F_c(q_c(t), p_c(t)) = \mathrm{Tr}\left[\hat{\delta}_c(q_c(t), p_c(t)) \frac{i}{\hbar}[\hat{H}, \hat{F}]\right] \tag{1.3.38}$$

and another equation of motion for this one and so on. For most systems this series never terminates, so we would need an infinite number of first order differential equations to capture the exact motion. The CMD approximation terminates this series at the equation of motion for the momentum centroid symbol so that the system of equations is still reminiscent of Hamilton's equations. The CMD equations of motion are then

$$\frac{d}{dt} q_c(t) = \frac{p_c(t)}{m} \tag{1.3.39}$$

$$\frac{d}{dt} p_c(t) = -\frac{1}{\beta} \ln\left[\rho_c(q_c(t))\right] \tag{1.3.40}$$

The CMD method is only able to capture the exact dynamics of the QHO due to the fact that its force operator is linear in position; this will be expounded upon in chapter 3.

### 1.3.4 Correlation functions

Now that the time evolution of observables and their expectation values can be captured exactly in the centroid formalism and approximately via CMD, we wish to extend this to the calculation of real time quantum correlation functions between the static operator $\hat{B}(0) \equiv \hat{B}$ and the time evolving operator $\hat{A}(t)$. Using the QDO, their real time correlation function may be written as

$$\langle \hat{B}\hat{A}(t) \rangle := \frac{1}{Z} \mathrm{Tr}\left[e^{-\beta \hat{H}} \hat{B} \hat{A}(t)\right] \tag{1.3.41}$$

$$= \frac{1}{Z} \int_{-\infty}^{\infty} \int_{-\infty}^{\infty} \frac{dq_c\, dp_c}{2\pi\hbar} \rho_c(q_c, p_c) \mathrm{Tr}\left[\hat{\delta}_c(q_c, p_c) \hat{B} \hat{A}(t)\right] \tag{1.3.42}$$

The quantum correlation function of $\hat{B}$ and $\hat{A}$ is therefore the time evolution of the centroid distribution for the operator product $\hat{B}\hat{A}(t)$ and cannot be expressed as a correlation function between their centroid symbols $B_c$ and $A_c(t)$, respectively. It can be shown that when $\hat{B}$ is is

a linear function of the position and momentum operators, then the correlation function of the centroid symbols is equal to a so-called Kubo transformed quantum time correlation function[3]

$$\langle B_c A_c(t)\rangle := \int_{-\infty}^{\infty}\int_{-\infty}^{\infty} \frac{dq_c\, dp_c}{2\pi\hbar}\rho_c(q_c,p_c)B_c A_c(t) \tag{1.3.43}$$

$$= \frac{1}{Z}\int_0^1 du\, \mathrm{Tr}\Big[e^{-(1-u)\beta\hat{H}}\hat{B}e^{-\beta u\hat{H}}\hat{A}(t)\Big] \tag{1.3.44}$$

$$= \frac{1}{Z}\mathrm{Tr}\Big[e^{-\beta\hat{H}}\int_0^1 du\, \hat{B}(-iu\beta\hbar)\hat{A}(t)\Big] \tag{1.3.45}$$

$$\equiv \int_0^1 du\langle\hat{B}(-iu\beta\hbar)\hat{A}(t)\rangle =: \langle\hat{B}\hat{A}(t)\rangle_{(K)} \tag{1.3.46}$$

where the operator $\hat{B}$ is said to have been Kubo transformed

$$\int_0^1 du\, \hat{B}(-iu\beta\hbar) \equiv \int_0^1 du\, e^{u\beta\hat{H}}\hat{B}e^{-u\beta\hat{H}} \tag{1.3.47}$$

Assuming that the Hamiltonian governing the time evolution of $\hat{A}(t)$ is the same as $\hat{H}$ then it is possible to undo the single Kubo transform and so retrieve the original correlation function by taking the Fourier transform from time to frequency space and evaluating the trace in the basis of the eigenstates of $\hat{H}$.[4] The relationship between the Fourier transforms, $\mathcal{F}\{f(t)\}(\omega)$, of both correlations function is

$$\mathcal{F}\{\langle\hat{B}\hat{A}(t)\rangle\}(\omega) = \frac{\beta\hbar\omega}{1-e^{-\beta\hbar\omega}}\mathcal{F}\{\langle\hat{B}\hat{A}(t)\rangle_{(K)}\}(\omega) \tag{1.3.48}$$

which leads to the following Fourier transform relation between the correlation functions

$$\langle\hat{B}\hat{A}(t)\rangle = \frac{1}{2\pi}\int_{-\infty}^{\infty} d\omega\, e^{i\omega t}\frac{\beta\hbar\omega}{1-e^{-\beta\hbar\omega}}\int_{-\infty}^{\infty} dt'\, e^{-i\omega t'}\langle\hat{B}\hat{A}(t')\rangle_{(K)} \tag{1.3.49}$$

It is stressed that these equations are exact if the centroid symbol $A_c(t)$ is evolved exactly, so if the dynamics of the symbol is determined approximately via the CMD method then the correlation function is exact at zero time and approximate thereafter. When $B_c$ is nonlinear in the centroid variables then the correlation function corresponds to higher order Kubo-transformed correlation functions; in the case of $B_c = (q_c)^n$ this corresponds to the $n^{th}$ order Kubo transform [23]. Unlike in the single Kubo transform case where a relation exists through a simple frequency factor as seen in (1.3.49), no such relation exists in general for the higher order Kubo transformed correlation functions.

Now that the basic background information has been presented, we can progress to the specialized topics contained within this thesis. Chapter 2 presents a generalized method for tackling rotational dynamics and by extension any system which can be represented as motion on a constrained surface embedded in Euclidean space. Chapter 3 contains the work performed in the area of state projected centroid dynamics, which allows for the centroid formalism to be extended to microcanonical systems. Formal derivations for these chapters are present in Appendices B and C, respectively, in order to maintain the flow of the text.

[3] Refer to A.2
[4] Refer to A.3

# Chapter 2

# Centroid quantum statistical mechanics in constrained spaces

## 2.1 Introduction

Past attempts to reformulate the centroid formalism to accommodate systems undergoing rotational motion have so far been unsuccessful [24]. Here we present a method to properly capture the dynamics of rotating systems by viewing the system as having been topologically constrained from the regular motion in Euclidean space. Specifically, we include the theory and results for a system constrained to move on the 1-sphere or circle, hereafter referred to as a ring. The theoretical extension to motion on the 2-sphere, also called the sphere, is also shown. We will do this by instead beginning with the Euclidean path integral representation of the centroid density and applying topological constraints to reduce the phase space so that the system moves on the desired manifold. The centroid symbols are not restricted directly; the phase space reduction will however result in physically significant changes in the nature of the centroid phase space.

The naïve method to extend the centroid formalism to that of a particle on a ring would be to define the centroids for the angular position and angular momentum, $\varphi_c$ and $p_{\varphi,c}$, which would be associated with the path integral variables $\varphi$ and $p_\varphi$ and therefore the original quantum operators $\hat{\varphi}$ and $\hat{J}$. Formal problems arise when attempting to define an angle operator $\hat{\varphi}$. One way of quantizing a classical system is to use the canonical quantization relation

$$(\text{Poisson bracket}) \to \frac{1}{i\hbar}(\text{Commutator}) \tag{2.1.1}$$

where the Poisson bracket is defined as

$$[f,g]_P := \sum_{n=1}^{N} \frac{\partial f}{\partial q_n}\frac{\partial g}{\partial p_n} - \frac{\partial f}{\partial p_n}\frac{\partial g}{\partial q_n} \tag{2.1.2}$$

where the summation is over all sets of canonical coordinates in the $2N$-dimensional classical phase space. The Poisson bracket also has the same properties of the commutator. The quantization procedure (2.1.1) works in the case of Cartesian variables with a Euclidean phase space, but the process of quantizing the angle in polar coordinates

$$[\varphi, p_\varphi]_P = 1 \quad \to \quad [\hat{\varphi}, \hat{J}] = i\hbar \tag{2.1.3}$$

is inherently problematic [25, 26]. If one were to assume the operator is continuous, then its spectral range is the entire real line and hence the operator belongs to the Hilbert space $L^2(\mathbb{R})$, however the corresponding angular momentum operators will lose its hermiticity since it is only hermitian on the Hilbert space $L^2(S^1)$ where the vectors are $2\pi$-periodic. If we instead define the operator as being $2\pi$-periodic using a modulo operation then it will have a discontinuity at $2\pi$; this results in a problematic appearance of an infinite number of discontinuities in the commutation relation of $\hat{\varphi}$ and $\hat{J}$. It was also demonstrated in [27] that the behaviour of the time evolution of expectation value of the angle operator gives results which are inconsistent with those for free motion on a ring, but that the cosine of the angle did not have this problem. The use of the cosine has an advantage for comparison with experiments since it corresponds with the dipole moment of the particle; if the centroid symbol was the angle $\varphi_c$ then the autocorrelation function of the dipole would be a difficult to replicate due to the nonlinear terms in the cosine which would result in higher order Kubo transform correlation functions. It would be advantageous to use the cosine and sine operators as the position variables for the centroid distribution since they may be directly compared to the $x$ and $y$ Cartesian coordinates. The only problem is that it is not immediately obvious how to construct momentum operators to construct the equations of motion. The theory of constraints in path integrals is used in an attempt to provide a rigourous method to generate these operators and derive the centroid density.

The cosine and sine operators, $\cos\hat{\varphi}$ and $\sin\hat{\varphi}$ respectively, have previously been suggested [25,28] as suitable replacements for $\hat{\varphi}$ since they are naturally continuous, $2\pi$-periodic, hermitian, and have physically appropriate uncertainty relations [26]. Using the angle variable representation of the trigonometric and the angular momentum operator allows one to determine the commutator relations

$$[\cos\hat{\varphi}, \sin\hat{\varphi}] = 0 \qquad [\hat{J}, \cos\hat{\varphi}] = -i\hbar\sin\hat{\varphi} \qquad [\hat{J}, \sin\hat{\varphi}] = i\hbar\cos\hat{\varphi} \tag{2.1.4}$$

We can instead use the complex exponential form of the trigonometric functions to define a new pair of operators

$$\hat{U} := e^{i\hat{\varphi}} \equiv \cos\hat{\varphi} + i\sin\hat{\varphi} \tag{2.1.5}$$

$$\hat{U}^\dagger := e^{-i\hat{\varphi}} \equiv \cos\hat{\varphi} - i\sin\hat{\varphi} \tag{2.1.6}$$

which obviously form a unitary operator pair, $\mathbb{1} = \hat{U}\hat{U}^\dagger = \hat{U}^\dagger\hat{U}$. The set of commutator relations is then

$$[\hat{U}, \hat{U}^\dagger] = 0 \qquad [\hat{J}, \hat{U}] = \hbar\hat{U} \qquad [\hat{J}, \hat{U}^\dagger] = -\hbar\hat{U}^\dagger \tag{2.1.7}$$

From this we can determine how these operators act on the basis of the eigenstates of the angular momentum operator, $\{|j\rangle, j \in \mathbb{Z}\}$

$$\hat{J}|j\rangle = \hbar j|j\rangle \qquad \hat{U}|j\rangle = |j+1\rangle \qquad \hat{U}^\dagger|j\rangle = |j-1\rangle \tag{2.1.8}$$

so $\hat{U}$ and $\hat{U}^\dagger$ are ladder operators for angular momentum and act as raising and lowering operators, respectively. Their eigenstates are the angle eigenstates, $\{|\varphi\rangle, \varphi \in [0, 2\pi)\}$

$$\hat{U}|\varphi\rangle = e^{i\varphi}|\varphi\rangle \qquad \hat{U}^\dagger|\varphi\rangle = e^{-i\varphi}|\varphi\rangle \tag{2.1.9}$$

We can work out that the inner products between the eigenstates are

$$\langle\varphi'|\varphi\rangle = \delta(\varphi' - \varphi) \qquad \langle j'|j\rangle = \delta_{j'j} \qquad \langle\varphi|j\rangle = \frac{1}{\sqrt{2\pi}}e^{ij\varphi} \tag{2.1.10}$$

where $\delta_{j'j}$ is the Kronecker delta. This background information will be useful when defining the QDO and observables for the particle on a ring.

## 2.2 Theory of Constraints

### 2.2.1 Constraints in classical mechanics

Implementing constraints in the operator formulation of quantum mechanics is difficult due to the non-commuting nature of operators in a Hilbert space. We instead formulate the classical constraints for the system which can be used to constrain the commuting symbols present in the path integral. If some extra conditions are fulfilled it may be possible to generate a set of quantum operators via canonical quantization. We will focus on the relevant sections of the method required to derive constraints for a Hamiltonian system as initially devised by Dirac [29]; a very detailed explanation can be found in chapter 1 of reference [30]. We will be using Einstein notation for this section[5]. We begin with the Lagrangian for a system with a $2N$-dimensional phase space, $\mathcal{L}(q^k, \dot{q}^k)$, and recall that the equations of motion may be obtained by invoking the principle of least action which results in the Euler-Lagrange equations

$$0 = \frac{d}{dt}\left(\frac{\partial \mathcal{L}}{\partial \dot{q}^n}\right) - \frac{\partial \mathcal{L}}{\partial q^n} \tag{2.2.1}$$

$$= -\frac{\partial \mathcal{L}}{\partial q^n} + \ddot{q}^k \frac{\partial^2 \mathcal{L}}{\partial \dot{q}^k \partial \dot{q}^n} + \dot{q}^k \frac{\partial^2 \mathcal{L}}{\partial q^k \partial \dot{q}^n} \tag{2.2.2}$$

where we have used the definition of the total derivative

$$\frac{d}{dt} f(q,t) = \frac{\partial}{\partial t} f(q,t) + \dot{q}^k \frac{\partial}{\partial q^k} f(q,t) \tag{2.2.3}$$

An equation for the acceleration term $\ddot{q}^\alpha$ can be found in the case that the velocity Hessian matrix is invertible and therefore has a non-zero determinant. The elements of the $N \times N$ Hessian matrix in this case are

$$\mathbf{H}^j{}_k = \frac{\partial^2 \mathcal{L}}{\partial \dot{q}_j \partial \dot{q}^k} \tag{2.2.4}$$

If the determinant is 0 then the rank of the Hessian is less than $N$ and so one or more rows is a linear combination of the others, so the accelerations are not all uniquely determined. As a result the conjugate momenta in the Hamiltonian formulation

$$p_n = \frac{\partial \mathcal{L}}{\partial \dot{q}^n} \tag{2.2.5}$$

will not be functions of just the phase space coordinates, but will also have some unknown explicit time dependent terms. There will be relations dependent on both the position and momentum generated by the definition of the momenta (2.2.5)

$$\phi_m(q^k, p_k) \approx 0, \quad m = 1, \ldots, M \tag{2.2.6}$$

These relations are called *primary constraints* in the literature, and will constrain the system to move in some subspace of the full phase space called the constrained subspace. The symbol " $\approx$ " in (2.2.6) denotes a so-called *weak equality*; the quantities $f$ and $g$ are said to be weakly equal, $f \approx g$, when they are equal in the subspace but not necessarily throughout the full phase space. If the quantities $f$ and $g$ are equal throughout the entire phase space they are said to be *strongly*

[5] Refer to section B.1

*equal*, this is denoted by the usual equality sign $f = g$. If we truly are in the classical subspace where the constraints are satisfied then we should remain there given the following transformation of the Hamiltonian

$$\mathcal{H} \to \mathcal{H} + u^m(q^k, p_k)\phi_m =: \mathcal{H}_T \tag{2.2.7}$$

where the $u^m$ are Lagrange multipliers. This is because the constraints are expected to be weakly equal to zero in entire phase space. The quantity $\mathcal{H}_T$ is referred to as the total Hamiltonian. It is not necessarily the case that the primary constraints are sufficient to remain in the constrained subspace. Although the primary constraints are defined to be strongly equal to zero there, if the system is to remain in the constrained subspace the equations of motion of the constraints must vanish there or else the system could drift into a region where the constraints are non-zero and hence not satisfied. We therefore define the following consistency equation for a constraint $\phi_m$ based on the classical Hamiltonian equations of motion

$$[\phi_m, \mathcal{H}_T] = [\phi_m, \mathcal{H}] + u^k[\phi_m, \phi_k] \approx 0 \tag{2.2.8}$$

We must solve the left side for all the primary constraints. There are two possible outcomes when solving this equation:

1. The left side is exactly 0, generates a restriction for the $u^k$ Lagrange multipliers, or else generates a constraint dependent on a previously known constraint. In this case the consistency equation is satisfied since it will be exactly zero in the constrained subspace.

2. The left side returns a function which does not satisfy any of the previous conditions and as such is not dependent on some previous constraint. The consistency equation has therefore generated a new constraint for the system, called a *secondary constraint* since it is not fixed in the Hamiltonian via a Lagrange multiplier. In this case, we must apply the consistency equation (2.2.8) to the new constraint, and repeat this process until one of conditions in 1. is satisfied. We may then end up generating a series of secondary constraints, though it is assumed this process terminates.

Assuming that the process has generated some additional constraints we can discard those that are dependent constraints as redundant. If the we have generated $S$ unique secondary constraints then we will have $M + S = R$ constraints in total. The dimension of the constrained subspace is then $2N - R$. Now that we have a full set of constraints, we consider an even more important classification, that of *first-class constraints* and *second-class constraints*. First-class constraints are constraints which have a vanishing Poisson bracket with every other constraint in the set, while second-class constraints have a non-zero Poisson bracket with at least one other constraint of the system. We must now define a new canonical bracket in the constrained subspace which generalizes the Poisson bracket called the *Dirac bracket*, after its developer. The Dirac bracket will be developed in such a way that all constraints will have a vanishing Dirac bracket. This is used so that the second-class constraints can be strongly set to zero in the constrained subspace, and as a result any primary second-class constraints can be set to zero so they vanish from the Hamiltonian. This is not true for primary first class constraints which will survive as additional terms in the Hamiltonian, though these do not appear in the systems under consideration here and so we will not talk about their effects. We construct a skew-symmetric matrix whose elements are the Poisson brackets between the known secondary constraints

$$C^j{}_k = [\phi^j, \phi_k] \tag{2.2.9}$$

which is guaranteed to be invertible. If it were not then the rank would be less than the number of constraints used to build it which would indicate that one or more of the constraints is not uniquely defined and hence a first-class constraint. The Dirac bracket is now defined as

$$[f,g]_D = [f,g]_P + (C^{-1})^j{}_k\,[f,\phi_j]_P[\phi^k,g]_P \tag{2.2.10}$$

$$\equiv [f,g]_P + C_j{}^k\,[f,\phi_j]_P[\phi^k,g]_P \tag{2.2.11}$$

where $C^{-1}$ is the inverse matrix of $C$, and the summation is over total number of second-class constraints. The Dirac bracket can be shown to satisfy all of the same properties of the Poisson bracket. However, we can now see that the Dirac brackets of all the constraints are zero. The Dirac bracket between the canonical variables of the system will also differ from their original Poisson brackets which shows how the constraints have manifested as a new interdependence between the phase space variables in the constrained subspace.

We note that this formalism is important when applying constraints to the Lagrangian, and by extension the Hamiltonian, in the form of Lagrange multipliers. The Lagrange multipliers constitute extra degrees of freedoms for the system and so act as an additional set of coordinates; they will therefore increase the size of the classical phase space and generate their own equations of motion. If the Lagrangian with these Lagrange multipliers is singular then this provides the avenue to constrain the Hamiltonian.

### 2.2.2 Constraints in quantum mechanics

#### Operators

Assume we have a system in a $2N$-dimensional phase space with a set coordinates $x^j$ which is restricted to some subspace by a set of second-class constraints

$$\phi_m(x^j) \approx 0, \quad m = 1,\ldots,R \tag{2.2.12}$$

which is also equipped with a Dirac bracket. It may be possible to find a set of variables $y^k$ in the constrained subspace such that the constraints are exactly equal to 0 when expressed as a function of these coordinates, or

$$x^j = F^j(y^k) \to \phi_m(F^j(y^k)) = 0 \tag{2.2.13}$$

where $\mathbf{F}$ is vector whose elements are functions of the new system of coordinates. Here the sets of coordinates $x^j$ and $y_k$ will contain both position and momentum phase space coordinates. If all second-class constraints are strongly equal to zero in this new set of coordinates then the Dirac bracket will reduce to the usual Poisson bracket, so we should have the relation

$$[x^a, x_b]_D = [x^a(y^k), x_b(y^k)]_P \tag{2.2.14}$$

It may then be possible to follow the canonical quantization procedure (2.1.1) and so obtain a set a operators with the desired set of commutation relations. Care must be taken here when defining the quantum analogue $\hat{x}^j$ for the phase space coordinates $x^j$. If the set of new phase space coordinates $y^k$ possess non-zero Poisson brackets then the analogous quantum operators $\hat{y}^k$ will be non-commuting; these non-zero commutators will result in operator ordering issues in $\hat{x}^j(\hat{y}^k)$ if $x^j$ is a nonlinear function of the reduced phase space coordinates $y^k$. There is some ambiguity

in choosing an operator ordering, though for this work we will select the one which generates the most symmetric ordering of the operators and gives the correct commutator relations in the $\hat{y}^k$ operator basis.[6]

**Path Integrals**

If we assume a set of variables $y^k$ exists such that condition (2.2.13) is satisfied[7] then the path integral for the system is

$$\int [\mathcal{D}y^k] \left(\det M^{-1}\right)^{1/2} \exp(iS[y^k(t)]) \tag{2.2.15}$$

where $S[y^k(t)]$ is the action corresponding to the Hamiltonian (2.2.7) where the original coordinates $x^j$ have been replaced by $y^k$. The $(2N-R)\times(2N-R)$ matrix $M$ has elements

$$M^k{}_l = [y^k, y_l]_D \equiv [y^k, y_l]_P \tag{2.2.16}$$

where the equivalence relation follows from our assumption that the constraints vanish in these coordinates. We can immediately write down the path integral in the original constrained phase space variables as

$$\int [\mathcal{D}x^j] \prod_m \delta(\phi_m) (\det C^{-1})^{1/2} \exp(iS[x^j(t)]) \tag{2.2.17}$$

where the action is the one expected for the Hamiltonian $\mathcal{H}$ without constraints, and the matrix $C$ is defined by (2.2.9). Using the Fourier representation of the delta function this may be rewritten as

$$\int [\mathcal{D}x^j][\mathcal{D}u] (\det C^{-1})^{1/2} \exp(iS[x^j(t), u^m(t)]) \tag{2.2.18}$$

$$S[x^k(t), u^m(t)] = S[x^k(t)] - \int u^m \phi_m \tag{2.2.19}$$

This can be extended to the partition function by instead using the imaginary time action.[8]

## 2.3 Theoretical Results

### 2.3.1 Constraining to the ring

In the case of the free particle moving on the circle, we begin with the classical Lagrangian for a free particle moving in the 2-dimensional plane but with a Lagrange multiplier constraint that the positions be fixed such that the motion is on a ring of radius $R$, so $x^2+y^2=R^2$. The Lagrangian with this additional Lagrange multiplier is then

$$\mathcal{L} = \frac{m}{2}\left(\dot{x}^2+\dot{y}^2\right) - \lambda\left(x^2+y^2-R^2\right) \tag{2.3.1}$$

[6] See chapter 13 of reference [30].

[7] As with the operator approach this is not necessarily true, in which case there will be added difficulties in defining a path integral. This problem does not arise for the systems considered here so we do not discuss the theory needed.

[8] See chapter 16 of reference [30].

The Lagrange multiplier must be treated here as an additional canonical coordinate with its own velocity, $\dot{\lambda}$. The Hamiltonian phase space will therefore be 6-dimensional since it will have its own canonically conjugate momentum. The Hessian with respect to the velocity for this Lagrangian is then

$$\mathbf{H} = \begin{bmatrix} m & 0 & 0 \\ 0 & m & 0 \\ 0 & 0 & 0 \end{bmatrix} \tag{2.3.2}$$

which is evidently singular, so we must use the theory of constraints laid out in the previous section. The total Hamiltonian in this case has the form

$$\mathcal{H}_T = (\dot{x}p_x + \dot{y}p_y + \dot{\lambda}p_\lambda) - \mathcal{L} = \frac{1}{2m}(p_x^2 + p_y^2) + \lambda(x^2 + y^2 - R^2) + \dot{\lambda}p_\lambda \tag{2.3.3}$$

To prevent the Lagrange multiplier from varying, the canonical momentum should be zero in the constrained subspace. This constitutes our primary constraint for the system

$$\phi_1 = p_\lambda \approx 0 \tag{2.3.4}$$

The $\dot{\lambda}$ term is then one of the $u^k$ Lagrange multiplier functions previously mentioned that will be fixed by constraining the system, so we instead define $\dot{\lambda} := u^\lambda$. Though the Lagrange multiplier term is present in the Hamiltonian, it is not itself a constraint. We will now apply the consistency equation to see if we generate any secondary constraints:

$$\dot{\phi}_1 = [\phi_1, \mathcal{H}]_P = -(x^2 + y^2 - R^2) \qquad \rightarrow \phi_2 = x^2 + y^2 - R^2 \approx 0 \tag{2.3.5}$$

$$\dot{\phi}_2 = [\phi_2, \mathcal{H}]_P = \frac{2}{m}(xp_x + yp_y) \qquad \rightarrow \phi_3 = xp_x + yp_y \approx 0 \tag{2.3.6}$$

$$\dot{\phi}_3 = [\phi_3, \mathcal{H}]_P = \frac{1}{m}(p_x^2 + p_y^2) - 2\lambda(x^2 + y^2) \qquad \rightarrow \phi_4 = \frac{1}{2}(p_x^2 + p_y^2) - \lambda m(x^2 + y^2) \approx 0 \tag{2.3.7}$$

$$\dot{\phi}_4 = [\phi_4, \mathcal{H}]_P = -4\lambda(xp_x + yp_y) - mu^\lambda(x^2 + y^2) \qquad \rightarrow u^\lambda = -\frac{4\lambda}{m(x^2 + y^2)}(xp_x + yp_y) \approx 0 \tag{2.3.8}$$

The last consistency equations fixes $u^\lambda$ which terminates our series of constraints. We can see that $\phi_2 \approx 0$ forces the position of the system to be fixed on the ring. The quantity $p_r := xp_x + yp_y$ is also a representation of the radial momentum, just as $p_\varphi := xp_y - yp_x$ is the angular momentum, so the constraint $\phi_3 \approx 0$ can be interpreted as fixing the radial momentum to be zero. We also note that $\phi_2$ ensures that Lagrange multiplier term will be zero in the constrained subspace, and $\phi_4$ can be used to explicitly find an expression for the Lagrange multiplier. With all constraints determined the second class constraints in the Hamiltonian are strongly equal to zero. As a result the Lagrange multiplier term $\lambda(x^2 + y^2 - R^2) \equiv \lambda\phi_2$ will also disappear. Since we have generated 4 independent constraints, the constrained subspace will have dimension $6 - 4 = 2$ which is the expected phase space size for the 1 dimensional ring. We can now construct the $C$ matrix using the definition from (2.2.9)

$$C = \begin{bmatrix} 0 & 0 & 0 & mq^k q_k \\ 0 & 0 & 2q^k q_k & 2q^k p_k \\ 0 & -2q^k q_k & 0 & p^k p_k + 2m\lambda q^k q_k \\ -mq^k q_k & -2q^k p_k & -p^k p_k - 2m\lambda q^k q_k & 0 \end{bmatrix} \tag{2.3.9}$$

where the vectors are $q_k = (x, y)$ and $p_k = (p_x, p_y)$. The matrix is non-singular since the determinant is $\det C = 4m^2(q^k q_k)^4$ and its inverse is

$$C^{-1} = \frac{1}{2m(q^k q_k)^2} \begin{bmatrix} 0 & -p^k p_k - 2m\lambda q^k q_k & q^k p_k & -2q^k q_k \\ p^k p_k + 2m\lambda q^k q_k & 0 & -mq^k q_k & 0 \\ -q^k p_k & mq^k q_k & 0 & 0 \\ 2q^k q_k & 0 & 0 & 0 \end{bmatrix} \tag{2.3.10}$$

The Dirac bracket can now be defined, and the relations between the canonical variables worked out

$$\begin{aligned} [x, p_x]_D &= \frac{y^2}{R^2} & [y, p_y]_D &= \frac{x^2}{R^2} & [x, y]_D &= 0 \\ [x, p_y]_D &= -\frac{xy}{R^2} & [y, p_x]_D &= -\frac{xy}{R^2} & [p_x, p_y]_D &= \frac{1}{R^2}(yp_x - xp_y) \end{aligned} \tag{2.3.11}$$

We note that the Dirac bracket of the Lagrange multiplier and its conjugate momentum is $[\lambda, p_\lambda] = 0$ and so has vanished in the constrained subspace. Expressing these symbols as functions of the canonical variables for motion on a ring, $\varphi$ and $p_\varphi$, allows us to reduce the Dirac brackets above to the Poisson bracket

$$[f, g]_P = \frac{\partial f}{\partial \varphi}\frac{\partial g}{\partial p_\varphi} - \frac{\partial f}{\partial p_\varphi}\frac{\partial g}{\partial \varphi} \tag{2.3.12}$$

if we define the constrained variables as follows

$$x := R\cos\varphi \qquad y := R\sin\varphi \qquad p_x := -\frac{1}{R}p_\varphi \sin\varphi \qquad p_y := \frac{1}{R}p_\varphi \cos\varphi \tag{2.3.13}$$

where the definition of $x$ and $y$ is as expected. If we substitute these definitions for the original coordinates into the constraints, it can be seen that the constraints will are strongly equal to zero in the reduced phase space coordinates, ie $\phi_m(\varphi, p_\varphi) = 0$. This is also true for the Lagrange multiplier function, $u^\lambda(\varphi, p_\varphi) = 0$. Now that the terms $\lambda\phi_2$ and $u^\lambda p_\lambda$ can be strongly set to zero in the total Hamiltonian, the free Hamiltonian in the constrained subspace is then

$$\mathcal{H} = \frac{1}{2m}(p_x^2 + p_y^2) = \frac{1}{2mR^2}((-p_\varphi \sin\varphi)^2 + (p_\varphi \cos\varphi)^2) = \frac{p_\varphi^2}{2mR^2} \tag{2.3.14}$$

which is the expected classical Hamiltonian corresponding to free motion of a particle on a ring. All of the generated constraints and $u^\lambda$ have vanished from the Hamiltonian when written in this basis, though for $\phi_4$ to go to zero we have to fix the value of the Lagrange multiplier

$$\phi_4 = \frac{1}{2R^2}p_\varphi^2 - \lambda m R^2 = 0 \quad \rightarrow \quad \lambda = \frac{p_\varphi^2}{2mR^4} \tag{2.3.15}$$

The Lagrange multiplier is directly proportional to Hamiltonian (2.3.14), which is a conserved quantity thereby implying that the Lagrange multiplier will not vary in time; this is consistent with the constraint $p_\lambda = 0$. Since we can write all of (2.3.11) using Poisson brackets, the way is paved to quantize our system. We must now establish a set of operators which have the following commutation relations

$$\begin{aligned} [\tilde{x}, \tilde{p}_x] &= -i\hbar\frac{\tilde{y}^2}{R^2} & [\tilde{y}, \tilde{p}_y] &= -i\hbar\frac{\tilde{x}^2}{R^2} & [\tilde{x}, \tilde{y}] &= 0 \\ [\tilde{x}, \tilde{p}_y] &= i\hbar\frac{\tilde{x}\tilde{y}}{R^2} & [\tilde{y}, \tilde{p}_x] &= i\hbar\frac{\tilde{x}\tilde{y}}{R^2} & [\tilde{p}_x, \tilde{p}_y] &= -i\hbar\frac{1}{R^2}(\tilde{y}\tilde{p}_x - \tilde{x}\tilde{p}_y) \end{aligned} \tag{2.3.16}$$

where the tilde is used to indicate that although these are operators they are not the usual Cartesian operators. It is also useful to have the following relationship between the two pairs of position and momentum operators

$$\frac{d}{dt}\tilde{q} \equiv \frac{i}{\hbar}[\hat{H}, \tilde{q}] = \frac{\tilde{p}}{m} \tag{2.3.17}$$

so that the equation of motion for the position centroid variables (1.3.33) remains consistent allowing for the use of CMD. The quantum operators from $L^2(S^1)$ introduced in the introduction to this chapter can be used to define a set of operators which satisfy this condition as well as the commutator relations (2.3.16). These operators may then be written as

$$\tilde{x} := R\cos\hat{\varphi} \qquad \tilde{y} := R\sin\hat{\varphi} \qquad \tilde{p}_x := -\frac{1}{2R}\{\hat{J}, \sin\hat{\varphi}\} \qquad \tilde{p}_y := \frac{1}{2R}\{\hat{J}, \cos\hat{\varphi}\} \tag{2.3.18}$$

where $\{A, B\} = AB + BA$ is the anti-commutator, and the commutators (2.3.16) can be worked out using (2.1.4). We note that the momentum operators are a symmetric product of the position operators and the angular momentum operator. Using these momentum operators the Hamiltonian is

$$\hat{H} = \frac{1}{2m}\left(\tilde{p}_x^2 + \tilde{p}_y^2\right) = \frac{1}{2mR^2}\left(\hat{J}^2 - \frac{1}{4}\right) \tag{2.3.19}$$

where we have an additional constant potential which introduces a shift constant potential term so that the expected free particle on a ring Hamiltonian is not obtained. These results, though independently obtained, are the same as those found in [31]. While this shift would need to be accounted for in the path integral, the centroid formalism is invariant under the addition of constant potential terms in the Hamiltonian. Although this derivation was specifically for the case of the free particle on the ring, the same constrained symbols and operators can be retrieved in the case where a position dependent potential is included in the Lagrangian though some of the constraints, and hence the Dirac bracket, will be defined differently.[9]

### 2.3.2 Constraining the centroid density

Here we begin with the path integral representation for the centroid density in two dimensions

$$\rho_c(x_c, y_c, p_{xc}, p_{yc}) = \int \mathcal{D}\mathbf{q}\,\mathcal{D}\mathbf{p}\,\delta(x_c - x_0)\,\delta(y_c - y_0)\,\delta(p_{xc} - p_{x\,0})\,\delta(p_{yc} - p_{y\,0})\exp(-S[\tau]/\hbar) \tag{2.3.20}$$

The theory explained in section 2.2.2 is used to constrain the variables in the path integral and then replace them with the equivalent symbols present in the reduced phase space. In this instance we will replace the constrained Cartesian phase space variables with those from the phase space for $S^1$ using the relations (2.3.13). While the path integral variables are constrained, the centroid phase space variables are not. The proposed centroid density is

$$\rho_c = \int \mathcal{D}\varphi\mathcal{D}p_\varphi\,\delta(x_c - x_0)\,\delta(y_c - y_0)\,\delta(p_{xc} - p_{x\,0})\,\delta(p_{yc} - p_{y\,0})\exp(-S[\tau]/\hbar) \tag{2.3.21}$$

where measures have changed, and the functional integral over the momentum is in fact a product of sums. The centroid constraints are no longer functions of the Cartesian path integral variables but have the form

$$a_0 = \int_0^{\beta\hbar} d\tau a(\varphi(\tau), p_\varphi(\tau)) \tag{2.3.22}$$

[9] Refer to B.1

and the imaginary time action undergoes the transformation

$$S[\tau] = \int_0^{\beta\hbar} d\tau \left[\mathcal{H} - ip_x\dot{x} - ip_y\dot{y}\right] \to S[\tau] = \int_0^{\tau} d\tau \left[\mathcal{H} - ip_\varphi\dot{\varphi}\right] \tag{2.3.23}$$

$$\mathcal{H} = \frac{1}{2m}\left(p_x^2 + p_y^2\right) + V(x,y) \to \mathcal{H} = \frac{1}{2mR^2}\left(p_\varphi^2 - \frac{1}{4}\right) + V(\varphi) \tag{2.3.24}$$

The constant potential present in the kinetic term of the Hamiltonian may be treated as a constant scaling factor since it is independent of the path integral variables. After the phase space reduction the partition function is now

$$Z = \mathrm{Tr}\left[\exp\left(\frac{1}{2mR^2}\left(\hat{J}^2 - \frac{1}{4}\right) + V(\hat{\varphi})\right)\right] = e^{-\frac{1}{8mR^2}}\,\mathrm{Tr}\left[\exp\left(\frac{1}{2mR^2}\hat{J}^2 + V(\hat{\varphi})\right)\right] \tag{2.3.25}$$

where the constant potential is again present. Since the centroid density is normalised by the partition function these terms will cancel, so the resultant density will be identical to the case where the Hamiltonian does not contain this term. The centroid formalism will always be invariant under the addition of a constant potential term in the Hamiltonian. An issue now presents itself when we try to undo the trace operation in the centroid density to try and obtain a QDO. The presence of cross terms involving the angular position and momentum path integral variables inhibits undoing the Trotter operation, which presents a theoretical issue for this method. In order to generate the desired Hamilton-like equations of motion among the centroid symbols, we conjecture that the symbol Hamiltonian is be replaced by the equivalent operator Hamiltonian in the QDO using the operators from (2.3.18). The QDO is then proposed to be

$$\begin{aligned}\hat{\delta}_c(x_c, y_c, p_{xc}, p_{yc}) = &\int d\xi_x\, d\xi_y\, d\eta_x\, d\eta_y\, e^{-i(\xi_x x_c + \xi_y y_c)}\, e^{-i(\eta_x p_{xc} + \eta_y p_{yc})} \\ &\times \exp\left(-\beta\hat{H} + i\xi_x R\cos\hat{\varphi} + i\xi_y R\sin\hat{\varphi} + i\eta_x\frac{1}{2R}\{\hat{J}, -\sin\hat{\varphi}\} + i\eta_y\frac{1}{2R}\{\hat{J}, \cos\hat{\varphi}\}\right)\end{aligned} \tag{2.3.26}$$

Whether the trace of this QDO is equal to the proposed centroid density is not yet known. Potential issues are discussed in the conclusion to this chapter. One way to test this is to build the centroid density using both the path integral definition (2.3.21) and as the trace of the QDO (2.3.26) for comparison, though this has currently not been done. This QDO has been used in all numerical calculations and computational results show that this QDO appears to return the expected centroid phase space distributions for the Cartesian position and momentum operators in our reduced Hilbert space

$$x_c = \mathrm{Tr}[\hat{\delta}_c\tilde{x}] \qquad y_c = \mathrm{Tr}[\hat{\delta}_c\tilde{y}] \qquad p_{xc} = \mathrm{Tr}[\hat{\delta}_c\tilde{p}_x] \qquad p_{yc} = \mathrm{Tr}[\hat{\delta}_c\tilde{p}_y] \tag{2.3.27}$$

Since Hamilton's equations of motion for the quantum operators are

$$\frac{d}{dt}\tilde{x} = \frac{i}{\hbar}[\hat{x}, \tilde{H}] = \frac{i}{2mR\hbar}[\hat{J}^2, \cos\hat{\varphi}] = -\frac{1}{2mR}\{\hat{J}, \sin\hat{\varphi}\} \equiv \frac{\tilde{p}_x}{m} \tag{2.3.28}$$

$$\frac{d}{dt}\tilde{p}_x = \frac{i}{\hbar}[\tilde{p}_x, \hat{H}] = -\frac{1}{2mR^2}\{\hat{J}, \tilde{p}_y\} + \frac{i}{\hbar}[\hat{V}, \tilde{p}_x] =: \hat{F}_x \tag{2.3.29}$$

for the $x$-direction and

$$\frac{d}{dt}\tilde{y} = \frac{1}{2mR}\{\hat{J}, \cos\hat{\varphi}\} \equiv \frac{\tilde{p}_y}{m} \tag{2.3.30}$$

$$\frac{d}{dt}\tilde{p}_y = \frac{1}{2mR}\{\hat{J}, \tilde{p}_x\} + \frac{i}{\hbar}[\hat{V}, \tilde{p}_y] =: \hat{F}_y \tag{2.3.31}$$

for the $y$-direction, we can formulate a similar set using the centroid variables to use in CMD calculations. Noting that both force operators are dependent on the position and momentum operators, the associated centroid distributions are also not expected to be separable in the position and momentum centroid variables and so the definition of the force operator (1.3.37) therefore does not hold for the rotational formulation.

## 2.4 Computational Results

### 2.4.1 Numerical Structure

Due to the significant difficulty we faced in obtaining any analytic results, the bulk of the work has been computational in nature. The production code used was written from scratch in C++ with linear algebra structures and operations provided by the Armadillo linear algebra package. All operators are represented as matrices using some finite number of the momentum operator eigenstates, $\{|j\rangle, j \in [-j_{max}, \ldots, j_{max}]\}$, as the basis. In this basis the momentum operator is diagonal, and the raising and lowering operators are constant on the upper and lower diagonal, respectively. Since all periodic potentials can be written using a Fourier series of sines and cosines, we will need to represent these as higher powers of the raising and lowering operators

$$\cos(m\hat{\varphi}) = \frac{1}{2}\left(\hat{U}^m + (\hat{U}^\dagger)^m\right) \qquad \sin(m\hat{\varphi}) = \frac{1}{2i}\left(\hat{U}^m - (\hat{U}^\dagger)^m\right) \tag{2.4.1}$$

A uniform grid is constructed for each of the four Fourier variables, and a matrix representation of the centroid Hamiltonian is constructed at each grid point. Eigenvalue decomposition is performed on the centroid Hamiltonian and the matrix exponentials then constructed. We can then replace the quantum operators of interest with this object and so obtain Fourier space functions for the centroid density and various centroid symbols. The continuous Fourier transform (CFT) can then be performed along each Fourier variable axis to retrieve centroid distribution functions in terms of the four centroid variables. If the phase space integral of the centroid density is not closely equal to $Z$ then the maximum value of all axes of the Fourier space are increased. Performing the CFT using Riemann sums is very inefficient for a system with four dimensions so to greatly improve computation time we used the method detailed in [32] which involves the use of two forward and one inverse fast Fourier transforms to compute the one dimensional CFT. The one downside is that the range of the output function is inversely proportional to the grid spacing of the input function, and the grid spacing of the output is inversely proportional to the range of the input by the following relations

$$\Delta a = 2\frac{a_{\max}}{a_{\text{size}}} \qquad b_{\max} = \frac{\pi}{\Delta a} \qquad \Delta b = 2\pi\frac{a_{\text{size}}}{\Delta a} \qquad a_{\text{size}} = b_{\text{size}} \tag{2.4.2}$$

where $\Delta q$ gives the grid spacing, the $q_{\text{size}}$ is the maximum point, $q_{\text{size}}$ is the number of grid points. The variables $a$ and $b$ indicate whether the properties are associated with the input or output function, respectively. Since the rotational centroid density is zero when the radial distance in the position coordinates is greater than the radius of the system

$$\rho_c = 0, \quad x_c^2 + y_c^2 > R^2 \tag{2.4.3}$$

for non-zero $\beta$ the only useful points are located within this radius. To obtain a fine grid spacing within this radius would require the exponential of the centroid Hamiltonian to be built at 'a large

number of points, which becomes impractical with a large number of dimensions in the Fourier space. To circumvent this, we choose to build the exponential of the centroid Hamiltonian to a maximum point in the Fourier space where it has sufficiently decayed. We can then increase the input range by padding the matrix with zeroes before passing the function to the CFT routine. This will increase the number of grids points and therefore give us a smaller value for $\Delta b$ while leaving $\Delta a$ fixed with only a minor increase in computation time. The accumulated errors from performing this for each of the four dimensions in Fourier space results in some anomalies in the centroid phase space distributions. Having built the centroid density and distributions for the two force operators, we use the CMD algorithm to approximate the dipole autocorrelation function. The system of Hamilton's equations are computed using the explicit fourth order Runge-Kutta algorithm.

### 2.4.2 Free particle on a ring

We begin by examining the results for the particle on a ring with no potential, where the Hamiltonian is given by

$$\hat{H} = B\hat{J}^2 \tag{2.4.4}$$

and where we have chosen $\hbar = 1$, $m = 0.5$, $R = 1$ and therefore $B = 1$. The maximum radial value in the centroid phase space should therefore be $r_c = 1$. Some centroid densities are shown in Fig. 2.1 for temperatures $\beta$ =2, 5, 8 and 12. The densities in the left column have been integrated over the centroid momentum coordinates while those in the right column have been integrated over the position centroid coordinates. We can see that the position distribution is uniform in $\varphi_c$ due to the lack of a potential in the Hamiltonian, but that the density is only non-zero within the radius $r_c = R$. The reason for this is that the thermal paths are confined to move on the ring so the centroid of the thermal paths must be located within this arc. This is why the centroid density is heavily localized near the radius of the ring in the low temperature limit where the thermal paths are short. As the temperature increases the paths can wind around the circle, and so the centroid is more likely to be located near the origin. It can be seen that in this case the outer portion of the density becomes wider and moves towards the origin while another hump begins to rise centred at the origin. It can be shown that the high and low temperature limit of the position centroid density are respectively[10]

$$\lim_{\beta\to 0} \rho_c(x_c, y_c) = \sum_{j=-\infty}^{\infty} \frac{1}{2\pi r_c}\delta(r_c - R) \tag{2.4.5}$$

$$\lim_{\beta\to \infty} \rho_c(x_c, y_c) = \frac{1}{2\pi r_c}\delta(r_c) \tag{2.4.6}$$

where $r_c = \sqrt{x_c^2 + y_c^2}$, which is in agreement with what we observe in these systems. In the case of the momentum distribution, when integrated over the position centroid variables, the shape appears to be a Gaussian which which has a width directly proportional to the temperature and a height inversely proportional to the temperature. We can surmise that in the low temperature limit the density will approach a delta function, much like the position centroid distribution, so that the phase space integral is equal to $Z = 1$. It is currently unclear what the limiting behaviour is in the high temperature limit.

[10]Refer to section B.3.1

We have also included cuts of the total centroid density at constant $y_c$ and $p_{yc}$ is Fig. 2.2. In the right column $y_c$ is held constant and $p_{yc}$ is varied and in the left column $p_{yc}$ is held constant and $y_c$ is varied. The plots demonstrate the correlation which exists between the four centroid variables. This correlation frustrates attempts at efficient computation of the centroid density since it cannot be decomposed into a product of centroid distributions, as is the case with Euclidean space. Examining these cuts also gives us insight into the trajectories the centroid will take through the phase space when performing CMD calculations. It is not possible for the centroid to visit regions where the density becomes zero, so the shape of the non-zero regions gives insight into how the centroid coordinates are correlated.

We can see that for $y_c = 0.6$ the centroid density is zero outside the range $x_c \in [-0.8, 0.8]$ as expected from (2.4.3). As the value of $p_{yc}$ is increased the bulk of the density starts to accumulate at the extremes of the $x_c$ axis and broadens along the $p_{xc}$ axis such that the density appears to twist about the origin in the $x_c - p_{xc}$ plane. This broadening is towards negative values of $p_{xc}$ for positive values of $x_c$, and towards positive values of $p_{xc}$ for negative values of $x_c$. This behaviour in the centroid density demonstrates that as trajectories move closer to $r_c = R$ the momentum density changes such that the trajectories are directed away from this barrier. The same trend is seen when $y_c$ is at a constant positive value and $p_{yc}$ is made more negative. When $y_c$ is at a constant negative value the correlation between $x_c$ and $p_{yx}$ is reversed. When the magnitude of the $p_{yc}$ coordinate value is increased the bulk of the distribution will move towards positive values of $p_{xc}$ for positive values of $x_c$, and towards negative values of $p_{xc}$ when $x_c$ is negative.

When $p_{yc}$ is fixed and the $y_c$ coordinate increased the range of the density along the $x_c$ axis begins to shrink, as expected. The density also begins to broaden along the $p_{xc}$ axis, and this broadening is again dependent on the $x_c$ coordinate. For positive values of $x_c$ the broadening is towards negative values of $p_{xc}$ and for negative values of $x_c$ it is towards positive values of $p_{xc}$. This broadening in the $p_{xc}$ axis is again to direct trajectories away from the barrier at $r_c = R$. We notice that as $y_c$ becomes closer to the radius of the ring and the range of $x_c$ begins to shrink in turn that the $x_c$ dependence of the broadening along the $p_{xc}$ axis becomes less noticeable as a result.

CMD calculations were also performed for the centroid symbol $x_c(t)$ at a variety of temperatures and the resulting centroid dipole autocorrelation results are displayed in Fig. 2.3, along with the exact Kubo transformed dipole function. A time step of $\Delta t = 0.01$ was chosen for all calculations which proved to give stable results. Since the CMD results are expected to converge to the classical results in the $\beta \to 0$ limit, we have also plotted this function as given by B.4.6 except the functions has been rescaled by $2\langle x_c x_c(0)\rangle$ so that the time zero values match. We do this since we only want to show that the CMD results will eventually match the decaying exponential behaviour in the classical result. As can be seen in Fig. 2.3a the CMD results do indeed match the rate of Gaussian decay expected from the classical autocorrelation function and displays no recurrence. The drift of the CMD results away from zero here and in all other plots in Fig. 2.3 is due to accumulated instabilities in the individual $x_c(t)$ trajectories. As temperature is increased, the CMD results begin the match the exact result at very early times but quickly dephase and decohere. Even at very low temperatures the CMD results have difficulty matching the exact Kubo transformed correlation function to the first minimum, as can be seen in Fig. 2.3e. The difference is very slight but still present even in Fig. 2.3f which has twice the $\beta$ value. The phase matching is also poor, with the CMD results matching the exact case for 0.75 oscillations in Fig. 2.3d, 1.25 oscillations in Fig. 2.3e and 2.25 oscillations in Fig. 2.3f. That the CMD results are so slow to converge to the exact results with decreasing temperature demonstrates the difficulty the method has with capturing the quantum dynamics of the free particle on a ring.

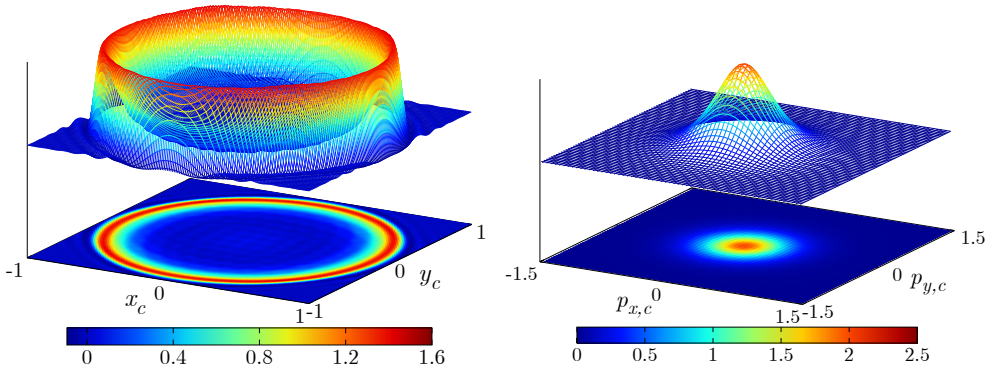


(a) $\rho_c(x_c, y_c)$ for $\beta = 2$




(b) $\rho_c(p_{xc}, p_{yc})$ for $\beta = 2$

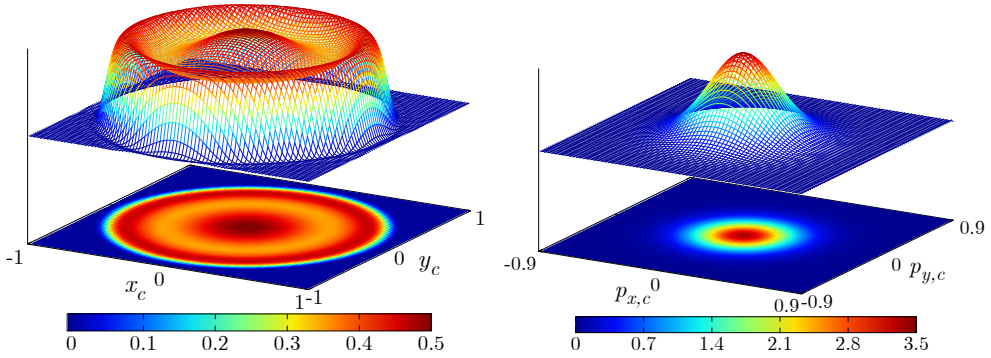


(c) $\rho_c(x_c, y_c)$ for $\beta = 5$




(d) $\rho_c(p_{xc}, p_{yc})$ for $\beta = 5$

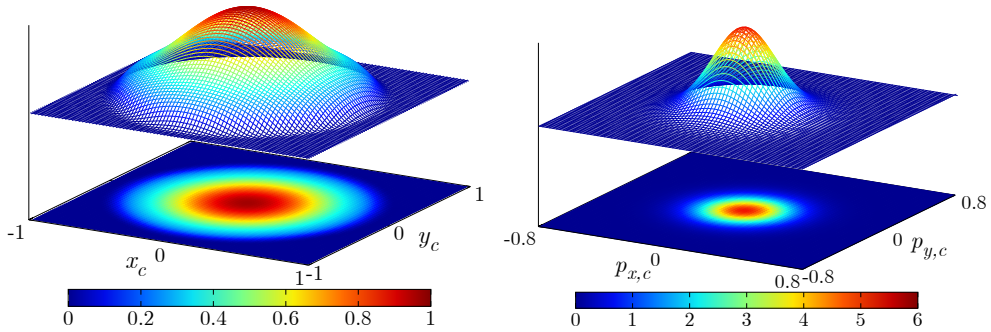


(e) $\rho_c(x_c, y_c)$ for $\beta = 8$




(f) $\rho_c(p_{xc}, p_{yc})$ for $\beta = 8$

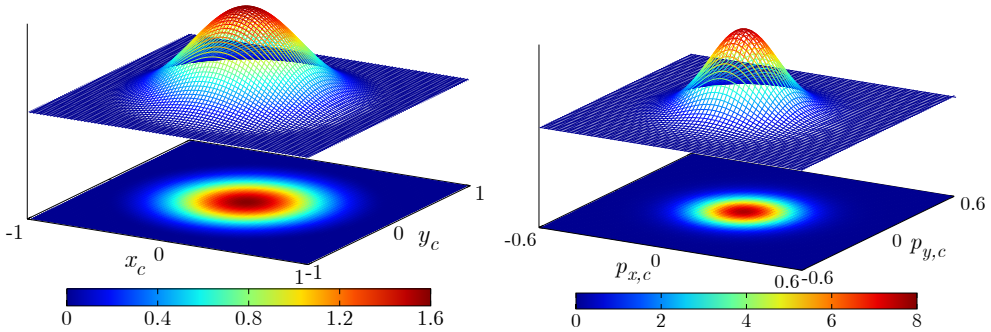


(g) $\rho_c(x_c, y_c)$ for $\beta = 12$




(h) $\rho_c(p_{xc}, p_{yc})$ for $\beta = 12$

Figure 2.1: Position and momentum centroid densities for the free particle on a ring

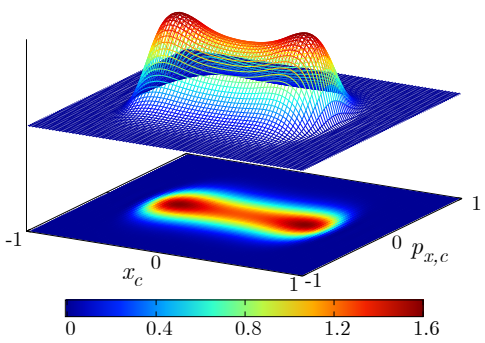


(a) $\rho_c$ for $\beta = 5$, $y_c = 0.6$, $p_{yc} = 0$

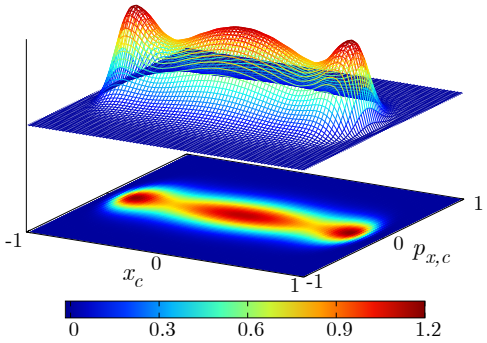


(b) $\rho_c$ for $\beta = 5$, $y_c = 0$, $p_{yc} = 0.2$

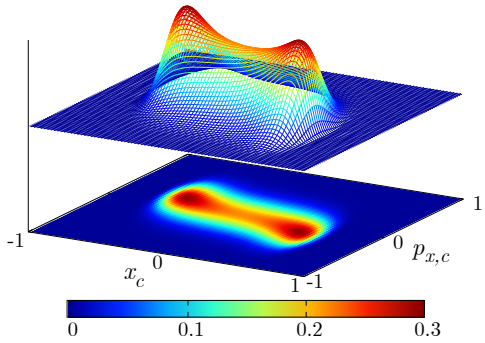


(c) $\rho_c$ for $\beta = 5$, $y_c = 0.6$, $p_{yc} = 0.4$

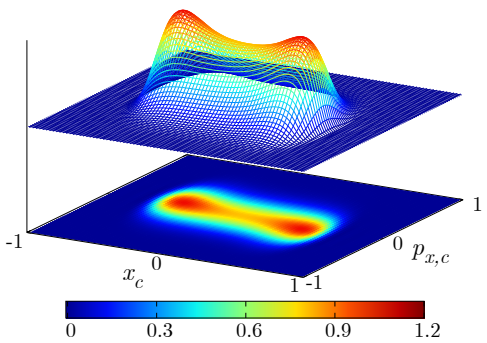


(d) $\rho_c$ for $\beta = 5$, $y_c = 0.6$, $p_{yc} = 0.2$

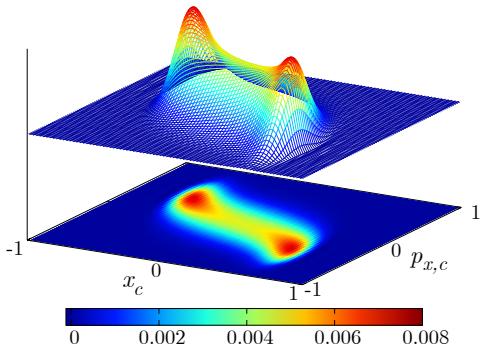


(e) $\rho_c$ for $\beta = 5$, $y_c = 0.6$, $p_{yc} = 0.7$

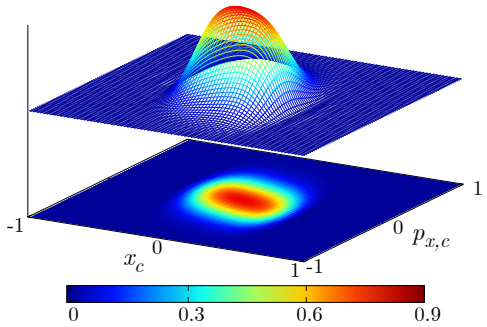


(f) $\rho_c$ for $\beta = 5$, $y_c = 0.8$, $p_{yc} = 0.2$

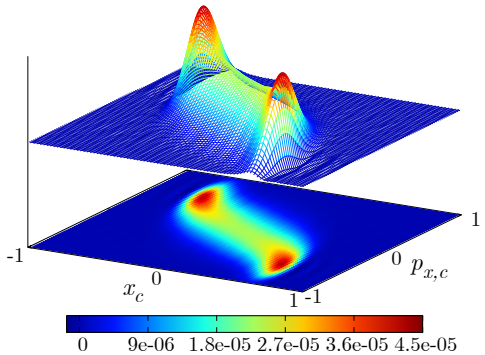


(g) $\rho_c$ for $\beta = 5$, $y_c = 0.6$, $p_{yc} = 1.0$

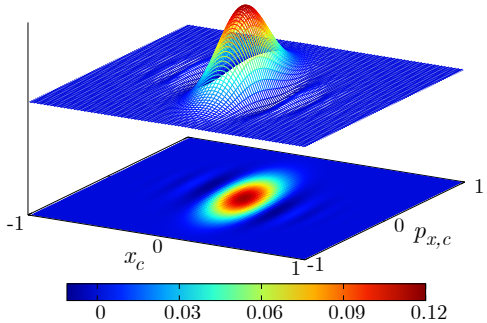


(h) $\rho_c$ for $\beta = 5$, $y_c = 0.9$, $p_{yc} = 0.2$

Figure 2.2: Centroid density for the free POR at constant $y_c$ and $p_{yc}$

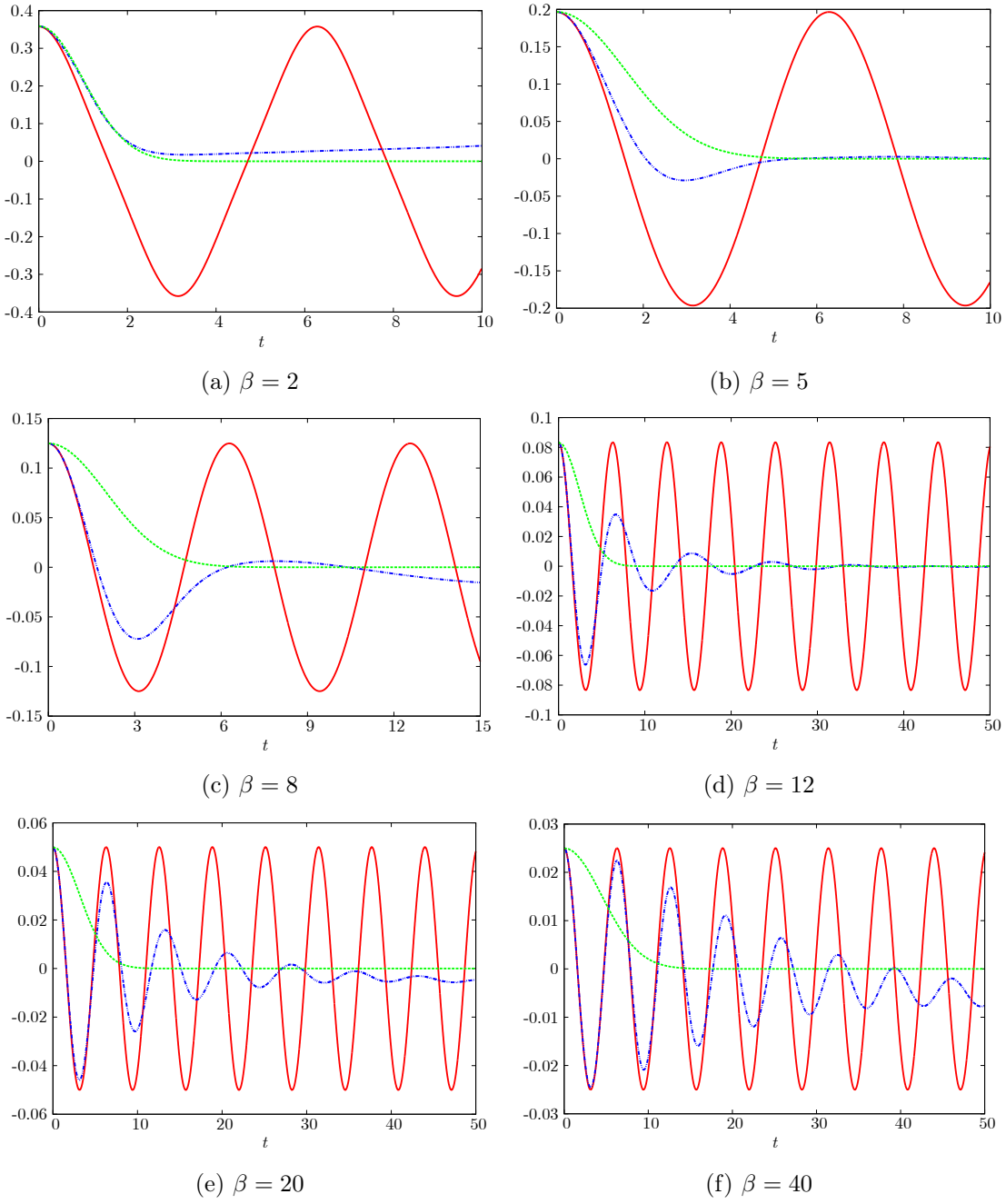


(a) $\beta = 2$

(b) $\beta = 5$

(c) $\beta = 8$

(d) $\beta = 12$

(e) $\beta = 20$

(f) $\beta = 40$

Figure 2.3: Comparison of exact Kubo transformed autocorrelation function (red), approximate CMD dipole autocorrelation function (blue), and the classical dipole autocorrelation function (green).

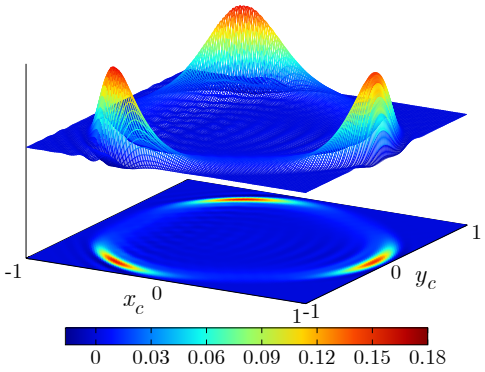


(a) $\rho_c(x_c, y_c)$ for $\beta = 2$

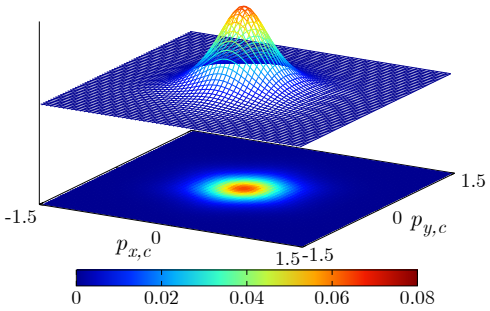


(b) $\rho_c(p_{xc}, p_{yc})$ for $\beta = 2$

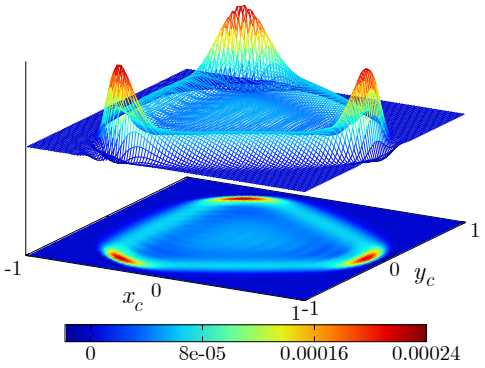


(c) $\rho_c(x_c, y_c)$ for $\beta = 5$

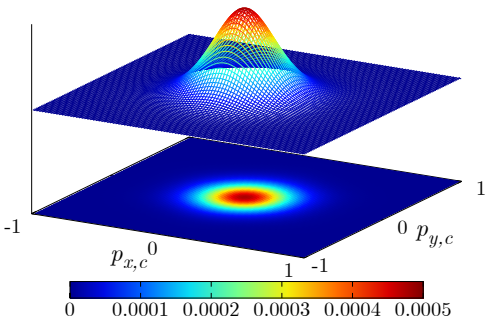


(d) $\rho_c(p_{xc}, p_{yc})$ for $\beta = 5$

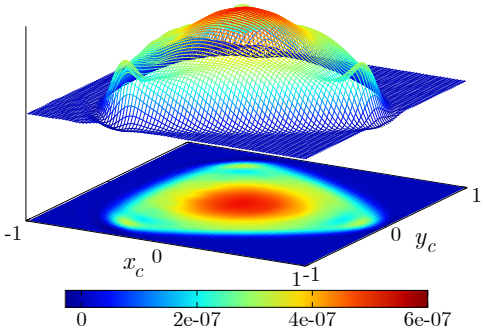


(e) $\rho_c(x_c, y_c)$ for $\beta = 8$

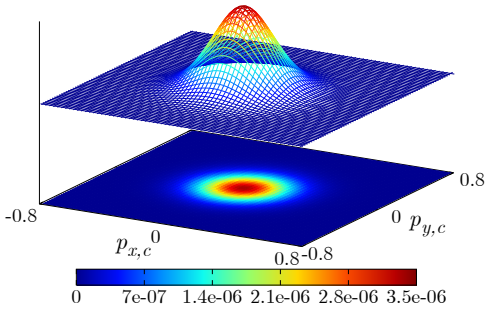


(f) $\rho_c(p_{xc}, p_{yc})$ for $\beta = 8$

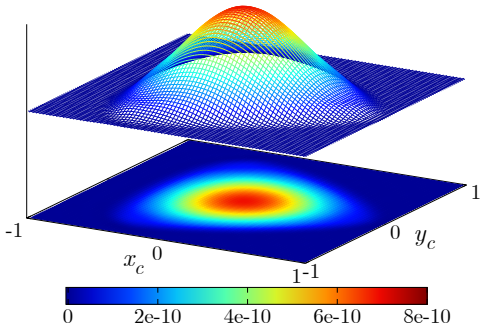


(g) $\rho_c(x_c, y_c)$ for $\beta = 12$

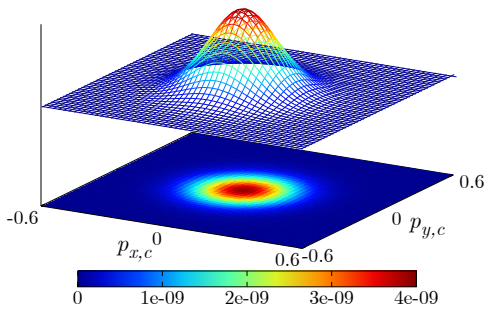


(h) $\rho_c(p_{xc}, p_{yc})$ for $\beta = 12$

Figure 2.4: Position and momentum centroid densities for the Hamiltonian (2.4.7)

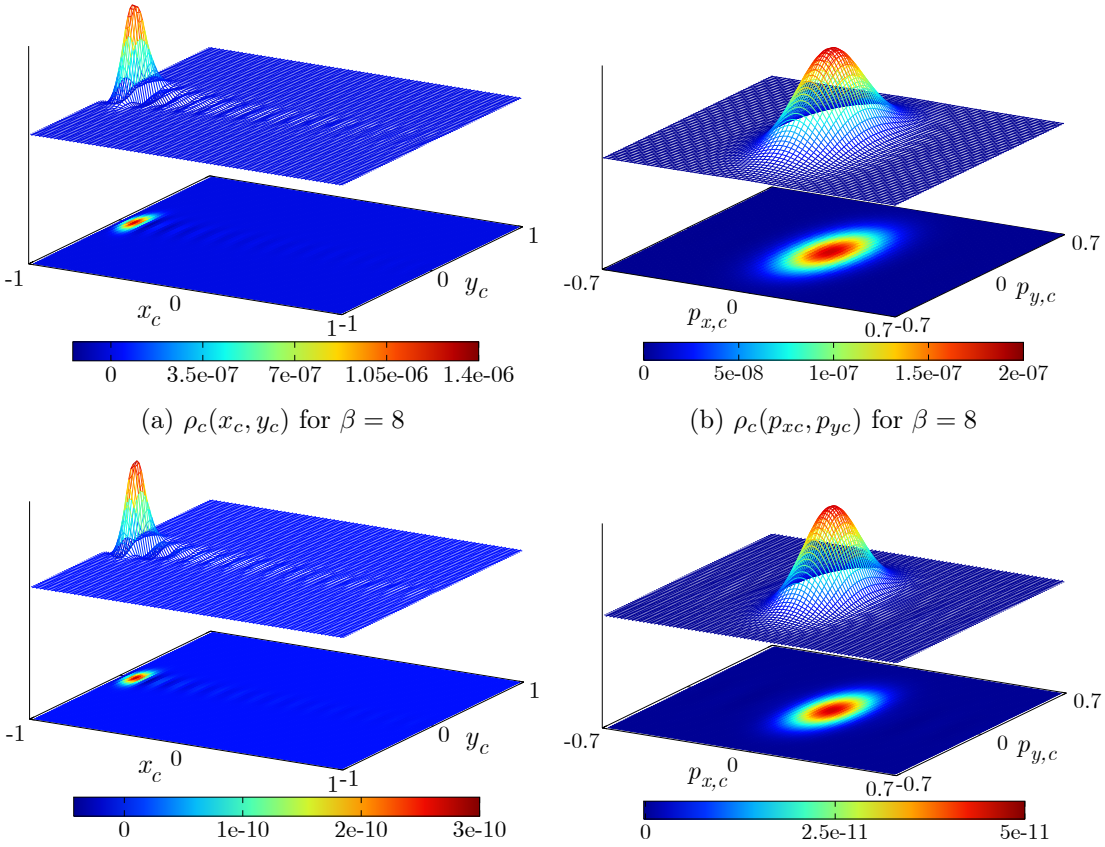


(a) $\rho_c(x_c, y_c)$ for $\beta = 8$

(b) $\rho_c(p_{xc}, p_{yc})$ for $\beta = 8$

(c) $\rho_c(x_c, y_c)$ for $\beta = 12$

(d) $\rho_c(p_{xc}, p_{yc})$ for $\beta = 12$

Figure 2.5: Position and momentum centroid densities for the Hamiltonian (2.4.8)

### 2.4.3 Hindered rotor model

We now move on to systems with a periodic potential in the Hamiltonian, which are collectively referred to as hindered rotor models. For consistency purposes we have taken $\hbar = 1$ and $B = 1$. The first model under consideration has a potential with three wells and the following Hamiltonian

$$\hat{H} = \hat{J}^2 + 2(1 - \cos(3\hat{\varphi})) \tag{2.4.7}$$

We again calculated the centroid density for the temperatures $\beta = 2, 5, 8, 12$, which are displayed in Fig. 2.4. The left column has been integrated over the momentum coordinates and the right column has been integrated over the position coordinates. The position density shows the same behaviour as the free particle case, with the density being localized near the radius of ring in the high temperature limit and showing a growing hump localized about the origin at progressively lower temperatures. The localizing effect of the potential is also evident as the centroid density has three humps located at $\varphi_c = 0, 2\pi/3, 4\pi/3$ corresponding with the location of the minima in the potential. Although these peaks eventually disappear a distortion is still apparent in the density at these points causing a triangular shape, though this too disappears with decreasing temperature. The shape of the momentum distributions are seemingly unaffected by the potential and still appear to be Gaussian in shape with a width which is inversely proportional to the temperature.

We also considered a system with a strongly confining potential with only one well given by the Hamiltonian

$$\hat{H} = \hat{J}^2 + 10(\cos(\hat{\varphi}) + 1) \tag{2.4.8}$$

and the resulting centroid densities are shown in Fig. 2.5 for $\beta = 8, 12$. We can see that the confining potential is so strong that the position densities are very similar in both cases. It also causes the position density to be strongly peaked at $\varphi_c = \pi$ and very near the radius of the ring. For both temperatures, the non-zero portion of the density are the width of one grid space. The ripples in the density are artefacts from the Fourier transform. A test calculation was also performed at $\beta = 40$ and the results for the position density were nearly identical, demonstrating that a sufficiently strong potential can severely inhibit the bulk of the density making the expected appearance around the origin of the centroid phase space in the low temperature limit. The potential also results in the momentum densities becoming squeezed in the $p_{yc}$ direction. The momentum distribution does broaden with a decrease in temperature, which is the expected trend.

CMD calculations were performed for all given temperatures and both hindered rotor Hamiltonians, and despite having a correct $t = 0$ value the dipole autocorrelation function was highly unstable even for a small time step. As a result, no comparison of CMD and exact Kubo transformed correlation functions are shown for the hindered rotor models. The issue is with the centroid force fields, which we expect to become infinitely repulsive at the radius of ring since the centroid should not be allowed beyond this point in phase space. This is problematic for calculating the centroid trajectories; if they get too close to the radius of the ring and have sufficient momentum the centroid will sometimes clip outside the ring on the next time step and avoid the repulsive force field. If this occurs to a sufficient number of orbits the centroid correlation function results become unusable. The system is therefore *stiff*, meaning that smooth and stable results can only be achieved when the time step is taken to be extremely small. In our case this would also necessitate a larger number of grid points for the force fields so that the centroid trajectories can move closer to the ring. Since this would increase the computation time and memory, we wish to approach this problem by using an implicit method rather than explicit method for the integrator. Explicit integrators use current and past positions in phase space to compute the next time step while implicit integrators also require knowledge about the next position in phase space. To determine the position of the next time step using an implicit integrator therefore requires use of a root finding algorithm which will also increase computation time, but should allow us to better avoid any instability by restricting the search to phase space points located within the ring.

### 2.4.4 Summary and future work

In this chapter we have successfully extended the centroid formalism to systems which can be considered to inhabit constrained spaces. This includes rotational motion and internal torsions within molecules. We have seen that this necessitates considering the constrained space as being embedded in some Euclidean space, and using the number of centroid phase space variables associated with the Euclidean space. The centroid densities for the operators will also no longer be separable in the phase space coordinates, so the force fields had to be generated from the force operators. Performing the exact centroid dynamics for the free particle on a ring yielded a dipole time correlation function which was exactly equal to the one generated using a finite dimensional matrix representation for the quantum operators. We also tested the CMD approximation by introducing parametric dependence into the centroid force symbols in order to calculate

the approximate dipole autocorrelation function. Only the CMD results for the free particle are currently usable, but these show that the CMD approximation will have difficulty capturing the exact nature of quantum mechanical motion on a ring. A recent formulation of rotational RPMD has shown good results for a particle on a ring system with a highly confining potential at a high temperature [33, 34] and we hope to replicate these results using our formalism.

We now discuss in the issue presented in section 2.3.2, that is whether

$$\rho_c(x_c, y_c, p_{xc}, p_{yc}) \stackrel{?}{=} \mathrm{Tr}\, \hat{\delta}_c(x_c, y_c, p_{xc}, p_{yc}) \tag{2.4.9}$$

for the proposed quantities. We assume that the content of the QDO is correct since it generates the desired equations of motion, so the issue then is with the centroid density. The terms coupling the position and angular momentum operators in the QDO makes the process of rewriting the trace as a path integral difficult. It seems likely that the constrained momentum operators will generate additional phases proportional to the Fourier variables $\eta_x$ and $\eta_y$ which are not present in $\rho_c$. This discrepancy may be a result of us constraining the Hamiltonian

$$\hat{H} = \frac{1}{2m}\left(\hat{p}_x^2 + \hat{p}_y^2\right) + V(\hat{x}, \hat{y}) \tag{2.4.10}$$

instead of the effective centroid Hamiltonian

$$\hat{H}' = \frac{1}{2m}\left(\hat{p}_x^2 + \hat{p}_y^2\right) + V(\hat{x}, \hat{y}) - i\frac{\xi_x}{\beta}\hat{x} - i\frac{\xi_y}{\beta}\hat{y} - i\frac{\eta_x}{\beta}\hat{p}_x - i\frac{\eta_y}{\beta}\hat{p}_y \tag{2.4.11}$$

The additional momentum terms will effect the Dirac brackets of the system and therefore the constrained phase space symbols. Preliminary work has been done dealing with this issue, but is not shown in this thesis. Another potential problem may come from the functional integral over the momentum. In the path integral the angular momentum coordinates should still only take on integer values, however, when we generated the constrained phase space symbols the classical angular momentum symbol was used. The classical angular momentum can be any real number, so the question is whether the functional integral is an integral over the all of the reals or a sum over all of the integers. Again, this is an open problem. We note that if we were to only consider the position centroid constraints, then the statement

$$\rho_c(x_c, y_c) = \mathrm{Tr}\left[\hat{\delta}_c(x_c, y_c)\right] \tag{2.4.12}$$

is true assuming the angular momentum functional integral is in fact a product of sums[11]. The reason is that the Dirac brackets are totally independent of any position dependent potential, which includes the position centroid constraints.

We have also worked out the constrained operators corresponding to motion on a 2-sphere, which is equivalent to the motion of a linear rigid rotor which has no orientation. The constrained operators are given in section B.2 where the action of the position operators on the $|l, m\rangle$ basis was found in [35]. The proposed QDO for the motion of a particle on a 2-sphere of radius R to given by (B.2.22). The centroid phase space is naturally 6-dimensional, which will pose significant problems for our method of performing test calculations.

Lastly, we present a scheme for connecting the motion of the rigid rotating tops to motion on a constrained surface. The motion of the rigid tops is associated with the group $SO(3)$ and

[11] Refer to section B.3

is generally parametrized in terms of the Euler angles. The topology of $SO(3)$ is that of a half 3-sphere in $\mathbb{R}^4$, with antipodal points on the boundary. Quaternions may also be used to describe the motion of rigid bodies; these are associated with the group $S^3$, the 3-sphere, which forms the boundary of a ball in $\mathbb{R}^4$. The group $S^3$ therefore acts as double cover of $SO(3)$, with antipodal points on the 3-sphere mapping to the same Euler angles. Use of the 3-sphere is preferable to that of the half 3-sphere since we do not have to account for the discontinuous boundary. It follows from the method laid out in this chapter that the centroid phase space would therefore be 8-dimensional. Work has been done to determine the constrained phase space variables in terms of the hyper-spherical coordinates, but the mapping to Euler angles has not yet been completed. This approach assumes that all three moments of inertia are identical, that is where the motion corresponds to a spherical top. The 4-dimensional surfaces corresponding to the spherical top, where only two of the moments of inertia are identical, and the asymmetric top, where no moments of inertia are the same, will likely be different, and is currently presumed to be a 3-ellipsoid. We note that the method described in this chapter is not limited to motion on $n$-spheres, but can be extended to other constrained spaces such as ellipses and tori.

# Chapter 3

# State projected centroid quantum statistical mechanics

## 3.1 Projection operators in the centroid formalism

The formulation of centroid dynamics as presented in chapter 1 was defined for the canonical ensemble, where the temperature, volume and number of particles were constant. We will now adapt the centroid formulation for the microcanonical ensemble where instead the energy, volume and number of particles are fixed. Specifically, we wish to study the statistical mechanics associated with the normalized state $|\psi\rangle$ with associated energy level $E_\psi$.[12] To do this we construct a density operator associated with this pure state

$$\hat{\mathcal{P}}_\psi := |\psi\rangle \langle\psi| \tag{3.1.1}$$

which is idempotent and a projection operator. In particular, we will be interested in the case where the projection is onto an eigenstate of the system Hamiltonian, which has some special properties that will not prove to hold for projection onto an arbitrary pure state. For now, we use the fact that the eigenstates of the Hamiltonian form a complete basis for the Hilbert space, and write the state $|\psi\rangle$ in this basis

$$|\psi\rangle = \sum_n c_n |\chi_n\rangle \tag{3.1.2}$$

where the set $\{c_n\}$ are complex numbers satisfying $\sum_n |c_n|^2 = 1$ and $\{|\chi_n\rangle\}$ are the eigenstates of the Hamiltonian with associated eigenenergies $\{E_n\}$. The normalisation constant associated with the microcanonical ensemble is

$$Z_\psi := \mathrm{Tr}\left[e^{-\beta\hat{H}}\hat{\mathcal{P}}_\psi\right] = \langle\psi|e^{-\beta\hat{H}}|\psi\rangle = \sum_n |c_n|^2 e^{-\beta E_n} \tag{3.1.3}$$

We can now define the centroid density for the microcanonical formulation, also called the state projected centroid density,

$$\rho_c^{(\psi)}(q_c, p_c) = \mathrm{Tr}\left[\hat{\varphi}_c(q_c, p_c)\hat{\mathcal{P}}_\psi\right] = \langle\psi|\hat{\varphi}_c(q_c, p_c)|\psi\rangle \tag{3.1.4}$$

[12] It is noted that since a mixed state may be represented as a linear combination of pure states, $\hat{\rho} = \sum p_i |\psi\rangle \langle\psi|$, the following work would also apply to mixed states even in the case where it is not a projection operator by simply using a linear combination of the results for each pure state

which by construction will have the correct phase space average

$$Z_\psi \equiv \iint \frac{dq_c\, dp_c}{2\pi\hbar} \rho_c^{(\psi)}(q_c, p_c) \tag{3.1.5}$$

This centroid density can in general contain regions of negative density and so is no longer guaranteed to be a positive semi-definite function and is no longer separable in the momentum and position centroid symbols. From here we could naïvely define the state projected version of the QDO as

$$\hat{\delta}_c^{(\psi)}(q_c, p_c) := \hat{\delta}_c(q_c, p_c)\hat{\mathcal{P}}_\psi \text{ (wrong)} \tag{3.1.6}$$

which is not Hermitian unlike the QDO for the canonical ensemble. This will result in a loss of consistency when defining the centroid symbols due to an ordering ambiguity since the QDO and projection operator possess a non-zero commutator in general; thusly

$$A_c \neq \mathrm{Tr}\Big[\hat{\delta}_c(q_c, p_c)\hat{\mathcal{P}}_\psi \hat{A}\Big] \neq \mathrm{Tr}\Big[\hat{\mathcal{P}}_\psi \hat{\delta}_c(q_c, p_c)\hat{A}\Big] \tag{3.1.7}$$

The correct method, as shown in Roy and Blinov [36], is to Kubo-transform the projection operator with the effective centroid Hamiltonian $\hat{H}'$, see (1.3.16), as follows

$$\hat{\delta}_c^{(\psi)}(q_c, p_c) := \frac{\hbar}{2\pi\rho_c^{(\psi)}(q_c, p_c)} \int_{-\infty}^{\infty}\int_{-\infty}^{\infty} d\xi\, d\eta\, e^{i\xi q_c} e^{i\eta p_c} \left[\int_0^1 du\, e^{-(1-u)\beta\hat{H}'} \hat{\mathcal{P}}_\psi e^{-u\beta\hat{H}'}\right] \tag{3.1.8}$$

Though the work in [36] was for exchange operators for particles following Bose-Einstein and Fermi-Dirac statistics, the general results apply to the case of our state projection operators and so this paper forms the theoretical basis of this chapter. The state projected centroid density remains unchanged due to the cyclic property of the trace which effectively cancels the Kubo transform. The time dependent QDO is also defined in the same way as in equation (1.3.24). It can be shown that the consistency equations for the position and momentum operators, (1.3.17) and (1.3.18), still hold regardless of the projection operator

$$q_c = \mathrm{Tr}\Big[\hat{\delta}_c^{(\psi)}(q_c, p_c)\hat{q}\Big] \tag{3.1.9}$$

$$p_c = \mathrm{Tr}\Big[\hat{\delta}_c^{(\psi)}(q_c, p_c)\hat{p}\Big] \tag{3.1.10}$$

The definition of time evolved centroid symbols for $q_c$ and $p_c$ and their equation of motions still hold under state projection, so the formulation of CMD is the same. In general, the time dependent centroid symbol for an operator $\hat{A}$ is now defined as

$$A_c^{(\psi)}(t; q_c, p_c) := \mathrm{Tr}\Big[\hat{\delta}_c^{(\psi)}(t; q_c, p_c)\hat{A}\Big] \tag{3.1.11}$$

where the superscript is used due to denote state projection. The definition of the centroid force (1.3.37) does not hold any longer since it relied on the separability of the centroid distribution in the momentum and position symbols. When performing CMD calculations then we must use the more general definition of the centroid force as the centroid symbol associated with the force operator. The centroid force will is also uniquely determined by the Hamiltonian and the projection operator. While the linear position and momentum centroid symbols remain the same in the case of state projection, the same cannot be said for the centroid symbols corresponding to operators which are a nonlinear combination of the canonical operators. So, while the force operator may be a function of the position operator in general, the distribution in the state

projected centroid phase will not be constant along the centroid momentum axis. This can cause problems in the case when the state projected centroid density oscillates wildly between areas with positive and negative density, since the force will not be well defined near the crossover region. We also note that in the case of the high temperature limit, $\beta \to 0$, that the state projected QDO becomes

$$\lim_{\beta\to 0} \hat{\delta}_c^{(\psi)}(q_c,p_c) := \frac{\hbar}{2\pi\rho_c^{(\psi)}(q_c,p_c)} \int_{-\infty}^{\infty}\int_{-\infty}^{\infty} d\xi\, d\eta\, e^{i\xi q_c} e^{i\eta p_c} \left[\int_0^1 du\, e^{-(1-u)(i\xi\hat{x}+i\eta\hat{p})} \hat{\mathcal{P}}_\psi e^{-u(i\xi\hat{x}+i\eta\hat{p})}\right] \tag{3.1.12}$$

and so the associated centroid density in this limit is

$$\lim_{\beta\to 0} \rho_c^{(\psi)}(q_c,p_c) = \frac{\hbar}{2\pi}\int_{-\infty}^{\infty}\int_{-\infty}^{\infty} d\xi\, d\eta\, \mathrm{Tr}\left[e^{i\xi\hat{x}+i\eta\hat{p}}\hat{\mathcal{P}}_\psi\right] \tag{3.1.13}$$

We can immediately establish a connection with the Wigner distribution function, defined as

$$W_\psi(q,p) = \frac{1}{\pi\hbar}\int_{-\infty}^{\infty} dy\, \langle q-y|\hat{\mathcal{P}}_\psi|q+y\rangle\, e^{2ipy/\hbar} \tag{3.1.14}$$

$$= \frac{1}{(2\pi\hbar)^2}\int_{-\infty}^{\infty}\int_{-\infty}^{\infty} d\sigma\, d\tau\, e^{-i(\sigma q+\tau p)/\hbar}\mathrm{Tr}\left[e^{i(\sigma\hat{q}+\tau\hat{p})/\hbar}\hat{\mathcal{P}}_\psi\right] \tag{3.1.15}$$

The high temperature centroid distribution and Wigner distribution function are then related as follows

$$\lim_{\beta\to 0} \rho_c^{(\psi)}(q_c,p_c) \equiv 2\pi\hbar W_\psi(q_c,p_c) \tag{3.1.16}$$

## 3.2 Microcanonical correlation functions

Due to the inclusion of the projection operator via a Kubo transform in the QDO, the following state projected centroid correlation function

$$\langle B_c A_c(t)\rangle^{(\psi)} := \frac{1}{Z_\psi}\int_{-\infty}^{\infty}\int_{-\infty}^{\infty}\frac{dq_c\, dp_c}{2\pi\hbar}\rho_c^{(\psi)}(q_c,p_c) B_c^{(\psi)} A_c^{(\psi)}(t) \tag{3.2.1}$$

where $B_c$ is linear in the position and momentum centroid symbols, is no longer related to the single Kubo transformed correlation function, but instead to the double Kubo transform of the microcanonical correlation function.[13] The microcanonical ensemble real time quantum correlation function is defined as

$$\langle \hat{B}\hat{A}(t)\rangle^{(\psi)} := \frac{1}{Z_\psi}\mathrm{Tr}\Big[\hat{\mathcal{P}}_\psi e^{-\beta\hat{H}}\hat{B}\hat{A}(t)\Big] = \frac{1}{Z_\psi}\langle\psi|e^{-\beta\hat{H}}\hat{B}\hat{A}(t)|\psi\rangle \tag{3.2.2}$$

In the case of the double Kubo transform both the stationary operator $\hat{B}$ and the state projection operator $\hat{\mathcal{P}}_\psi$ undergo a Kubo transform

$$\langle \hat{B}\hat{A}(t)\rangle_{(DK)}^{(\psi)} := \frac{1}{Z_\psi}\mathrm{Tr}\left[e^{-\beta\hat{H}}\int_0^1 du\left(\int_u^1 dv\, \hat{B}(-iv\beta\hbar)\hat{\mathcal{P}}_\psi(-iu\beta\hbar) + \int_0^u dv\, \hat{\mathcal{P}}_\psi(-iu\beta\hbar)\hat{B}(-iv\beta\hbar)\right)\hat{A}(t)\right] \tag{3.2.3}$$

$$= \frac{2}{Z_\psi}\mathrm{Tr}\left[e^{-\beta\hat{H}}\int_0^1 du\int_u^1 dv\, \hat{B}(-iv\beta\hbar)\hat{\mathcal{P}}_\psi(-iu\beta\hbar)\hat{A}(t)\right] \tag{3.2.4}$$

[13] Refer to section C.4

For the canonical ensemble it was possible to undo the Kubo transform by transforming to frequency space, multiplying by a common frequency factor, then transforming back to time space. In the case of the double Kubo transform it is not always possible to define a common frequency factor, see section C.5.2 where it is shown to be impossible for projection onto an arbitrary state as the frequency factors are different for each peak in the spectrum and therefore require knowledge of the energy eigenstates. However, it is possible to define a common frequency factor in the case where $\hat{\mathcal{P}}_\psi$ is a sum of projection operators each of which projects onto an eigenstate of the Hamiltonian

$$\hat{\mathcal{P}}_\psi = \sum_n c_n \hat{\mathcal{P}}_n = \sum_n c_n |\chi_n\rangle \langle\chi_n| \tag{3.2.5}$$

The results here therefore generalise the results from [37], where two projection operators were used to project onto the symmetric and antisymmetric energy eigenstates. Working in the basis of the Hamiltonian's eigenfunctions, the relationship between the two Fourier transform correlation functions when the projection operator is of the form (3.2.5) can be shown to be[14]

$$\mathcal{F}\{\langle \hat{B}\hat{A}(t)\rangle^{(\psi)}\}(\omega) = \frac{(\beta\hbar\omega)^2}{2(e^{-\beta\hbar\omega} + \beta\hbar\omega - 1)} \mathcal{F}\{\langle \hat{B}\hat{A}(t)\rangle^{(\psi)}_{(DK)}\}(\omega) \tag{3.2.6}$$

and so the relationship between the correlation functions is

$$\langle \hat{B}\hat{A}(t)\rangle^{(\psi)} = \frac{1}{2\pi}\int_{-\infty}^{\infty} d\omega\, e^{i\omega t} \frac{(\beta\hbar\omega)^2}{2(e^{-\beta\hbar\omega} + \beta\hbar\omega - 1)} \int_{-\infty}^{\infty} dt'\, e^{-i\omega t'} \langle \hat{B}\hat{A}(t')\rangle^{(\psi)}_{(DK)} \tag{3.2.7}$$

However since establishing a physical connection between the double Kubo transformed correlation function, and hence state projected CMD results, and the exact correlation function cannot generally be done without solving the TISE performing state projected CMD is not always useful for determining the dynamics of microcanonical ensembles. We do know however that in the case where the projection operator is the identity operator the double Kubo transform reduces to a single Kubo transform, which can be undone in general as shown in section (C.4.37). Therefore if state projection is performed onto a each individual state from a known complete basis, which are not necessarily the energy eigenstates, the sum of the double Kubo transform correlation functions will give the regular Kubo transform correlation function.

## 3.3 Results

### 3.3.1 Computational setup

The program was written from scratch in C++ using the Armadillo linear algebra library. All operators here are constructed as matrices in the basis of the QHO number eigenstates using normal ordered combinations of the creation and annihilation operators. The eigenvectors of the Hamiltonian in this basis representation are used to construct the state projection operator. The rest of the program is identical in structure to the one described in section 2.4.1 with the exception of the Fourier space function of the centroid symbols, except the operator exponential of the centroid Hamiltonian was traced with the projection operator for the centroid density. In the case of the centroid symbols the Kubo transform had to be performed, so these functions where instead defined on a grid

$$\hat{\mathcal{P}}_\varphi e^{-\beta u \hat{H}'} \hat{A} e^{-\beta(u-1)\hat{H}'} \quad u = k/\kappa,\, k = 0, \ldots, \kappa \tag{3.3.1}$$

[14] Refer to section C.5.1

where $\kappa$ is the grid size of the interval $[0, 1]$. The Kubo transform integral was computed using a Riemann sum, with the grid size chosen to be $\kappa = 50$.

### 3.3.2 Quantum harmonic oscillator

The state projected formalism is first applied to the quantum harmonic oscillator. We will be working in the basis of the QHO eigenstates, called the number eigenstates and denoted by $\{|n\rangle, n \in \mathbb{N}\}$, so it useful to express all operators in terms of the creation and annihilation operators. First recall that the Hamiltonian for the QHO is

$$\hat{H} = \frac{\hat{p}^2}{2m} + \frac{1}{2}m\omega^2\hat{q}^2 \equiv \hbar\omega\left(\hat{a}^\dagger\hat{a} + \frac{1}{2}\right) \tag{3.3.2}$$

where $\hat{a}^\dagger$ is the creation operator and $\hat{a}$ is the annihilation operator. The force operator corresponding to the QHO system is

$$\hat{F} = \frac{i}{\hbar}[m\omega^2\hat{q}^2/2, \hat{p}] = -m\omega^2\hat{q} \tag{3.3.3}$$

and so given that the consistency conditions for the position and momentum operators still hold under the state projection, the associated static force symbol is

$$F_c^{(\psi)} = -m\omega^2 q_c \tag{3.3.4}$$

which is independent of the state we are projecting on to. The equation of motion for $q_c(t)$ can then be determined analytically by solving Hamilton's equation of motion, which will yield

$$q_c(t; q_c, p_c) = q_c\cos(\omega t) + \frac{p_c}{m\omega}\sin(\omega t) \tag{3.3.5}$$

This result is independent of whether we make the CMD assumption or not, and so the QHO is the one case where the exact centroid dynamics and CMD results are equivalent. This is a result of the force operator being proportional to the position operator, which means the corresponding force symbol will be proportional to the centroid position symbol. The CMD approximation usually results in a loss of information about the time evolution of the force symbol since the force symbol loses its explicit time dependence and there are no additional equations of motion included to allow for the time evolution of the centroid symbol. To accurately capture the dynamics of the system one would need another differential equation to accurately capture the time evolution of the force symbol, and another to account for the time evolution of this equation, etcetera. In general this would result in an infinite number of extra differential equations, however since the position symbol has an equation of motion included in the set of Hamilton's equations for the centroid symbols these additional equations of motion are redundant, so we can terminate this hierarchy for the QHO knowing that no information is lost in using CMD. Since the equation of motion for $q_c(t)$ is independent of the state projection, the position autocorrelation function will always be given by

$$\langle q_c q_c(t)\rangle^{(\psi)} = \frac{1}{Z_\psi}\left(\cos(\omega t)\iint\frac{dq_c\,dp_c}{2\pi\hbar}\rho_c^{(\psi)}(q_c, p_c)q_c q_c + \sin(\omega t)\iint\frac{dq_c\,dp_c}{2\pi\hbar}\rho_c^{(\psi)}(q_c, p_c)q_c p_c\right) \tag{3.3.6}$$

so the phase space integrals will only set the amplitude of the correlation function. The state projected centroid densities can also be analytically solved for the QHO system, and we present the results in the case of projection onto a canonical coherent state with eigenvalue $z$[15]

$$\rho_c^{(z)}(q_c,p_c)=\frac{\beta\hbar\omega}{\sinh(\beta\hbar\omega/2)}\frac{1}{1+\alpha}\exp\left(-\frac{2}{1+\alpha}|z|^2\right)\exp\left(-\left(\beta\hbar\omega+\frac{2}{1+\alpha}\right)\left(\frac{m\omega}{2\hbar}q_c^2+\frac{1}{2m\omega\hbar}p_c^2\right)\right)$$
$$\times\exp\left(\frac{2}{1+\alpha}\left(\sqrt{\frac{2m\omega}{\hbar}}\,\mathrm{Re}(z)q_c+\sqrt{\frac{2}{m\omega\hbar}}\,\mathrm{Im}(z)p_c\right)\right) \tag{3.3.7}$$

and also for projection onto an individual QHO eigenstate with quantum number $n$[16]

$$\rho_c^{(n)}(q_c,p_c)=\frac{\beta\hbar\omega}{\sinh(\beta\hbar\omega/2)}\frac{(-1)^n}{1+\alpha}\exp\left[-\left(\beta\hbar\omega+\frac{2}{1+\alpha}\right)|a_c|^2\right]\left(\frac{1-\alpha}{1+\alpha}\right)^n L_n\left(\frac{4}{1-\alpha^2}|a_c|^2\right) \tag{3.3.8}$$

A selection of eigenstate projected centroid densities are presented in Fig. 3.2 for the parameters $\hbar=1$, $m=1$, and $\omega=1$. It is noted that the functions are entirely even in $q_c$ and $p_c$, and from this it can be deduced that the second integral in (3.3.7) will evaluate to zero as both $q_c$ and $p_c$ are odd functions. Equation (3.3.6) can then be simplified to

$$\langle q_c q_c(t)\rangle^{(\psi)}=\cos(\omega t)\frac{1}{Z_\psi}\iint\frac{dq_c\,dp_c}{2\pi\hbar}\rho_c^{(\psi)}(q_c,p_c)q_c q_c \tag{3.3.9}$$

So for our chosen parameters we expect the answer to be a cosine with period $2\pi$. CMD calculations were performed for a total time of $t=20$ with a time step of $\Delta t=0.1$ and the results are presented in Fig. 3.3 along with the results using exact quantum dynamics, and as expected the CMD results are identical.

### 3.3.3 Quartic well

We next consider a Hamiltonian with only a quartic anharmonic potential term

$$\hat{H}=\frac{\hat{p}^2}{2m}+d_4\hat{q}^4 \tag{3.3.10}$$

The force operator for the quartic well is then of the form

$$\hat{F}=\frac{i}{\hbar}d_4[\hat{q}^4,\hat{p}]=-4d_4\hat{q}^3=-4d_4\left(\frac{\hbar}{2m\omega}\right)^{3/2}(a+a^\dagger)^3 \tag{3.3.11}$$

The state projected centroid densities for the lowest three eigenenergies are shown in Fig. 3.4, where we selected the parameter values $\hbar=1$, $m=1$, $\omega=1$ and $d_4=1/4$ and the temperatures $\beta=1,8$ in order to match those from [37]. The centroid densities are no longer symmetric under rotation in $q_c-p_c$ plane as was the case in with the QHO, though this is difficult to discern from the plots since the anharmonic term is weak. CMD calculations were performed next with a time step of $\Delta t=0.0025$ and a total time of $t=40$ for $\beta=1$ and $t=100$ for $\beta=8$ and the results shown in Fig. 3.5. We can see that the $\beta=1$ correlation functions show better matching for the phase and amplitude in the case of projection onto higher energy eigenstates with some slight

[15] Refer to section C.1
[16] Refer to section C.2

drifting from the exact results, though the results are very quick to decorrelate. The $\beta = 8$ CMD results are a poorer approximation to the exact results for higher energy eigenstates. The CMD results for the ground state match the exact phase for roughly 5 oscillations as seen in Fig. 3.5b while the CMD results for the first excited state results only match for about 3 oscillations, see Fig. 3.5d. The results for the second excited state at $\beta = 8$ are included in Fig. 3.5f despite the presence of numerical errors which proved to be very persistent. Although not noticeable, the time zero value for the CMD results is exact, but the individual trajectories proved to be unstable even at a very short time step.

### 3.3.4 Double well

The final system under consideration is the double well, which has the Hamiltonian

$$\hat{H} = \frac{\hat{p}^2}{2m} + d_2\hat{q}^2 + d_4\hat{q}^4 \tag{3.3.12}$$

and associated force operator

$$\hat{F} = \frac{i}{\hbar}[d_2\hat{q}^2 + d_4\hat{q}^4, \hat{p}] = -2d_2\hat{q} - 4d_4\hat{q}^3 = -2d_2\sqrt{\frac{\hbar}{2m\omega}}(a+a^\dagger) - 4d_4\left(\frac{\hbar}{2m\omega}\right)^{3/2}(a+a^\dagger)^3 \tag{3.3.13}$$

For the numerical computations we again selected parameter values from [37], which correspond to $\hbar = 1$, $m = 1$, $\omega = 1$, $d_2 = -1/2$ and $d_4 = 1/10$. The state projected centroid densities are presented for the lowest three energy eigenstates at $\beta = 1, 8$ in Fig. 3.6. CMD calculations were performed with a time step of $\Delta t = 0.0025$ for a total time of $t = 40$ for $\beta = 1$ and $t = 100$ for $\beta = 8$ and the results are displayed in Fig. 3.7. In the case of the $\beta = 1$ results we can see the results becoming progressively better for higher energy eigenstates, however the results still fail to match the exact results to the first local minimum and as such are very poor though this is expected for the double well. The results for $\beta = 8$ are reversed like the quartic well system, with the ground state CMD results matching the exact results better than the first excited state. The results in Fig. 3.7f are again a result of instability in the CMD trajectories which would not disappear, and so cannot be analyzed further. It was expected that the energy levels above the central maximum in the double well would perform better since tunneling would not occur, though it is unclear why this would not be the case at lower temperatures.

In an attempt to better understand the effect of the two wells on the centroid dynamics we also show the time evolution of the centroid distribution $\rho_c^{(1)}(q_c, p_c) \cdot q_c(t; q_c, p_c)$ for $\beta = 1$ using exact centroid dynamics and CMD in Figs. 3.8 and 3.9. The $q_c$ axis is on the horizontal and the $p_c$ axis is along the vertical. The ranges for each axis are $q_c \in [2.5, 2.5]$ and $p_c \in [1.5, 1.5]$. Since we do not expect the centroid trajectories to cross the point where the density become zero we can deduce from Fig. 3.6c that there are two regions of motion here, one in the centre of the plane where the density is negative and everywhere outside this region where the density is positive. The times shown span $t = 0$ to $t = 20$ which is almost the period of one oscillation in the exact results, see Fig. 3.3c. We first note that the minima of the double well are located at $\pm\sqrt{5/2}$. The centroid density is greater than zero for $q_c = \pm\sqrt{5/2}$, and we see initially in the $t = 0$ densities in Fig. 3.8 that the bulk of the density in this region is just slightly offset from this position. As time progresses, the exact centroid trajectories never cross the $\rho_c^{(1)}(q_c, p_c) = 0$ boundary resulting in two regions of motion. Generally speaking, in the exact results we see the two blobs of positive and negative density swirling counter-clockwise about the origin of the phase space. The same

behaviour is also present in the CMD plots, but we can see in the CMD densities in Figs. 3.8 and 3.9 that a well is also present which traps some of the trajectories. As time progresses these trajectories move around in this well while the rest rotate counter-clockwise about the origin. This well in the phase space is very nearly centered at $p_c = 0$ and $q_c = \pm\sqrt{5/2}$, indicating that this is a lingering effect of the double wells. For this system the energy of the first excited eigenstate is slightly above the hump in the middle of the potential so the poor performance of the CMD simulation is not due to tunneling by the first excited eigenstate.

Lastly, we combined the energy eigenstate projected CMD position autocorrelation functions to obtain an approximate of the Kubo transformed position autocorrelation function. Results are shown for $\beta = 1, 8$ in Fig. 3.1 where we also show the results obtained using exact quantum dynamics, regular CMD and symmetry-adapted CMD (SA-CMD). SA-CMD was introduced in [37], and as previously stated involved projecting onto the symmetric and antisymmetric eigenstates

$$\mathcal{P}_S = \frac{1}{Z_S} \sum_{n \text{ even}} |\chi_n\rangle \langle\chi_n| \qquad \mathcal{P}_A = \frac{1}{Z_A} \sum_{n \text{ odd}} |\chi_n\rangle \langle\chi_n| \tag{3.3.14}$$

and then recombining the results

$$\langle q_c q_c(t)\rangle^{(SA)} = \frac{Z_S}{Z}\langle q_c q_c(t)\rangle^{(S)} + \frac{Z_A}{Z}\langle q_c q_c(t)\rangle^{(A)} \tag{3.3.15}$$

Here we also recombine the state-projected CMD (SP-CMD) results as follows

$$\langle q_c q_c(t)\rangle^{(SP)} = \sum_n \frac{Z_n}{Z}\langle q_c q_c(t)\rangle^{(n)} \tag{3.3.16}$$

For the $\beta = 1$ case the double Kubo transformed autocorrelation functions for the lowest ten eigenstates are used, and for the $\beta = 8$ case we recombined the results for the the lowest four eigenstates. As can be seen, the SA-CMD results are slightly better than those from regular CMD but they still fail to match the exact result to the first local minimum in both cases. The SP-CMD results are a bit better and do match the exact results to the first minimum in the $\beta = 1$ results before failing, which is unexpected given the generally poor results seen in Fig. 3.7. The $\beta = 8$ SP-CMD results are very slightly better than that SA-CMD results, and it is expected that the two will converge in the low temperature limit where the entire population is in the ground state.

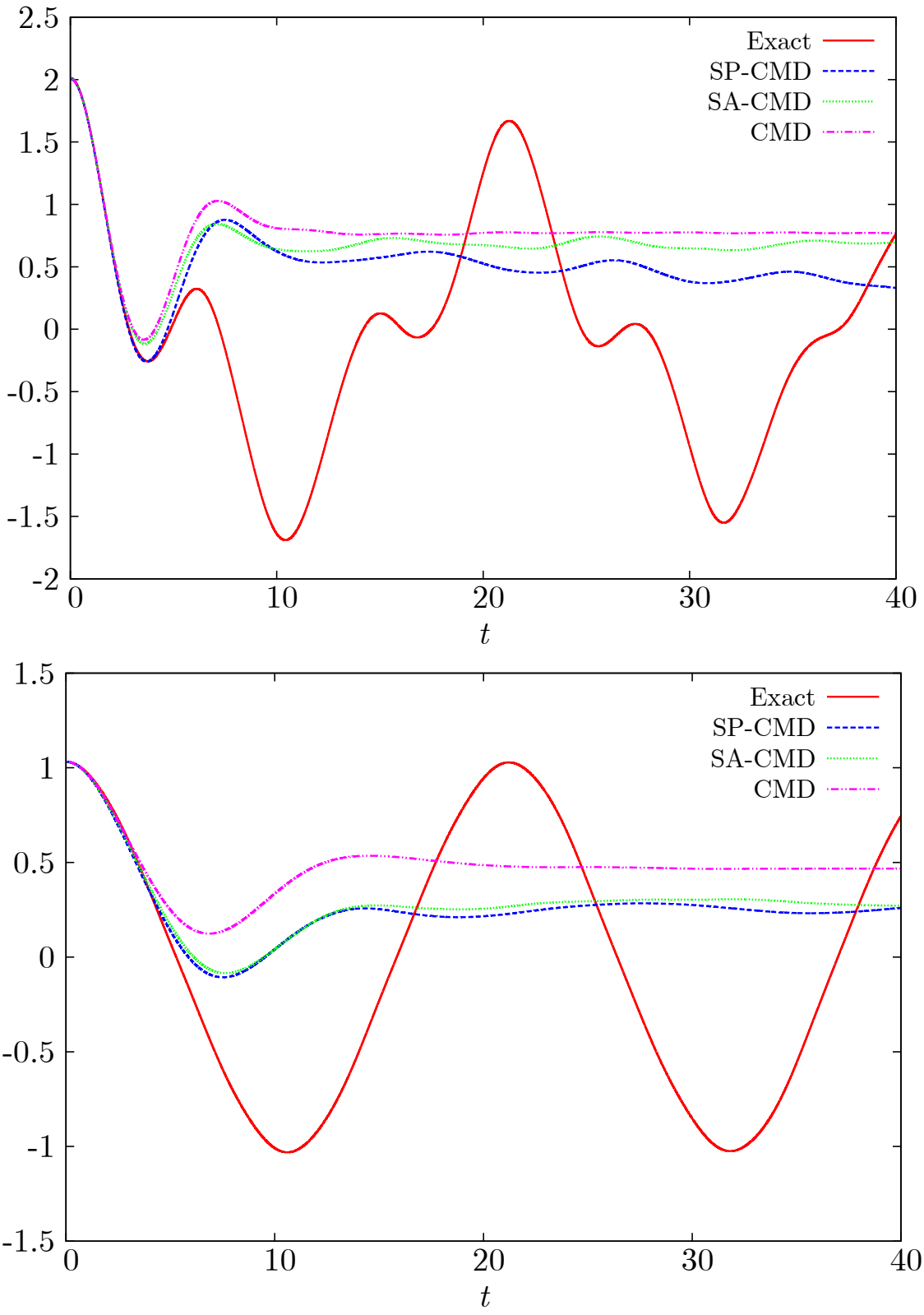


Figure 3.1: Comparison of the Kubo transformed position autocorrelation function as computed using exact quantum dynamics, CMD, symmetry-adapted CMD (SA-CMD) and state-projected CMD (SP-CMD) for the double well system with $\beta = 1$ at top and $\beta = 8$ below.

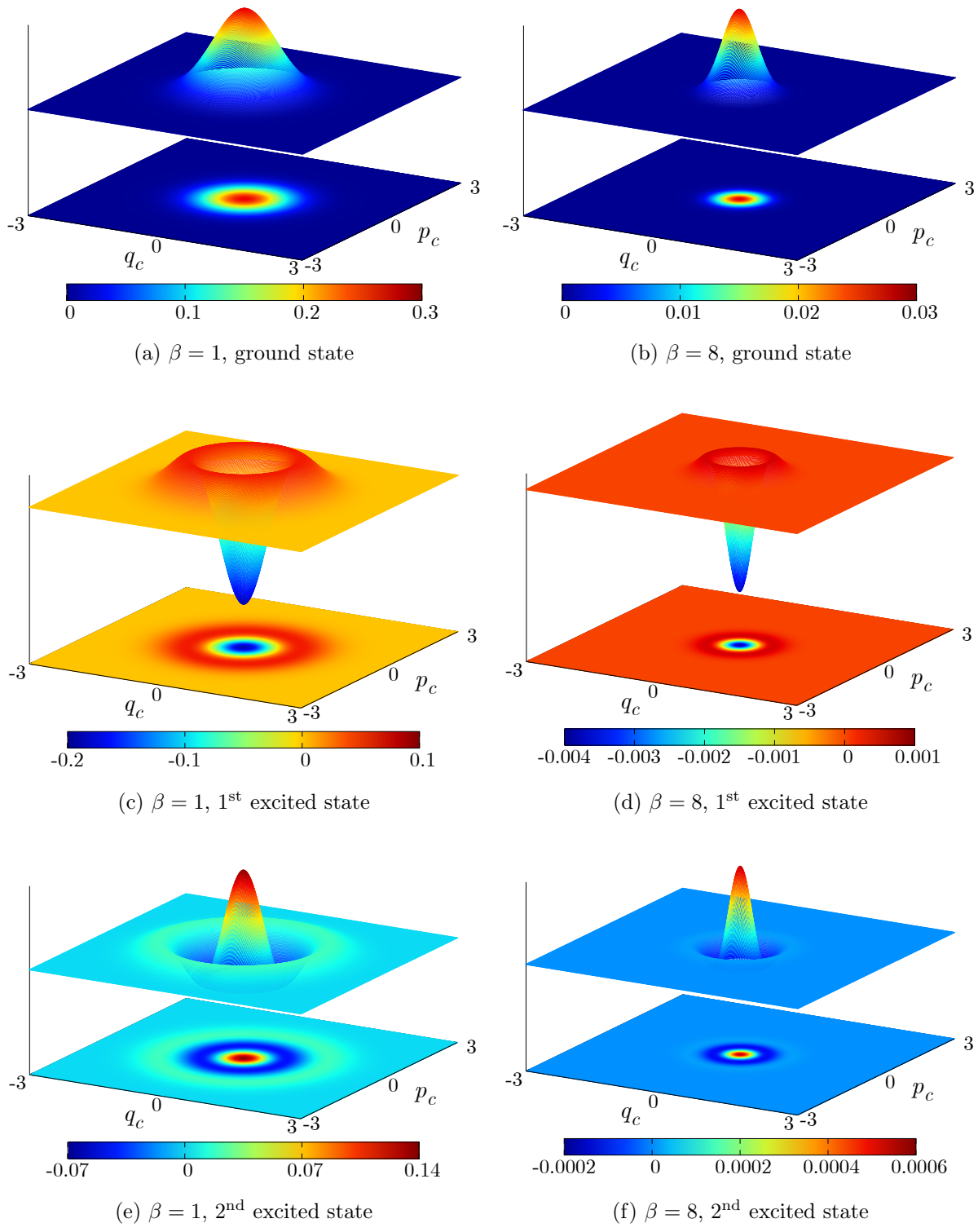


(a) $\beta = 1$, ground state

(b) $\beta = 8$, ground state

(c) $\beta = 1$, 1st excited state

(d) $\beta = 8$, 1st excited state

(e) $\beta = 1$, 2nd excited state

(f) $\beta = 8$, 2nd excited state

Figure 3.2: State projected centroid densities for the quantum harmonic oscillator with temperatures $\beta = 1, 8$ for the three lowest energy eigenstates

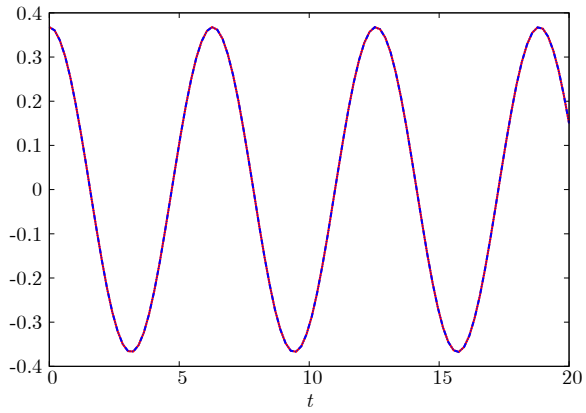


(a) $\beta = 1$, ground state

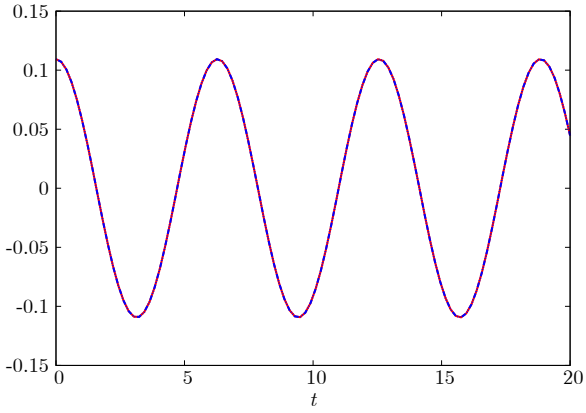


(b) $\beta = 8$, ground state

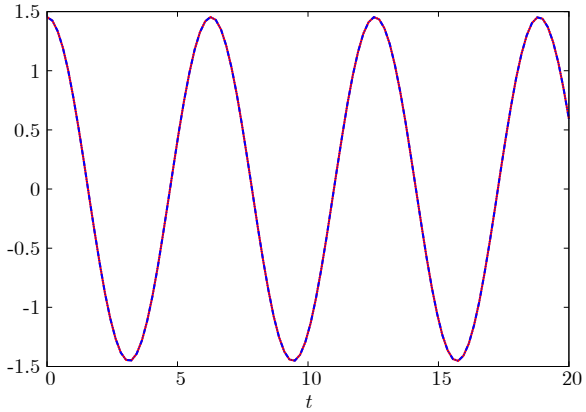


(c) $\beta = 1$, $1^{\text{st}}$ excited state

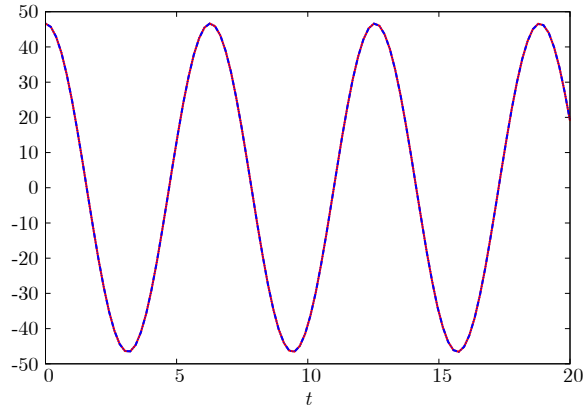


(d) $\beta = 8$, $1^{\text{st}}$ excited state

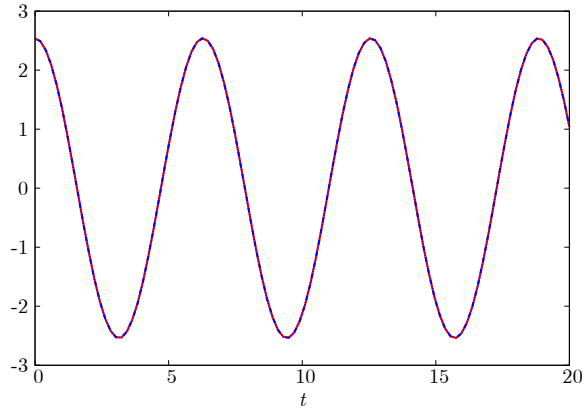


(e) $\beta = 1$, $2^{\text{nd}}$ excited state

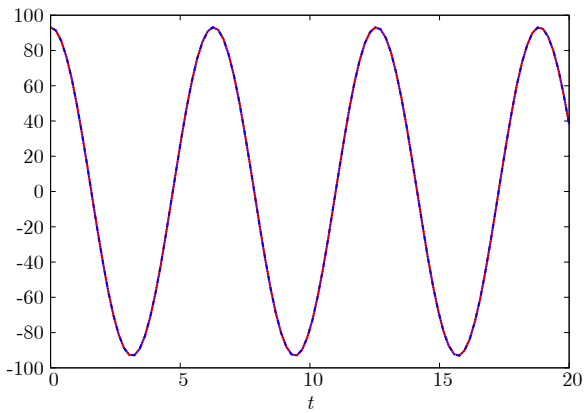


(f) $\beta = 8$, $2^{\text{nd}}$ excited state

Figure 3.3: Double Kubo transformed state projected position autocorrelation functions calculated using exact quantum dynamics (red) and CMD (blue) for the temperatures $\beta = 1, 8$ and the three lowest energy eigenstates of the quantum harmonic oscillator

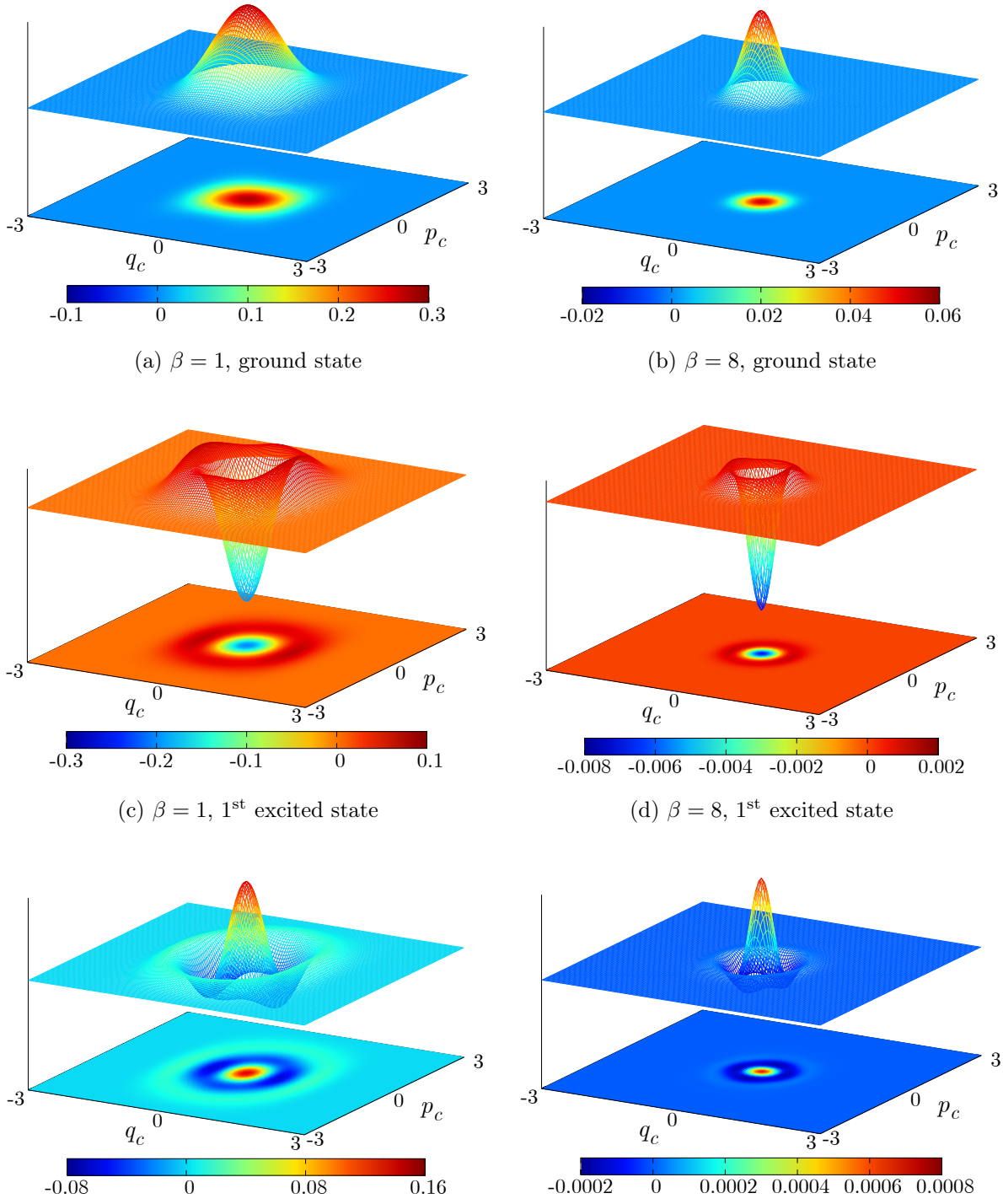


(a) $\beta = 1$, ground state

(b) $\beta = 8$, ground state

(c) $\beta = 1$, 1st excited state

(d) $\beta = 8$, 1st excited state

(e) $\beta = 1$, 2nd excited state

(f) $\beta = 8$, 2nd excited state

Figure 3.4: State projected centroid densities for the quartic well system with temperatures $\beta = 1, 8$ for the three lowest energy eigenstates

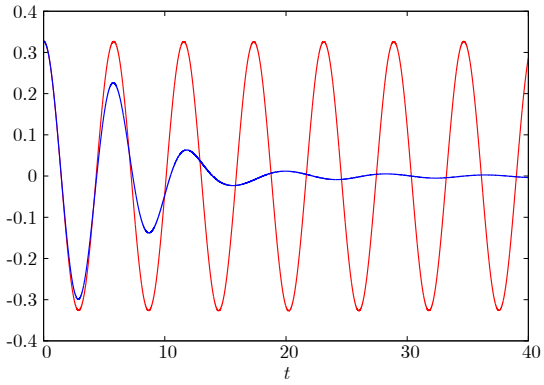


(a) $\beta = 1$, ground state

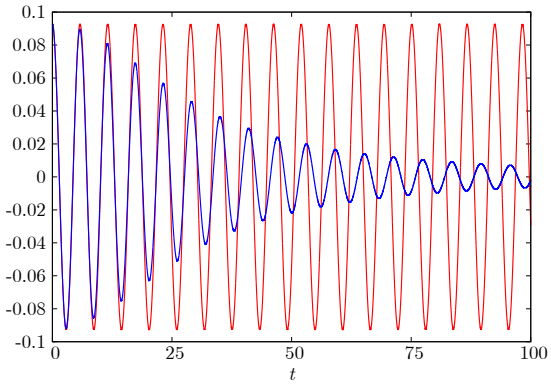


(b) $\beta = 8$, ground state

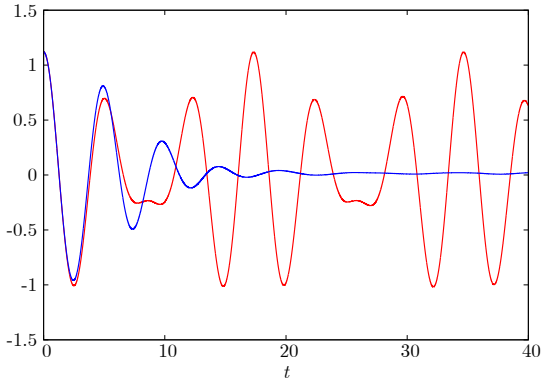


(c) $\beta = 1$, $1^{\text{st}}$ excited state

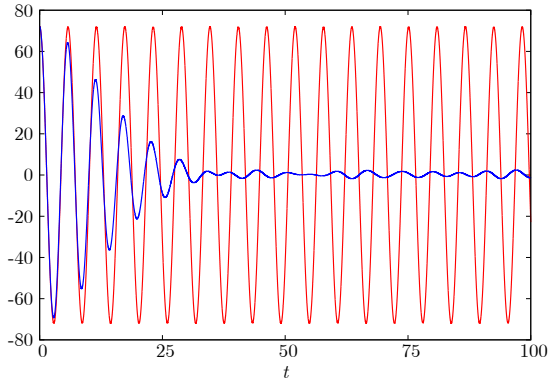


(d) $\beta = 8$, $1^{\text{st}}$ excited state

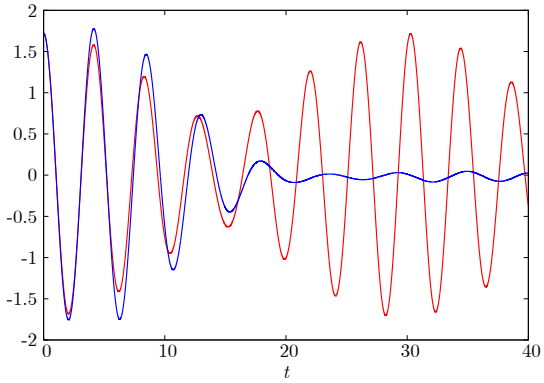


(e) $\beta = 1$, $2^{\text{nd}}$ excited state

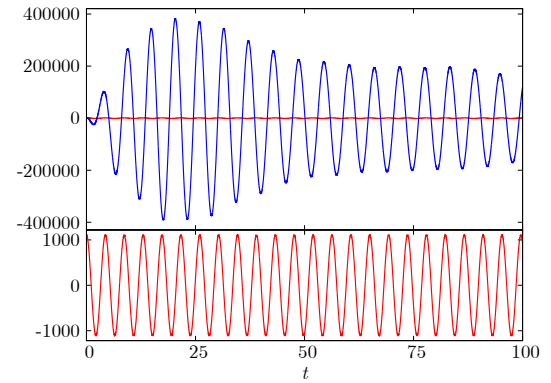


(f) $\beta = 8$, $2^{\text{nd}}$ excited state

Figure 3.5: Double Kubo transformed state projected position autocorrelation functions calculated using exact quantum dynamics (red) and CMD (blue) for the temperatures $\beta = 1, 8$ and the three lowest energy eigenstates of the quartic well system

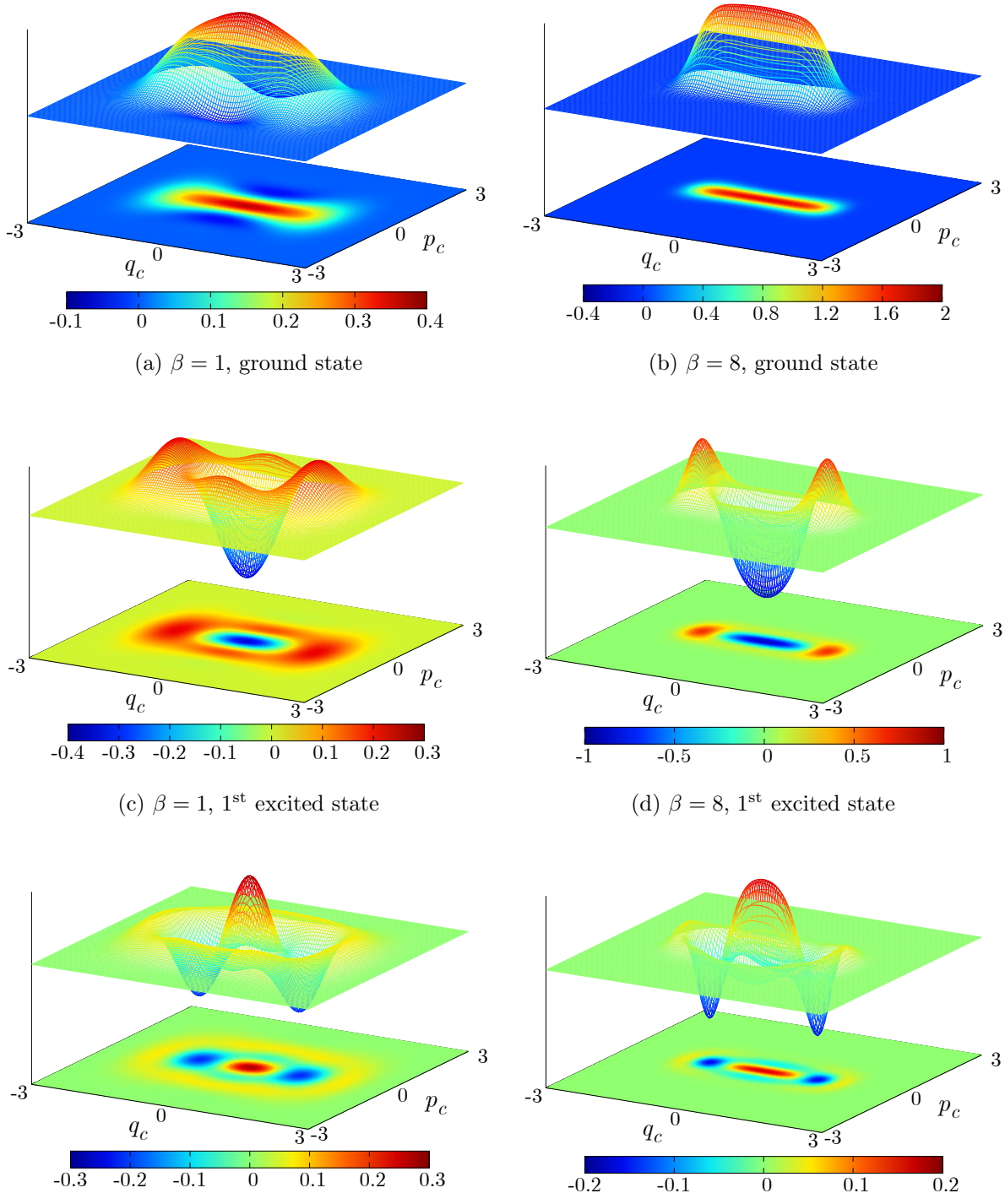


(a) $\beta = 1$, ground state

(b) $\beta = 8$, ground state

(c) $\beta = 1$, 1st excited state

(d) $\beta = 8$, 1st excited state

(e) $\beta = 1$, 2nd excited state

(f) $\beta = 8$, 2nd excited state

Figure 3.6: State projected centroid densities for the double well system with temperatures $\beta = 1, 8$ for the three lowest energy eigenstates

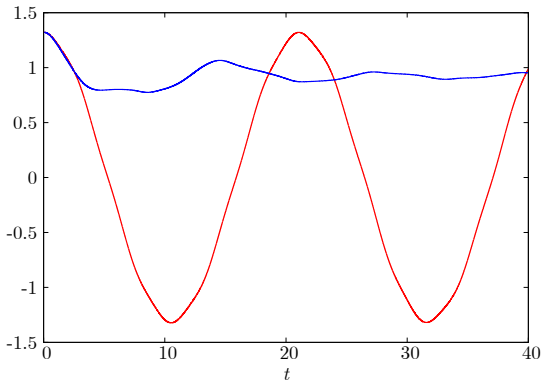


(a) $\beta = 1$, ground state

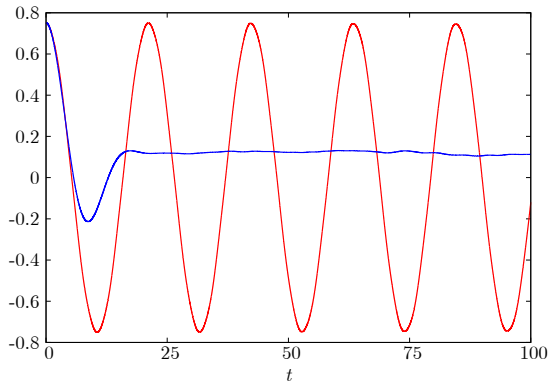


(b) $\beta = 8$, ground state

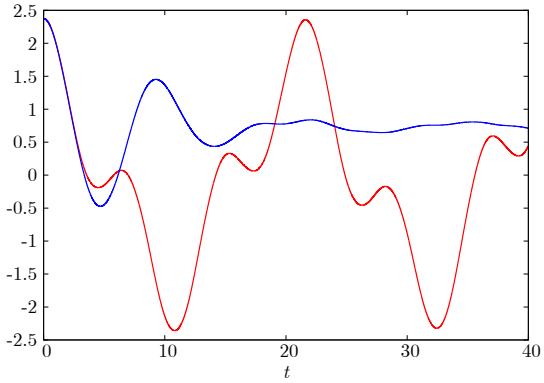


(c) $\beta = 1$, $1^{\text{st}}$ excited state

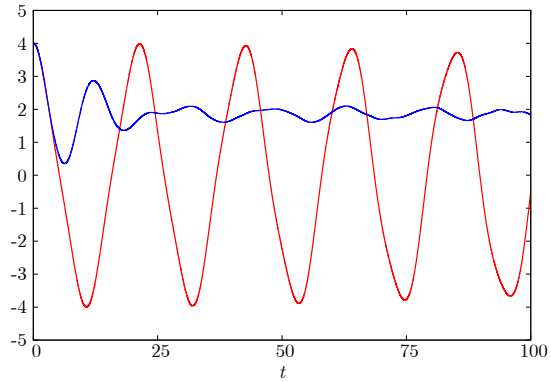


(d) $\beta = 8$, $1^{\text{st}}$ excited state

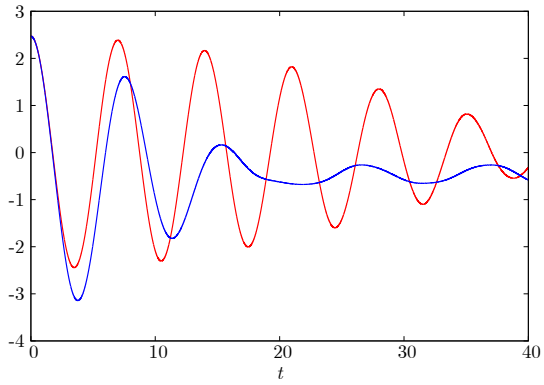


(e) $\beta = 1$, $2^{\text{nd}}$ excited state

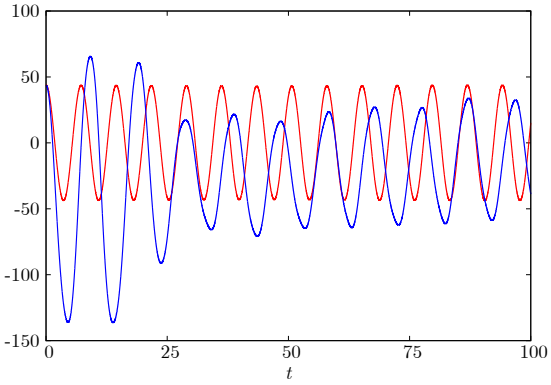


(f) $\beta = 8$, $2^{\text{nd}}$ excited state

Figure 3.7: Double Kubo transformed state projected position autocorrelation functions calculated using exact quantum dynamics (red) and CMD (blue) for the temperatures $\beta = 1, 8$ and the three lowest energy eigenstates of the double well system

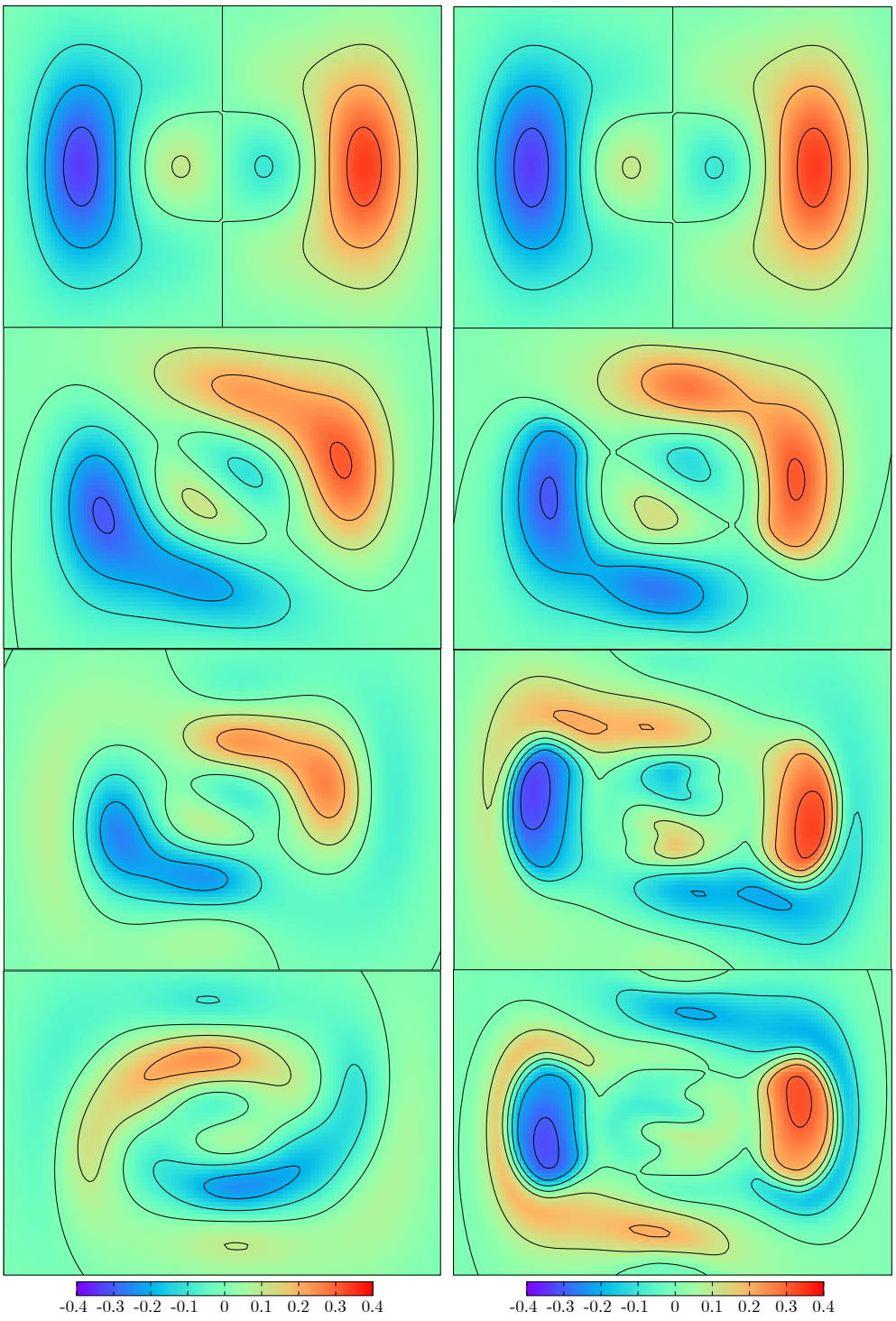


Figure 3.8: Time evolution of $\rho_c(q_c, p_c)q_c(t)$ using exact centroid dynamics (left column) and CMD (right column) at times $t = 0, 2, 4, 6$ (figures are in descending order) for the double well system

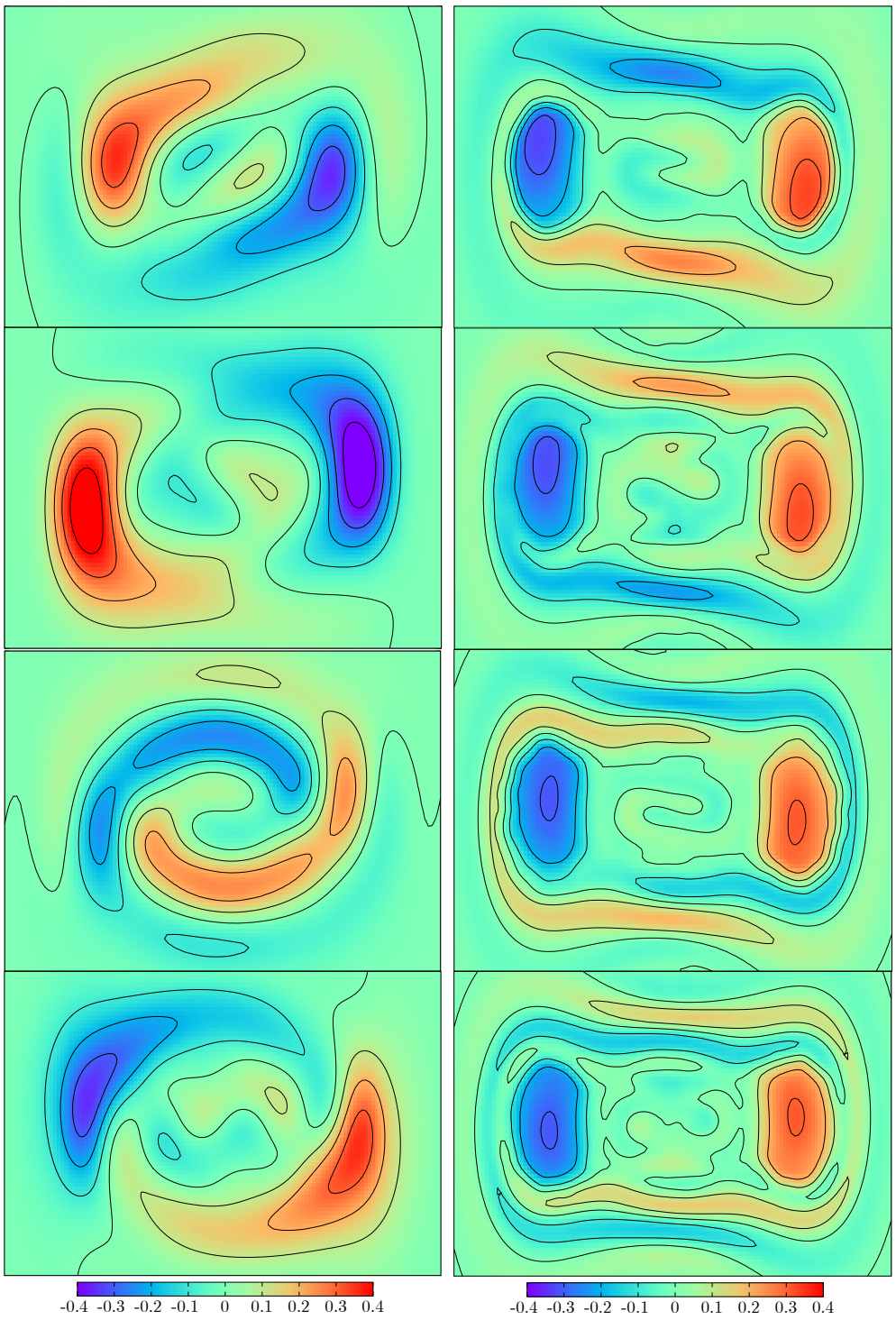


Figure 3.9: Time evolution of $\rho_c(q_c, p_c)q_c(t)$ using exact centroid dynamics (left column) and CMD (right column) at times $t = 8, 12, 16, 20$ (figures are in in descending order) for the double well system.

# Chapter 4

# Conclusions

In chapter 2 a general method was devised to formulate centroid statistical mechanics for systems undergoing rotational and torsional motion using the theory of constraints initially laid out by Dirac. This was worked out in detail motion on any n-dimensional ellipsoid with an arbitrary position dependent potential. The case of a particle moving on a ring was used as a test, and centroid densities were generated for the case of free motion as well as motion in the presence of periodic potentials. These centroid densities were not separable in the each of the centroid coordinates, as is the case for centroid densities of systems in Euclidean space. The CMD results for the free particle case gave a dipole autocorrelation function which showed closer agreement with the classical autocorrelation function at higher temperatures. Limits were worked out to show that the high temperature classical limit of the dipole autocorrelation function does not have the recurrences as are expected with the high temperature limit quantum results, as seen in section B.4. As temperature was decreased the results better matched the expected quantum Kubo transformed autocorrelation function, but still decorrelated rapidly and quickly drifted out of phase with the exact result. The CMD results for the hindered rotor models were not given due to numerical instability of the $x_c(t)$ trajectories, and therefore as of now only equilibrium properties can be successfully computed.

In chapter 3 we extended the used of projection operators in the centroid formalism to the case of state projection. We saw that in the case of state projection the centroid density is no longer positive definite and is again not separable in the position and momentum coordinates. Analytic results were obtained for the QHO, which demonstrated that the CMD results are again exact for this system. Equilibrium and dynamical properties were also obtained for the quartic well and double well systems. The recombined correlation functions for the double well showed improvement over the CMD and SA-CMD results. It was also shown that it is in general not possible to undo a double Kubo transformed time correlation function without prior knowledge of the eigenenergies to modify the height of the peaks in the Fourier transform spectrum.

## 4.1 Future work

The initial attempts at computing time correlation functions for the hindered rotor model were not successful due to numerical instabilities in the CMD trajectories. Obtaining useable results will necessitate use of an improved integrator along with a finer grid force field. The case of a hindered rotor with a highly confining potential is another matter, since it is difficult to obtain a grid fine

enough to accurately represent the highly localized centroid density. We will therefore tackle this case by approximating the centroid density for highly confined systems as a one dimensional Euclidean centroid density since the position and momentum densities are effectively squeezed in one direction. Once this work has been completed we hope to perform CMD calculations for multiple interacting rotors. We also note that motion on a circle is identical to motion of a particle in a one-dimensional Euclidean space with periodic boundary conditions, and so we hope to extend the CMD method to optical lattices. The next step is to move to higher dimensions, and here the first step is to test the centroid formalism for motion of a particle on a sphere. Significant optimizations will need to be made for the storage of the centroid densities, since the memory demands for higher dimensional objects will grow exponentially with each additional pair of position-momentum centroid variables. The motion of the rotating tops is the final goal, but at this stage the map between the Euler angles and the hyperspherical angles has not be constructed.

A new integrator must also be implemented for the state projected CMD calculations given the instability seen in some of the autocorrelation functions. We also wish to perform simulations with increased degrees of freedom which includes particles moving in a multidimensional Cartesian space and collections of coupled systems. We also wish to connect this work with current methods for computing low temperature and ground state dynamics.

# Appendix A

# Introductory Material

## A.1 Consistency equations for centroid symbols

Here we wish to show that the associated centroid phase space distributions for the position and momentum operators, $\hat{q}$ and $\hat{p}$, are $q_c$ and $p_c$, respectively. We will show this in general for the centroid distribution of an arbitrary operator $\hat{A}$

$$\rho_c(A_c) = \mathrm{Tr}\left[\int_{-\infty}^{\infty} \frac{d\xi}{\sqrt{2\pi}} e^{-\beta\hat{H}+i\xi\hat{A}} e^{-i\xi A_c}\right] \tag{A.1.1}$$

The goal then is to show that the following consistency equation holds

$$A_c = \frac{1}{\rho_c(A_c)} \mathrm{Tr}\left[\int_{-\infty}^{\infty} \frac{d\xi}{\sqrt{2\pi}} e^{-\beta\hat{H}+i\xi\hat{A}} e^{-i\xi A_c} \hat{A}\right] \tag{A.1.2}$$

The addition of other centroid constraints will not affect this derivation, so the results are easily generalized. This derivation depends on the application of the product rule and the cyclic property of the trace. We begin by writing

$$\begin{aligned} &\int_{-\infty}^{\infty} \frac{d\xi}{\sqrt{2\pi}} \left(\frac{\partial}{\partial\xi} e^{-i\xi A_c}\right) \mathrm{Tr}\left[e^{-\beta\hat{H}+i\xi\hat{A}}\right] + \int_{-\infty}^{\infty} \frac{d\xi}{\sqrt{2\pi}} e^{-i\xi A_c} \left(\frac{\partial}{\partial\xi} \mathrm{Tr}\left[e^{-\beta\hat{H}+i\xi\hat{A}}\right]\right) \\ &= \lim_{z\to\infty} \frac{1}{\sqrt{2\pi}} e^{-i\xi A_c} \mathrm{Tr}\left[e^{-\beta\hat{H}+i\xi\hat{A}}\right] \Big|_{\xi=-z}^{z} \end{aligned} \tag{A.1.3}$$

The centroid is assumed to be an entirely real and even function of $A_c$, implying that trace of the exponential of the effective centroid Hamiltonian is also a real and even function of $\xi$. Further assuming that it is Fourier integrable implies that the function decays to zero in the $\xi \to \pm\infty$ limit, so that the left hand side of (A.1.3) is independent of the undefined behaviour of $e^{-i\xi A_c}$ at the boundaries and goes to zero in both limits. We are aware that this argument is not rigourous but the analysis required is beyond the scope of this thesis. Moving on, we must now solve both sides of

$$\int_{-\infty}^{\infty} \frac{d\xi}{\sqrt{2\pi}} \left(\frac{\partial}{\partial\xi} e^{-i\xi A_c}\right) \mathrm{Tr}\left[e^{-\beta\hat{H}+i\xi\hat{A}}\right] = -\int_{-\infty}^{\infty} \frac{d\xi}{\sqrt{2\pi}} e^{-i\xi A_c} \mathrm{Tr}\left[\frac{\partial}{\partial\xi} e^{-\beta\hat{H}+i\xi\hat{A}}\right] \tag{A.1.4}$$

We first solve the left hand side

$$\int_{-\infty}^{\infty} \frac{d\xi}{\sqrt{2\pi}} \left(\frac{\partial}{\partial\xi} e^{-i\xi A_c}\right) \mathrm{Tr}\left[e^{-\beta\hat{H}+i\xi\hat{A}}\right] = -iA_c \int_{-\infty}^{\infty} \frac{d\xi}{\sqrt{2\pi}} e^{-i\xi A_c} \mathrm{Tr}\left[e^{-\beta\hat{H}+i\xi\hat{A}}\right] = -iA_c\rho_c(A_c) \tag{A.1.5}$$

We can evaluate the right hand side using the following operator derivative identity [38] to evaluate the derivative within the trace

$$\frac{\partial}{\partial\lambda}e^{-\hat{L}} = -\int_0^1 e^{-(1-u)\hat{L}}\,\frac{\partial\hat{L}}{\partial\lambda}\,e^{-u\hat{L}}du \tag{A.1.6}$$

Using the cyclic property of the trace this expression can be simplified

$$\mathrm{Tr}\left[\frac{\partial}{\partial\lambda}e^{-\hat{L}}\right] = -\mathrm{Tr}\left[\int_0^1 e^{-(1-u)\hat{L}}\,\frac{\partial\hat{L}}{\partial\lambda}\,e^{-u\hat{L}}du\right] = -\mathrm{Tr}\left[\int_0^1 e^{-\hat{L}}\,\frac{\partial\hat{L}}{\partial\lambda}du\right] = -\mathrm{Tr}\left[e^{-\hat{L}}\frac{\partial\hat{L}}{\partial\lambda}\right] \tag{A.1.7}$$

The right hand side is then

$$-\int_{-\infty}^{\infty}\frac{d\xi}{\sqrt{2\pi}}e^{-i\xi A_c}\mathrm{Tr}\left[\frac{\partial}{\partial\xi}e^{-\beta\hat{H}+i\xi\hat{A}}\right] = \int_{-\infty}^{\infty}\frac{d\xi}{\sqrt{2\pi}}e^{-i\xi A_c}\mathrm{Tr}\left[e^{-\beta\hat{H}+i\xi\hat{A}}\frac{\partial}{\partial\xi}\left(-\beta\hat{H}+i\xi\hat{A}\right)\right] \tag{A.1.8}$$

$$= i\int_{-\infty}^{\infty}\frac{d\xi}{\sqrt{2\pi}}e^{-i\xi A_c}\mathrm{Tr}\left[e^{-\beta\hat{H}+i\xi\hat{A}}\hat{A}\right] \tag{A.1.9}$$

The final result is then

$$-iA_c\rho_c(A_c) = i\int_{-\infty}^{\infty}\frac{d\xi}{\sqrt{2\pi}}e^{-i\xi A_c}\mathrm{Tr}\left[e^{-\beta\hat{H}+i\xi\hat{A}}\hat{A}\right] \tag{A.1.10}$$

$$A_c = \frac{1}{\rho_c(A_c)}\int_{-\infty}^{\infty}\frac{d\xi}{\sqrt{2\pi}}e^{-i\xi A_c}\mathrm{Tr}\left[e^{-\beta\hat{H}+i\xi\hat{A}}\hat{A}\right] \tag{A.1.11}$$

and thus the consistency equation holds. It follows that the centroid distributions for the operators $\hat{q}$ and $\hat{p}$ are $q_c$ and $p_c$, respectively.

## A.2 Kubo transformed correlation functions

The following derivation only holds for operators which are a linear function of $\hat{q}$ and $\hat{p}$, i.e. $\hat{B} = B_0\hat{I} + B_1\hat{q} + B_2\hat{p}$, which will by definition have the centroid symbol $B_c = B_0 + B_1q_c + B_2p_c$. Since we are generally interested in correlation functions involving the position or velocity this restriction is not limiting. The correlation function for two centroid symbols is then

$$\langle B_cA_c(t;q_c,p_c)\rangle = \frac{1}{Z}\int_{-\infty}^{\infty}\frac{dq_c\,dp_c}{2\pi\hbar}\rho_c(q_c,p_c)B_cA_c(t;q_c,p_c) \tag{A.2.1}$$

$$= \frac{1}{Z}\int_{-\infty}^{\infty}\frac{dq_cdp_c}{2\pi\hbar}B_c\int_{-\infty}^{\infty}\frac{d\xi\,d\eta}{2\pi}e^{-i\xi q_c}e^{-i\eta p_c}\mathrm{Tr}\left[e^{-\beta\hat{H}'}e^{it\hat{H}/\hbar}\hat{A}e^{-it\hat{H}/\hbar}\right] \tag{A.2.2}$$

For the $B_0$ term, the integrals over $q_c$ and $p_c$ can be immediately performed to yield delta functions $\sqrt{2\pi}\delta(\xi)$ and $\sqrt{2\pi}\delta(\eta)$, respectively. Performing the integrals over $\xi$ and $\eta$ reduces the centroid Hamiltonian to the system Hamiltonian, $\hat{H}' \to \hat{H}$. We therefore have

$$\frac{1}{Z}\int_{-\infty}^{\infty}\frac{dq_c\,dp_c}{2\pi\hbar}\,B_0\int_{-\infty}^{\infty}\hbar\frac{d\xi\,d\eta}{2\pi}e^{-i\xi q_c}e^{-i\eta p_c}\,\mathrm{Tr}\left[e^{-\beta\hat{H}'}e^{it\hat{H}/\hbar}\hat{A}e^{-it\hat{H}/\hbar}\right] \tag{A.2.3}$$

$$=\frac{1}{Z}B_0\int_{-\infty}^{\infty}\frac{d\xi\,d\eta}{2\pi}\delta(\xi)\delta(\eta)\mathrm{Tr}\left[e^{-\beta\hat{H}'}e^{it\hat{H}/\hbar}\hat{A}e^{-it\hat{H}/\hbar}\right] \tag{A.2.4}$$

$$=\frac{1}{Z}B_0\mathrm{Tr}\left[e^{-\beta\hat{H}}\hat{A}(t)\right] \tag{A.2.5}$$

The result here is the correlation function between the identity operator and the operator $\hat{A}(t)$. Next, for the $q_c$ term we can perform the integral over $p_c$, which will be replaced by the delta function $\sqrt{2\pi}\delta(\eta)$. The integral over $\eta$ is then performed, the result being that the centroid Hamiltonian is simplified to only include the $\xi$ term. We must then evaluate

$$\langle q_c A_c(t; q_c, p_c)\rangle = \frac{1}{Z}\int_{-\infty}^{\infty} \frac{dq_c\, d\xi}{2\pi}\, e^{-i\xi q_c} q_c \,\mathrm{Tr}\Big[e^{-\beta\hat{H}+i\xi\hat{q}}\hat{A}(t)\Big] \tag{A.2.6}$$

We now use the following Fourier transform property

$$\int_{-\infty}^{\infty} x^n e^{-i\omega x}\frac{dx}{\sqrt{2\pi}} = \sqrt{2\pi} i^n \delta^{(n)}(\omega) \tag{A.2.7}$$

and the following property of the distributional derivative of the delta function

$$\int_{-\infty}^{\infty}\delta'(x)f(x)dx = -\int_{-\infty}^{\infty}\delta(x)f'(x)dx \tag{A.2.8}$$

to evaluate the two integrals. The correlation function can now be written

$$\langle q_c A_c(t; q_c, p_c)\rangle = -\frac{i}{Z}\int_{-\infty}^{\infty}\frac{d\xi}{\sqrt{2\pi}}\delta(\xi)\mathrm{Tr}\left[\left(\frac{\partial}{\partial\xi}e^{-\beta\hat{H}+i\xi\hat{q}}\right)\hat{A}(t)\right] \tag{A.2.9}$$

We now make use of equation (A.1.6) to evaluate the derivative

$$\langle q_c A_c(t; q_c, p_c)\rangle = \frac{i}{Z}\int_{-\infty}^{\infty}\frac{d\xi}{\sqrt{2\pi}}\delta(\xi)\mathrm{Tr}\left[\int_0^1 du e^{-(1-u)(\beta\hat{H}-i\xi\hat{q})}\frac{\partial}{\partial\xi}\left(\beta\hat{H}-i\xi\hat{q}\right)e^{-u(\beta\hat{H}-i\xi\hat{q})}\hat{A}(t)\right] \tag{A.2.10}$$

$$= \frac{1}{Z}\int_{-\infty}^{\infty}\frac{d\xi}{\sqrt{2\pi}}\delta(\xi)\mathrm{Tr}\left[\int_0^1 du e^{-(1-u)(\beta\hat{H}-i\xi\hat{q})}\hat{q}e^{-u(\beta\hat{H}-i\xi\hat{q})}\hat{A}(t)\right] \tag{A.2.11}$$

$$= \frac{1}{Z}du\mathrm{Tr}\left[\int_0^1 e^{-(1-u)\beta\hat{H}}\hat{q}e^{-u\beta\hat{H}}\hat{A}(t)\right] = \frac{1}{Z}\int_0^1 du\mathrm{Tr}\Big[e^{-\beta H}\hat{q}(-iu\beta\hbar)\hat{A}\Big] \tag{A.2.12}$$

where in the previous line we have used the standard notation for time evolution of an operator and we say the correlation function has been Kubo transformed. The centroid correlation function is therefore equal to

$$\langle q_c A_c(t; q_c, p_c)\rangle = \langle\hat{q}\hat{A}(t)\rangle_{(K)} \equiv \frac{1}{Z}\int_0^1 du\langle\hat{q}(-iu\beta\hbar)\hat{A}\rangle \tag{A.2.13}$$

The same steps can be performed for the momentum operator to retrieve

$$\langle p_c A_c(t; q_c, p_c)\rangle = \langle\hat{p}\hat{A}(t)\rangle_{(K)} \tag{A.2.14}$$

Therefore it follows that for an arbitrary operator $\hat{A}$ and operator $\hat{B}$ which is a linear function of the position and momentum operators, the centroid correlation function is equal to the Kubo transformed correlation function

$$\langle B_c A_c(t; q_c, p_c)\rangle = \langle\hat{B}\hat{A}(t)\rangle_{(K)} \tag{A.2.15}$$

## A.3 Undoing the Kubo transform

We wish to establish a connection a connection between the usual quantum time correlation function and its Kubo transformed version. This is easily done when working in the basis of the Hamiltonian eigenstates. We begin with the regular correlation function

$$\langle \hat{B}\hat{A}(t)\rangle := \frac{1}{Z}\mathrm{Tr}\Big[e^{-\beta\hat{H}}\hat{B}\hat{A}(t)\Big] \tag{A.3.1}$$

$$= \frac{1}{Z}\sum_{n,m} e^{-\beta E_n}\,\langle\chi_n|\hat{B}|\chi_m\rangle\,\langle\chi_m|\hat{A}|\chi_n\rangle\,e^{it(E_m-E_n)/\hbar} \tag{A.3.2}$$

Performing the Fourier transform of the correlation function yields

$$\mathcal{F}\{\langle \hat{B}\hat{A}(t)\rangle\}(\omega) = \frac{1}{Z}\sum_{m,n} e^{-\beta E_n}\,\langle\chi_n|\hat{B}|\chi_m\rangle\,\langle\chi_m|\hat{A}|\chi_n\rangle\,\delta\Big(\omega - \frac{E_m-E_n}{\hbar}\Big) \tag{A.3.3}$$

Expanding the Kubo transformed correlation function in the basis of the energy eigenstates gives

$$\langle \hat{B}\hat{A}(t)\rangle_{(K)} := \frac{1}{Z}\int_0^1 du\,\mathrm{Tr}\Big[e^{-\beta\hat{H}}e^{u\beta\hat{H}}\hat{B}e^{-u\beta\hat{H}}\hat{A}(t)\Big] \tag{A.3.4}$$

$$= \frac{1}{Z}\sum_{n,m} e^{-\beta E_n}\int_0^1 du\,e^{u\beta(E_n-E_m)}\,\langle\chi_n|\hat{B}|\chi_m\rangle\,\langle\chi_m|\hat{A}|\chi_n\rangle\,e^{it(E_m-E_n)/\hbar} \tag{A.3.5}$$

$$= \frac{1}{Z}\sum_{n,m} e^{-\beta E_n}\frac{e^{\beta(E_n-E_m)}-1}{\beta(E_n-E_m)}\,\langle\chi_n|\hat{B}|\chi_m\rangle\,\langle\chi_m|\hat{A}|\chi_n\rangle\,e^{it(E_m-E_n)/\hbar} \tag{A.3.6}$$

$$\tag{A.3.7}$$

Taking the Fourier transform gives

$$\mathcal{F}\{\langle \hat{B}\hat{A}(t)\rangle_{(K)}\}(\omega) = \frac{1}{Z}\sum_{n,m} e^{-\beta E_n}\frac{e^{\beta(E_n-E_m)}-1}{\beta(E_n-E_m)}\,\langle\chi_n|\hat{B}|\chi_m\rangle\,\langle\chi_m|\hat{A}|\chi_n\rangle\,\delta\Big(\omega - \frac{E_m-E_n}{\hbar}\Big) \tag{A.3.8}$$

$$= \frac{1}{Z}\sum_{n,m} e^{-\beta E_n}\frac{e^{-\beta\hbar\omega}-1}{-\beta\hbar\omega}\,\langle\chi_n|\hat{B}|\chi_m\rangle\,\langle\chi_m|\hat{A}|\chi_n\rangle\,\delta\Big(\omega - \frac{E_m-E_n}{\hbar}\Big) \tag{A.3.9}$$

We can see that this is simply the Fourier transform of the usual correlation function multiplied by a constant frequency factor; the relation between the two Fourier transform is then

$$\mathcal{F}\{\langle \hat{B}\hat{A}(t)\rangle\}(\omega) = \frac{\beta\hbar\omega}{1-e^{-\beta\hbar\omega}}\mathcal{F}\{\langle \hat{B}\hat{A}(t)\rangle_{(K)}\}(\omega) \tag{A.3.10}$$

Undoing the Fourier transforms then gives us the following relation between the two correlation functions

$$\langle \hat{B}\hat{A}(t)\rangle = \frac{1}{2\pi}\int_{-\infty}^{\infty} d\omega\,e^{i\omega t}\frac{\beta\hbar\omega}{1-e^{-\beta\hbar\omega}}\int_{-\infty}^{\infty} dt'\,e^{-i\omega t'}\,\langle \hat{B}\hat{A}(t')\rangle_{(K)} \tag{A.3.11}$$

# Appendix B

# Constraints

## B.1 Constraining to an n-dimensional ellipsoid with a position dependent potential

Here we show how to constrain a system moving in $\mathbb{R}^{n+1}$ space to the n-ellipsoid. We will use Einstein notation for this section. Since all indices are Latin characters, we are working with spatial coordinates. The distinction between covariant and contravariant indices is not applicable here; the use of this notation is merely convenient. A symbol with an upper index, $q^k$, represent column vectors and symbols with a lower index, $q_k$, represent row vectors. The object $A^j{}_k$ is a matrix, quite literally a column vector whose entries are row vectors. Repeated indices denotes a contraction, so $q^k p_k$ is a dot product of vectors while $A^j{}_j$ represents a trace. The Poisson bracket may then be written as

$$[f,g]_P = \frac{\partial f}{\partial q^k}\frac{\partial g}{\partial p_k} - \frac{\partial f}{\partial p_k}\frac{\partial g}{\partial q^k} \tag{B.1.1}$$

First we consider the Lagrangian with a Lagrange multiplier term

$$\mathcal{L} = \frac{m}{2}\dot{q}^k\dot{q}_k - V + \lambda((q/a^2)^k q_k - 1) \tag{B.1.2}$$

where the equation for the n-dimensional ellipsoid is

$$1 = \left(\frac{q}{a^2}\right)^k q_k = \frac{q_{(1)}^2}{a_{(1)}^2} + \frac{q_{(2)}^2}{a_{(2)}^2} + \cdots \tag{B.1.3}$$

where $q$ are the Cartesian coordinates and $a$ are the lengths of the semi-principal axes. Since the Lagrangian is independent of $\dot{\lambda}$ the $(n+2)\times(n+2)$ Hessian with respect to the velocities will have one row and one column of all zeros and will hence be singular. The total Hamiltonian in this case is

$$\mathcal{H}_T = \frac{1}{2m}p^k p_k + V + \lambda((q/a^2)^k q_k - 1) + u^\lambda p_\lambda \tag{B.1.4}$$

where $u^\lambda$ is an additional Lagrange multiplier term, and it is understood that the potential term $V$ is purely dependent on the position coordinates $q^k$. The primary constraint is naturally that the momentum for the Lagrange multiplier be zero

$$\phi_1 = p_\lambda \approx 0 \tag{B.1.5}$$

Now we may generate the consistency conditions for this constraint in doing so generate additional constraints

$$\dot{\phi}_1 = -((q/a^2)^k q_k - 1) \qquad \to \phi_2 = (q/a^2)^k q_k - 1 \approx 0 \tag{B.1.6}$$

$$\dot{\phi}_2 = \frac{2}{m}(q/a^2)^k p_k \qquad \to \phi_3 = (q/a^2)^k p_k \approx 0 \tag{B.1.7}$$

The effects of the potential become noticeable in the consistency equation for the third constraint

$$\dot{\phi}_3 = \left[(q/a^2)^k p_k, \frac{p^l p_l}{2m} + V + \lambda(q/a^2)^l q_l\right]_P \tag{B.1.8}$$

$$= \frac{p_k}{2m}[(q/a^2)^k, p^l p_l]_P + (q/a^2)^k [p_k, V]_P + \lambda(q/a^2)^k [p_k, (q/a^2)^l q_l]_P \tag{B.1.9}$$

$$= \frac{(p/a^2)^k p_k}{m} - (q/a^2)^k \partial_k V - 2\lambda(q/a^4)^k q_k \tag{B.1.10}$$

$$\to \phi_4 = \frac{(p/a^2)^k p_k}{2} - \frac{m}{2}(q/a^2)^k \partial_k V - m\lambda(q/a^4)^k q_k \approx 0 \tag{B.1.11}$$

where we define $\partial_k := \partial/\partial q^k$. The consistency condition for $\phi_4$ will fix the value of $u^\lambda$ and terminate the series of constraints

$$\dot{\phi}_4 = \left[\frac{(p/a^2)^k p_k}{2} - \frac{m}{2}(q/a^2)^k \partial_k V - m\lambda(q/a^4)^k q_k, \frac{p^l p_l}{2m} + V + \lambda(q/a^2)^l q_l + u^\lambda p_\lambda\right]_P \tag{B.1.12}$$

$$= \frac{1}{2}[(p/a^2)^k p_k, V + \lambda(q/a^2)^l q_l]_P - \frac{1}{4}[(q/a^2)^k \partial_k V, p^l p_l]_P - m\left[\lambda(q/a^4)^k q_k, \frac{p^l p_l}{2m} + u^\lambda p_\lambda\right]_P \tag{B.1.13}$$

$$= -(p/a^2)^k \partial_k V - 2\lambda(q/a^4)^k p_k - \frac{p^k}{2}\partial_k\left((q/a^2)^l \partial_l V\right) - 2\lambda(q/a^4)^k p_k - m u^\lambda (q/a^4)^k q_k \approx 0 \tag{B.1.14}$$

$$\to u^\lambda = -\frac{1}{m((q/a^4)^k q_k)}\left((p/a^2)^k \partial_k V + 4\lambda(q/a^4)^k p_k + \frac{p^k}{2}\partial_k\left((q/a^2)^l \partial_l V\right)\right) \tag{B.1.15}$$

We can now construct the $C$ matrix using the Poisson bracket

$$C = \begin{bmatrix} 0 & 0 & 0 & m(q/a^4)^k q_k \\ 0 & 0 & 2(q/a^4)^k q_k & 2(q/a^4)^k p_k \\ 0 & -2(q/a^4)^k q_k & 0 & \begin{matrix}(p/a^4)^k p_k + 2m\lambda(q/a^6)^k q_k \\ + \frac{m}{2}(q/a^2)^k \partial_k((q/a^2)^l \partial_l V)\end{matrix} \\ -m(q/a^4)^k q_k & -2(q/a^4)^k p_k & \begin{matrix}-(p/a^4)^k p_k - 2m\lambda(q/a^6)^k q_k \\ -\frac{m}{2}(q/a^2)^k \partial_k((q/a^2)^l \partial_l V)\end{matrix} & 0 \end{bmatrix} \tag{B.1.16}$$

The determinant of this matrix is $\det C = 4m^2((q/a^4)^k q_k)^4$. The inverse therefore exists and is

$$C^{-1} = \frac{1}{2m((q/a^4)^l q_l)^2} \times \begin{bmatrix} 0 & \begin{matrix}-(p/a^4)^k p_k - 2m\lambda(q/a^6)^k q_k \\ -\frac{m}{2}(q/a^2)^l \partial_l((q/a^2)^k \partial_k V)\end{matrix} & (q/a^4)^k p_k & -2(q/a^4)^k q_k \\ \begin{matrix}(p/a^4)^k p_k + 2m\lambda(q/a^6)^k q_k \\ + \frac{m}{2}(q/a^2)^l \partial_l((q/a^2)^k \partial_k V)\end{matrix} & 0 & -m(q/a^4)^k q_k & 0 \\ -(q/a^4)^k p_k & m(q/a^4)^k q_k & 0 & 0 \\ 2(q/a^4)^k q_k & 0 & 0 & 0 \end{bmatrix} \tag{B.1.17}$$

We can now work out the Dirac brackets between the various position and momentum coordinates. The position variables only have a non vanishing Poisson bracket with $\phi_3$ and $\phi_4$, but the corresponding matrix elements in $C^{-1}$ are zero so the Dirac bracket between two position variables is simply the Poisson bracket

$$[q^j, q_k]_D = [q^j, q_k]_P = 0 \tag{B.1.18}$$

The momentum variables have a non-vanishing Poisson bracket with all the constraints except $\phi_1$. If we ignore the elements of $C^{-1}$ which are zero, then the Dirac bracket between two momentum coordinates is

$$[p^j, p_k]_D = [p^j, p_k]_P - (C^{-1})^2{}_3[p^j, \phi_3]_P[\phi_2, p_k]_P - (C^{-1})^3{}_2[p^j, \phi_2]_P[\phi_3, p_k]_P \tag{B.1.19}$$

$$= \frac{1}{2(q/a^4)^l q_l}\Big([p^j, (q/a^2)^b q_b]_P[(q/a^2)^c p_c, p_k]_P - [p^j, (q/a^2)^c p_c]_P[(q/a^2)^b q_b, p_k]_P\Big) \tag{B.1.20}$$

$$= \frac{1}{(q/a^4)^l q_l}\left((p/a^2)^j (q/a^2)_k - (q/a^2)^j (p/a^2)_k\right) \tag{B.1.21}$$

We now consider the Dirac bracket between a position and momentum variable

$$[q^j, p_k]_D = [q^j, p_k]_P - (C^{-1})^3{}_2[q^j, \phi_3]_P[\phi_2, p_k]_P \tag{B.1.22}$$

$$= \delta^j{}_k - \frac{1}{2(q/a^4)^l q_l}[q^j, (q/a^2)^b p_b]_P[(q/a^2)^c q_c, p_k]_P \tag{B.1.23}$$

$$= \delta^j{}_k - \frac{1}{(q/a^4)^l q_l}(q/a^2)^j (q/a^2)_k \tag{B.1.24}$$

where $\delta^j{}_k$ is the Kronecker delta tensor. Finally, we will evaluate the Dirac bracket between the $\lambda$ Lagrange multiplier and its conjugate momentum

$$[\lambda, p_\lambda]_D = [\lambda, p_\lambda]_P - (C^{-1})^1{}_4[\lambda, \phi_1]_P[\phi_4, p_\lambda]_P \tag{B.1.25}$$

$$= 1 + \frac{1}{m(q/a^4)^l q_l}(-m(q/a^4)^k q_k)[\lambda, p_\lambda]_P[\lambda, p_\lambda]_P = 0 \tag{B.1.26}$$

The Dirac brackets between all other variables and $\lambda$ and $p_\lambda$ are also zero. These terms may therefore be strongly set to zero; the total Hamiltonian is then

$$\mathcal{H}_T = \frac{p^k p_k}{2m} + V(q^j) \tag{B.1.27}$$

where the Dirac brackets between the constrained variables in the reduced phase space are

$$[q^j, q_k]_D = 0 \qquad [q^j, p_k]_D = \delta^j{}_k - \frac{1}{(q/a^4)^l q_l}(q/a^2)^j (q/a^2)_k$$

$$[p^j, p_k]_D = \frac{1}{(q/a^4)^l q_l}\left((p/a^2)^j (q/a^2)_k - (q/a^2)^j (p/a^2)_k\right) \tag{B.1.28}$$

We can see that the inclusion of the position dependent potential term in the Lagrangian had no effect on the Dirac brackets between the phase space variables. We also note that while the dimension of the original phase space was $2(n+2)$ due to the inclusion of the Lagrange multipliers in the Lagrangian, since we generated 4 constraints the restricted phase space will have dimension

$2n$ which is to be expected for the $n$-ellipsoid. The results for motion on an $n$-sphere may be retrieved by taking the length of all semi-principal axes to be the same value $a^k = R$,

$$1 = \Big(\frac{q}{R^2}\Big)^k q_k = \frac{q^k q_k}{R^2} \tag{B.1.29}$$

in which case the Dirac brackets reduce to

$$[q^j, q_k]_D = 0 \qquad [q^j, p_k]_D = \frac{1}{R^2}(\delta^j{}_k R^2 - q^j q_k) \qquad [p^j, p_k]_D = \frac{1}{R^2}\left(p^j q_k - q^j p_k\right) \tag{B.1.30}$$

## B.2 Constraining the particle to the 2-sphere

We can use the results from section B.1 to extend the centroid formalism to a particle moving on a 2-sphere with radius $R$ under an arbitrary potential. The set of Dirac brackets for the restricted phase space variables $\{x, y, z, p_x, p_y, p_z\}$ can be obtained by subbing these variables into equation (B.1.28). In the classical phase space on the sphere the position variables are $\varphi \in [0, 2\pi)$ and $\theta \in [0, \pi]$, each with an associated conjugate momentum $p_\varphi$ and $p_\theta$, respectively. The conjugate momenta may be written in terms of the velocities of the angle variables as follows

$$p_\theta = mR^2\dot{\theta} \qquad p_\varphi = mR^2 \sin^2\theta\dot{\varphi} \tag{B.2.1}$$

In this case quantum analogues of the conjugate momentum are not used due to issues quantizing $p_\theta$. Since the angular momentum operators are used instead to describe the motion of a particle on a sphere, we will use the classical versions of these operators

$$L_x = -p_\theta \sin\varphi - p_\varphi \cot\theta\cos\varphi \qquad L_y = p_\theta\cos\varphi - p_\varphi\cot\theta\sin\varphi \qquad L_z = p_\varphi \tag{B.2.2}$$

to allow for easy quantization of the constrained phase space variables. We begin by postulating that the expected position operators are the spherical coordinate versions of the Euclidean positions with the radial component fixed

$$x = R\sin\theta\cos\varphi \qquad y = R\sin\theta\sin\varphi \qquad z = R\cos\theta \tag{B.2.3}$$

Using the Poisson bracket

$$[f, g]_P = \frac{\partial f}{\partial\varphi}\frac{\partial g}{\partial p_\varphi} - \frac{\partial f}{\partial p_\varphi}\frac{\partial g}{\partial\varphi} + \frac{\partial f}{\partial\theta}\frac{\partial g}{\partial p_\theta} - \frac{\partial f}{\partial p_\theta}\frac{\partial g}{\partial\theta} \tag{B.2.4}$$

and expressing the relations (B.1.30) in spherical coordinates allows us to determine the expression for the momenta in the reduced phase space coordinates

$$p_x = \frac{1}{R^2}(zL_y - yL_z) = \frac{1}{R}(p_\theta\cos\theta\cos\varphi - p_\varphi\csc\theta\sin\varphi) \tag{B.2.5}$$

$$p_y = \frac{1}{R^2}(xL_z - zL_x) = \frac{1}{R}(p_\theta\cos\theta\sin\varphi + p_\varphi\csc\theta\cos\varphi) \tag{B.2.6}$$

$$p_z = \frac{1}{R^2}(yL_x - xL_y) = -\frac{1}{R}p_\theta\sin\theta \tag{B.2.7}$$

When converting the reduced phase space symbols to operators, we also demand that the Heisenberg equations of motion for the position operators still hold so that the CMD equations of motion remain self consistent. It can be worked out that the restricted position operators are

$$\tilde{x} = R\sin\hat{\theta}\cos\hat{\varphi} = R\hat{X}_x \tag{B.2.8}$$

$$\tilde{y} = R\sin\hat{\theta}\sin\hat{\varphi} = R\hat{X}_y \tag{B.2.9}$$

$$\tilde{z} = R\cos\hat{\varphi} = R\hat{X}_z \tag{B.2.10}$$

and the restricted momentum operators are

$$\tilde{p}_x = \frac{1}{2R^2}\left(\{\tilde{z},\hat{L}_y\} - \{\tilde{y},\hat{L}_z\}\right) = \frac{1}{2R}\left(\{\hat{X}_z,\hat{L}_y\} - \{\hat{X}_y,\hat{L}_z\}\right) \tag{B.2.11}$$

$$\tilde{p}_y = \frac{1}{2R^2}\left(\{\tilde{x},\hat{L}_z\} - \{\tilde{z},\hat{L}_x\}\right) = \frac{1}{2R}\left(\{\hat{X}_x,\hat{L}_z\} - \{\hat{X}_z,\hat{L}_x\}\right) \tag{B.2.12}$$

$$\tilde{p}_z = \frac{1}{2R^2}\left(\{\tilde{y},\hat{L}_x\} - \{\tilde{x},\hat{L}_y\}\right) = \frac{1}{2R}\left(\{\hat{X}_y,\hat{L}_x\} - \{\hat{X}_x,\hat{L}_y\}\right) \tag{B.2.13}$$

The $\hat{L}_n$ operators are the usual angular momentum operators for the sphere and the $\hat{X}_n$ operators act as position operators. The commutation relations for this set of operators are

$$[\hat{X}_l,\hat{X}_n] = 0 \qquad [\hat{L}_l,\hat{L}_m] = i\hbar\epsilon_{lmn}\hat{L}_n \qquad [\hat{L}_l,\hat{X}_m] = i\hbar\epsilon_{lmn}\hat{X}_n \tag{B.2.14}$$

where $\epsilon_{lmn}$ is the Levi-Civita symbol and the where the set $(l,m,n)$ can take the values $(1,2,3) \equiv (x,y,z)$. It is convenient to work in the usual $|l,m\rangle$ basis when building a matrix representation for these and other operators, and in order to work out how the operators act in the $x$ and $y$ directions it is easiest to construct ladder operators using the definitions

$$\hat{X}_+ = \hat{X}_x + i\hat{X}_y \qquad \hat{X}_- = \hat{X}_x - i\hat{X}_y \qquad \hat{L}_+ = \hat{L}_x + i\hat{L}_y \qquad \hat{L}_- = \hat{L}_x - i\hat{L}_y \tag{B.2.15}$$

Using the commutation relations and the knowledge that the angular momentum operators act on the $|l,m\rangle$ basis states as follows

$$\hat{L}_+|l,m\rangle = \sqrt{(l-m)(l+m+1)}\,|l,m+1\rangle \tag{B.2.16}$$

$$\hat{L}_-|l,m\rangle = \sqrt{(l+m)(l-m+1)}\,|l,m-1\rangle \tag{B.2.17}$$

$$\hat{L}_z|l,m\rangle = m\,|l,m\rangle \tag{B.2.18}$$

then it can be worked out that the position operators act on this basis in the following manner

$$\hat{X}_+|l,m\rangle = \sqrt{\frac{(l-m)(l-m-1)}{(2l-1)(2l+1)}}\,|l-1,m+1\rangle - \sqrt{\frac{(l+m+2)(l+m+1)}{(2l+1)(2l+3)}}\,|l+1,m+1\rangle \tag{B.2.19}$$

$$\hat{X}_-|l,m\rangle = -\sqrt{\frac{(l+m-1)(l+m)}{(2l-1)(2l+1)}}\,|l-1,m-1\rangle + \sqrt{\frac{(l-m+1)(l-m+2)}{(2l+1)(2l+3)}}\,|l+1,m-1\rangle \tag{B.2.20}$$

$$\hat{X}_z|l,m\rangle = \sqrt{\frac{(l-m)(l+m)}{(2l-1)(2l+1)}}\,|l-1,m\rangle + \sqrt{\frac{(l-m+1)(l+m+1)}{(2l+1)(2l+3)}}\,|l+1,m\rangle \tag{B.2.21}$$

Using the method described in chapter 2, the QDO for the particle on a sphere system may then be built by replacing the position and momentum operators in the 3-dimensional centroid QDO

with these restricted Hilbert space operators. Computations may then be performed using finite dimensional matrix representations in the $|l,m\rangle$ basis. Using the method from Chapter 2, the QDO for motion on the 2-sphere is then

$$\hat{\delta}_c(x_c,y_c,z_c,p_{x\,c},p_{y\,c},p_{z\,c}) = \int d\xi_x\, d\xi_y\, d\xi_z\, d\eta_x\, d\eta_y\, d\eta_z\, e^{-i(\xi_x x_c+\xi_y y_c+\xi_z z_c)}\, e^{-i(\eta_x p_{xc}+\eta_y p_{yc}+\eta_z p_{zc})} \times \exp\Big(-\beta\hat{H} + i\xi_x\tilde{x} + i\xi_y\tilde{y} + i\xi_z\tilde{z} + i\eta_x\tilde{p}_x + i\eta_y\tilde{p}_y + i\eta_z\tilde{p}_z\Big) \tag{B.2.22}$$

## B.3 The position centroid density for a particle on ring

If we only wish to consider the position centroid density for the particle on a sphere we begin with the unconstrained density

$$\rho_c(x_c,y_c) = \int \mathcal{D}\mathbf{q}\,\mathcal{D}\mathbf{p}\,\delta(x_c-x_0)\,\delta(y_c-y_0)\exp(-S[\tau]/\hbar) \tag{B.3.1}$$

and applying the method from Chapter 2 retrieve the following density

$$\rho_c(x_c,y_c) = \int \mathcal{D}\varphi\mathcal{D}p_\varphi\,\delta(x_c-x_0)\,\delta(y_c-y_0)\exp(-S[\tau]/\hbar) \tag{B.3.2}$$

$$= \int \mathcal{D}\varphi\mathcal{D}p_\varphi \iint \frac{d\xi_x d\xi_y}{2\pi} e^{-i(\xi_x x_c+\xi_y y_c)} \times \exp\left(-\frac{1}{\hbar}\int_0^{\beta\hbar} d\tau\left[\mathcal{H}(p_\varphi,\varphi) - ip_\varphi\varphi - i\frac{\eta_x}{\beta}R\cos\varphi - i\frac{\eta_y}{\beta}R\sin\varphi\right]\right) \tag{B.3.3}$$

The proposed QDO corresponding to this position centroid density is then

$$\hat{\delta}_c(x_c,y_c) = \iint \frac{d\xi_x d\xi_y}{2\pi} e^{-i(\xi_x x_c+\xi_y y_c)} \exp\left(-\beta\hat{H} + i\eta_x R\cos\hat{\varphi} + i\eta_y R\sin\hat{\varphi}\right) \tag{B.3.4}$$

The classical and quantum Hamiltonians here are

$$\mathcal{H} = Bp_\varphi^2 + V(\varphi) \qquad \hat{H} = B\hat{J}^2 + V(\hat{\varphi}) \tag{B.3.5}$$

where the potentials are both $2\pi$-periodic. We now wish to establish that

$$\rho_c(x_c,y_c) = \mathrm{Tr}\left[\hat{\delta}_c(x_c,y_c)\right] \tag{B.3.6}$$

We begin with the proposed centroid density, and write the trace as an integral over the angular position eigenstates

$$\mathrm{Tr}\left[\hat{\delta}_c(x_c,y_c)\right] = \int_0^{2\pi} d\varphi_{(0)}\,\langle\varphi_{(0)}|\hat{\delta}_c(x_c,y_c)|\varphi_{(0)}\rangle \tag{B.3.7}$$

The resolution of the identity for the angular position eigenstates and angular momentum eigenstates are

$$\mathbb{1} = \int_0^{2\pi} |\varphi\rangle\langle\varphi|\,d\varphi \qquad \mathbb{1} = \sum_{j=-\infty}^{\infty} |j\rangle\langle j| \tag{B.3.8}$$

Assuming that we can use the Trotter factorization[17] we decompose the exponential of the effective centroid Hamiltonian into position and momentum dependent parts

$$\mathrm{Tr}\left[\hat{\delta}_c(x_c,y_c)\right] = \iint \frac{d\xi_x d\xi_y}{2\pi} e^{-i(\xi_x x_c+\xi_y y_c)} \times \lim_{N\to\infty}\int_0^{2\pi} d\varphi_{(0)}\,\langle\varphi_{(0)}|\left(e^{(-\beta B\hat{J}^2)/N}e^{(-\beta V(\hat{\varphi})+i\eta_x R\cos\hat{\varphi}+i\eta_y R\sin\hat{\varphi})/N}\right)^N|\varphi_{(0)}\rangle \tag{B.3.9}$$

We now insert resolutions of the identity in the form of the angular position eigenstates between each of the terms in this product, and the resolution of the identity formed by the angular momentum eigenstates between the exponentials. A general element in this expansion is then

$$\langle\varphi_{(k+1)}|e^{(-\beta B\hat{J}^2)/N}|j_{(k)}\rangle\,\langle j_{(k)}|e^{(-\beta V(\hat{\varphi})+i\eta_x R\cos\hat{\varphi}+i\eta_y R\sin\hat{\varphi})/N}|\varphi_{(k)}\rangle \tag{B.3.10}$$

$$= \exp\Big[(-\beta B\hbar^2 j_{(k)}^2)/N\Big]\exp\big[(-\beta V(\varphi_{(k)})+i\eta_x R\cos\varphi_{(k)}+i\eta_y R\sin\varphi_{(k)})/N\big]\langle\varphi_{(k+1)}|j_{(k)}\rangle\langle j_{(k)}|\varphi_{(k)}\rangle \tag{B.3.11}$$

$$= \exp\Big[(-\beta[B\hbar^2 j_{(k)}^2+V(\varphi_{(k)})]+i\eta_x R\cos\varphi_{(k)}+i\eta_y R\sin\varphi_{(k)})/N\Big]\,\frac{1}{2\pi\hbar}e^{ij_{(k)}(\varphi_{(k+1)}-\varphi_{(k)})} \tag{B.3.12}$$

We now introduce the parameter $\epsilon=\beta\hbar/N$, and recombine the individual terms in the expansion

$$\lim_{N\to\infty}\langle\varphi_{(0)}|\left(e^{(-\beta B\hat{J}^2)/N}e^{(-\beta V(\hat{\varphi})+i\eta_x R\cos\hat{\varphi}+i\eta_y R\sin\hat{\varphi})/N}\right)^N|\varphi_{(0)}\rangle \tag{B.3.13}$$

$$= \lim_{N\to\infty}\int_0^{2\pi}\frac{1}{(2\pi)^N}d\varphi_{(0)}d\varphi_{(1)}\ldots d\varphi_{(N-1)}\sum_{j_{(0)}=-\infty}^{\infty}\cdots\sum_{j_{(N-1)}=-\infty}^{\infty} \times\exp\left[-\frac{\epsilon}{\hbar}\sum_{k=0}^{N-1}\left(\mathcal{H}(\varphi_{(k)},j_{(k)})-i\hbar j_{(k)}\frac{\varphi_{(k+1)}-\varphi_{(k)}}{\epsilon}-i\frac{\eta_x}{\beta}R\cos\varphi_{(k)}-i\frac{\eta_y}{\beta}R\sin\varphi_{(k)}\right)\right] \tag{B.3.14}$$

For notations sake we will define a functional measure for the angle variables

$$\int\mathcal{D}\varphi = \lim_{N\to\infty}\prod_{k=0}^{N-1}\int_0^{2\pi}d\varphi_{(k)} \tag{B.3.15}$$

and similarly a compact way of writing the many sums over the discrete angular momentum variables

$$\int\mathcal{D}p_\varphi = \lim_{N\to\infty}\frac{1}{(2\pi)^N}\prod_{k=0}^{N-1}\sum_{j_{(k)}=-\infty}^{\infty} \tag{B.3.16}$$

We now make the identification that we are in the limit $\epsilon\to 0$ and so substitute in the derivative

$$\lim_{\epsilon\to0}\frac{\varphi_{(k+1)}-\varphi_{(k)}}{\epsilon} = \lim_{\epsilon\to0}\frac{\varphi(\tau+\epsilon)-\varphi(\tau)}{\epsilon} = \dot{\varphi}_{(k)}(\tau) \tag{B.3.17}$$

where we have used an imaginary time unit $\tau$. The sum in the exponential is a Riemann sum and so can also be replaced by a Riemann integral over the imaginary time unit in the $\epsilon\to0$ limit,

[17] We could perform the time-slicing procedure, but the answers are equivalent in this case

which must run from 0 to $\beta\hbar$

$$\lim_{\epsilon\to 0}\frac{\epsilon}{\hbar}\sum_{k=0}^{N-1}\left(\mathcal{H}(\varphi_{(k)},j_{(k)})-i\hbar j_{(k)}\frac{\varphi_{(k+1)}-\varphi_{(k)}}{\epsilon}-i\frac{\eta_x}{\beta}R\cos\varphi_{(k)}-i\frac{\eta_y}{\beta}R\sin\varphi_{(k)}\right)$$
$$=\frac{1}{\hbar}\int_0^{\beta\hbar}d\tau\left[\mathcal{H}(\varphi,p_\varphi)-ip_\varphi\dot{\varphi}-i\frac{\eta_x}{\beta}R\cos\varphi-i\frac{\eta_y}{\beta}R\sin\varphi\right] \tag{B.3.18}$$

We have replaced the discrete momentum with the label $\hbar j_{(k)}=p_\varphi$ for consistency purposes. It should not be confused with the classical angular momentum, which is a continuous quantity. Putting everything back together we have the result

$$\mathrm{Tr}\left[\hat{\delta}_c(x_c,y_c)\right]=\iint\frac{d\xi_x d\xi_y}{2\pi}e^{-i(\xi_x x_c+\xi_y y_c)}$$
$$\times\int\mathcal{D}\varphi\mathcal{D}p_\varphi\exp\left[-\frac{1}{\hbar}\int_0^{\beta\hbar}d\tau\left[\mathcal{H}(\varphi,p_\varphi)-ip_\varphi\dot{\varphi}-i\frac{\eta_x}{\beta}R\cos\varphi-i\frac{\eta_y}{\beta}R\sin\varphi\right]\right] \tag{B.3.19}$$

which is what we wanted to show.

### B.3.1 The free particle on a ring position centroid density

We now consider the case of centroid density for the free particle on a ring. We begin by performing a change of coordinates on the Fourier variables $\xi_x$ and $\xi_y$ to polar coordinates as follows

$$\xi_x=\xi_r\cos\xi_\theta\qquad\xi_y=\xi_r\sin\xi_\theta \tag{B.3.20}$$

This allows us to to rewrite the centroid constraint terms as follows

$$\xi_x\cos\varphi+\xi_y\sin\varphi=\xi_r\cos(\varphi-\xi_\theta) \tag{B.3.21}$$

The Fourier integrals then change to

$$\int_{-\infty}^{\infty}\int_{-\infty}^{\infty}d\xi_x d\xi_y=\int_0^{\infty}\xi_r d\xi_r\int_0^{2\pi}d\xi_\theta \tag{B.3.22}$$

The integral over one of the $\varphi_{(k)}$ is then

$$\int_0^{2\pi}e^{i\varphi_{(k)}(j_{(k)}-j_{(k-1)})}e^{iR\xi_r\cos(\varphi_{(k)}-\xi_\theta)/N}d\varphi_{(k)}$$
$$=e^{-\xi_\theta(j_{(k)}-j_{(k-1)})}\int_{-\xi_\theta}^{2\pi-\xi_\theta}e^{i\theta_{(k)}(j_{(k)}-j_{(k-1)})}e^{iR\xi_r\cos\theta_{(k)}/N}d\theta_{(k)} \tag{B.3.23}$$

where we have made the coordinate change $\theta_{(k)}=\varphi_{(k)}-\xi_\theta$. Since the integrand is $2\pi$-periodic we can change the limits of integration back to $[0,2\pi)$. We will now make use of the following integral definition of the Bessel function of the first kind, hereafter called the Bessel function,

$$J_n(z)=\frac{1}{2\pi i^n}\int_0^{2\pi}e^{i(n\phi+z\cos\phi)}d\phi \tag{B.3.24}$$

The integral over $\theta_{(k)}$ may be readily evaluated to yield

$$e^{-\xi_\theta(j_{(k)}-j_{(k-1)})}\int_0^{2\pi} e^{i\theta_{(k)}(j_{(k)}-j_{(k-1)})}e^{iR\xi_r\cos\theta_{(k)}/N}d\theta_{(k)}=(ie^{-i\xi_\theta})^{(j_{(k)}-j_{(k-1)})}2\pi J_{(j_{(k)}-j_{(k-1)})}(R\xi_r/N) \tag{B.3.25}$$

The phase factor for each link will cancel, even at the end points due to the cyclic property of the trace. The path integral is then independent of the Fourier angle, so we can perform the integral over $\xi_\theta$. First we also rewrite the centroid phase space coordinates in polar coordinate form

$$x_c = r_c\cos\varphi_c \qquad y_c = r_c\sin\varphi_c \tag{B.3.26}$$

so we need to evaluate the following integral

$$\int_0^{2\pi} e^{-\xi_r r_c(\cos\xi_\theta\cos\varphi_c+\sin\xi_\theta\sin\varphi_c)}d\xi_\theta = \int_0^{2\pi} e^{-\xi_r r_c\cos(\xi_\theta-\varphi_c)} = 2\pi J_0(-r_c\xi_r r_c) \equiv 2\pi J_0(r_c\xi_r) \tag{B.3.27}$$

The centroid density is therefore independent of the angular coordinate, as would be expected for the free particle. The centroid density may now be written in the following form

$$\rho_c(r_c) = \lim_{N\to\infty}\int_0^\infty d\xi_r\,\xi_r\,J_0(r_c\xi_r)\sum_{j_{(N)}=-\infty}^{\infty}\delta_{j_{(0)}j_{(N)}}\left[\prod_{k=0}^{N-1}\sum_{j_{(k)}=-\infty}^{\infty} e^{-\beta B\hbar^2 j_{(k)}^2/N}J_{(j_{(k+1)}-j_{(k)})}(R\xi_r/N)\right] \tag{B.3.28}$$

$$= \lim_{N\to\infty}\int_0^\infty d\xi_r\,\xi_r\,J_0(r_c\xi_r)\sum_{j_{(N)}=-\infty}^{\infty}\delta_{j_{(0)}j_{(N)}}\left[\prod_{k=0}^{N-1}\sum_{j_{(k)}=-\infty}^{\infty} e^{-\beta B\hbar^2 j_{(k)}^2/N}J_{(j_{(k)}-j_{(k+1)})}(R\xi_r/N)\right] \tag{B.3.29}$$

where the Kronecker delta is required to ensure that the $k = 0$ and $k = N$ angular momentum variables are identical. We can simplify this form in the high and low temperature limits.

**The low temperature limit**

In the low temperature limit the following term

$$\lim_{\beta\to\infty}\exp\left[-\frac{1}{N}\beta B\hbar^2\sum_{k=0}^{N-1} j_{(k)}^2\right] \tag{B.3.30}$$

is only non-zero when the sum of the angular momentum variables is zero, which is only the case when each term $j_{(k)}$ is zero since they can only take non-negative values. Only the $j_{(k)} = 0$ term from each sum will survive and we can immediately write the low temperature limit as

$$\lim_{\beta\to\infty}\rho_c(r_c) = \int_0^\infty d\xi_r\,J_0(r_c\xi_r)\lim_{N\to\infty}\prod_{k=0}^{N-1}J_0(R\xi_r/N) \tag{B.3.31}$$

The Bessel functions can also be eliminated in this limit by repeated use of

$$\lim_{x\to 0}J_0(x) = \lim_{y\to\infty}J_0(1/y) = 1 \tag{B.3.32}$$

So the product is of Bessel functions merely evaluates to one. We are then left to evaluate the Hankel transform

$$\lim_{\beta\to\infty}\rho_c(r_c)=\int_0^\infty d\xi_r\, J_0(r_c\xi_r)=\frac{\delta(r_c)}{2\pi r_c} \tag{B.3.33}$$

Converting back to Cartesian centroid coordinates gives us the equivalent high temperature limit

$$\lim_{\beta\to\infty}\rho_c(x_c,y_c)=\delta(x_c)\delta(y_c) \tag{B.3.34}$$

which is only non-zero at the origin, $x_c^2+y_c^2=0$.

**The high temperature limit**

In the high temperature limit it can be seen that the exponential terms will go to one, so the position centroid density may be written as follows

$$\lim_{\beta\to0}\rho_c(r_c)=\lim_{N\to\infty}\int_0^\infty d\xi_r\,\xi_r\,J_0(\xi_r r_c)\sum_{j_{(N)}=-\infty}^{\infty}\delta_{j_{(0)}j_{(N)}}\left[\prod_{k=0}^{N-1}\sum_{j_{(k)}=-\infty}^{\infty}J_{(j_{(k)}-j_{(k+1)})}(R\xi_r/N)\right] \tag{B.3.35}$$

We can evaluate the product the sums of products of Bessel functions using the Bessel addition theorem

$$J_n(x+y)=\sum_{m=-\infty}^{\infty}J_m(x)J_{n-m}(y) \tag{B.3.36}$$

However, we must first reindex our infinite sums to use this theorem

$$\begin{aligned}&\sum_{j_{(k)}=-\infty}^{\infty}J_{(j_{(k)}-j_{(k+1)})}(\xi_rR/N)J_{(j_{(k-1)}-j_{(k)})}(\xi_rR/N)\\&=\sum_{h_{(k)}=-\infty}^{\infty}J_{h_{(k)}}(R\xi_r/N)J_{(j_{(k-1)}-j_{(k+1)}-h_{(k)})}(R\xi_r/N)\\&=J_{(j_{(k-1)}-j_{(k+1)})}(2R\xi_r/N)\end{aligned} \tag{B.3.37}$$

In this way the product of $N$ Bessel functions may be condensed to a single Bessel function by evaluating $N-1$ sums. Due to the cyclic nature of the indices, upon performing the $N-1$ sum the result is a Bessel function of order 0. We are therefore left with a single infinite sum which cannot be eliminated

$$\lim_{\beta\to0}\rho_c(r_c)=\lim_{N\to\infty}\int_0^\infty d\xi_r\,\xi_r\,J_0(r_c\xi_r)\sum_{j_{(0)}=-\infty}^{\infty}J_0(NR\xi_r/N) \tag{B.3.38}$$

$$=\sum_{j=-\infty}^{\infty}\int_0^\infty d\xi_r\,\xi_r\,J_0(r_c\xi_r)\,J_0(R\xi_r) \tag{B.3.39}$$

$$=\sum_{j=-\infty}^{\infty}\frac{1}{2\pi r_c}\delta(r_c-R) \tag{B.3.40}$$

so that we have an infinite number of delta functions located at the radius of the ring.

## B.4 Correlation functions for the free particle on a ring

### B.4.1 Classical system

We wish to compare the $\beta \to 0$ limit of the centroid dipole autocorrelation function for the free particle on a ring with the exact result. The classical Hamiltonian for this system is

$$\mathcal{H} = \frac{p_\varphi^2}{2mR^2} \equiv B p_\varphi^2 \tag{B.4.1}$$

and we can then determine the exact time evolution of the dipole moment $\cos\varphi(t)$ using the following system of differential equations and initial conditions

$$\frac{d}{dt}\varphi(t) = \frac{p_\varphi(t)}{mR^2},\ \varphi(0) = \varphi \qquad \frac{d}{dt}p_\varphi(t) = 0,\ p_\varphi(0) = p_\varphi \tag{B.4.2}$$

Solving these yields the solution

$$\varphi(t) = \frac{p_\varphi}{mR^2}t + \varphi \tag{B.4.3}$$

and so the equation for the time evolution of the dipole moment is

$$\cos\varphi(t) = \cos\left(\frac{p_\varphi}{mR^2}t\right)\cos(\varphi) - \sin\left(\frac{p_\varphi}{mR^2}t\right)\sin(\varphi) \tag{B.4.4}$$

The classical dipole autocorrelation function is then given by integration over the entire phase space

$$\langle \cos\varphi\cos\varphi(t)\rangle = \frac{\displaystyle\int_{-\infty}^{\infty} dp_\varphi \int_0^{2\pi} d\varphi\, e^{-\beta p_\varphi^2/2mR^2}\cos\varphi\cos\varphi(t)}{\displaystyle\int_{-\infty}^{\infty} dp_\varphi \int_0^{2\pi} d\varphi\, e^{-\beta p_\varphi^2/2mR^2}} \tag{B.4.5}$$

$$= \frac{1}{2}\exp\left(-\frac{t^2}{2\beta mR^2}\right) = \frac{1}{2}\exp\left(-B\frac{t^2}{\beta}\right) \tag{B.4.6}$$

Here we can see that the system decorrelates more rapidly with an increase in temperature, and in the $\beta \to 0$ limit we have

$$\lim_{\beta\to 0}\langle \cos\varphi\cos\varphi(t)\rangle = \begin{cases} 1/2 & \text{if } t = 0 \\ 0 & \text{if } t > 0 \end{cases} \tag{B.4.7}$$

### B.4.2 Quantum system

The Hamiltonian operator for the free particle on a ring is

$$\hat{H} = \frac{1}{2mR^2}\hat{J}^2 \equiv B\hat{J}^2 \tag{B.4.8}$$

The partition function for this Hamiltonian is

$$Z = \mathrm{Tr}\left[e^{-\beta B\hat{J}^2}\right] = \sum_{j=-\infty}^{\infty} e^{-\beta B j^2} = \vartheta_3\left(0, e^{-\beta B}\right) \tag{B.4.9}$$

where

$$\vartheta_3(z,q) := \sum_{j=-\infty}^{\infty} q^{j^2} e^{2ijz} \tag{B.4.10}$$

is one of the Jacobi theta functions. The dipole autocorrelation function for this system is

$$\langle \cos\hat{\varphi}\cos\hat{\varphi}(t)\rangle = \frac{1}{Z}\mathrm{Tr}\Big[e^{-\beta B\hat{J}^2}\cos\hat{\varphi}e^{iB\hat{J}^2t/\hbar}\cos\hat{\varphi}e^{-iB\hat{J}^2t/\hbar}\Big] \tag{B.4.11}$$

$$= \frac{1}{4Z}\sum_{j=-\infty}^{\infty} e^{-\beta Bj^2}\,\langle j|(\hat{U}+\hat{U}^\dagger)e^{iB\hat{J}^2t/\hbar}(\hat{U}+\hat{U}^\dagger)|j\rangle\, e^{-iBj^2t/\hbar} \tag{B.4.12}$$

$$= \frac{1}{4Z}\sum_{j=-\infty}^{\infty} e^{-\beta Bj^2}\left(e^{iB(j+1)^2t/\hbar}+e^{iB(j-1)^2t/\hbar}\right)e^{-iBj^2t/\hbar} \tag{B.4.13}$$

$$= \frac{1}{4Z}e^{iBt/\hbar}\sum_{j=-\infty}^{\infty} e^{-\beta Bj^2}\left(e^{2iBjt/\hbar}+e^{-2iBjt/\hbar}\right) \tag{B.4.14}$$

Using the fact that both sums are identical we can combine them to retrieve

$$\langle \cos\hat{\varphi}\cos\hat{\varphi}(t)\rangle = \frac{1}{2Z}e^{iBt/\hbar}\sum_{j=-\infty}^{\infty} e^{-\beta Bj^2}e^{2iBjt/\hbar} \tag{B.4.15}$$

$$= \frac{1}{2}e^{iBt/\hbar}\frac{\vartheta_3\Big(Bt/\hbar, e^{-\beta B}\Big)}{\vartheta_3\Big(0, e^{-\beta B}\Big)} \tag{B.4.16}$$

The Kubo transformed dipole autocorrelation function for this system is

$$\langle \cos\hat{\varphi}\cos\hat{\varphi}(t)\rangle_{(K)} = \frac{1}{Z}\mathrm{Tr}\left[\int_0^1 du\, e^{-\beta B\hat{J}^2}e^{uB\hat{J}^2}\cos\hat{\varphi}e^{-uB\hat{J}^2}e^{iB\hat{J}^2t/\hbar}\cos\hat{\varphi}e^{-iB\hat{J}^2t/\hbar}\right] \tag{B.4.17}$$

$$= \frac{1}{4Z}\sum_{j=-\infty}^{\infty}\int_0^1 du\, e^{-\beta Bj^2}e^{(u-it/\hbar)Bj^2}\,\langle j|(\hat{U}+\hat{U}^\dagger)e^{-uB\hat{J}^2}e^{iB\hat{J}^2t/\hbar}(\hat{U}+\hat{U}^\dagger)|j\rangle \tag{B.4.18}$$

$$= \frac{1}{4Z}\sum_{j=-\infty}^{\infty}\int_0^1 du\, e^{-\beta Bj^2}e^{(u-it/\hbar)Bj^2}\left(e^{-(u-it/\hbar)B(j+1)^2}+e^{-(u-it/\hbar)B(j-1)^2}\right) \tag{B.4.19}$$

$$= \frac{1}{4Z}e^{iBt/\hbar}\sum_{j=-\infty}^{\infty} e^{-\beta Bj^2}\left(e^{2iBjt/\hbar}\frac{1-e^{-\beta B(2j+1)}}{\beta B(2j+1)}+e^{-2iBjt/\hbar}\frac{1-e^{-\beta B(-2j+1)}}{\beta B(-2j+1)}\right) \tag{B.4.20}$$

Since both sums are again identical we can combine them

$$\langle \cos\hat{\varphi}\cos\hat{\varphi}(t)\rangle_{(K)} = \frac{1}{2Z}e^{iBt/\hbar}\sum_{j=-\infty}^{\infty} e^{-\beta Bj^2}e^{2iBjt/\hbar}\frac{1-e^{-\beta B(2j+1)}}{\beta B(2j+1)} \tag{B.4.21}$$

We now wish to compare these two quantum autocorrelation functions to the classical autocorrelation function in the $\beta \to 0$ limit. This is equivalent to the $e^{-\beta B} \to 1$ limit, and so the following limit of the Jacobi theta function will prove useful

$$\lim_{q\to 1}\vartheta_3(z,q) = \text{ш}(z/\pi) \tag{B.4.22}$$

We define the Shah function, also known as the Dirac comb, as

$$\text{ш}(t) := \sum_{j=-\infty}^{\infty} \delta(t-j) = \sum_{j=-\infty}^{\infty} e^{2\pi i k t} \tag{B.4.23}$$

where it follows that $\text{ш}(0) = \delta(0)$ and therefore the limit of the partition function is $\delta(0)$. The Shah function has the useful sampling property

$$f(t)\text{ш}(t) = \sum_{j=-\infty}^{\infty} f(j)\delta(t-j) \tag{B.4.24}$$

Although the appearance of the Dirac delta distribution in the limits is problematic, we will still be able to derive physical meaning from the results. The high temperature limit of the dipole autocorrelation function is

$$\lim_{\beta\to 0}\langle \cos\hat{\varphi}\cos\hat{\varphi}(t)\rangle = \frac{1}{2}\frac{\text{ш}\left(Bt/\pi\hbar\right)}{\delta(0)} \tag{B.4.25}$$

$$= \frac{1}{2\delta(0)} e^{iBt/\hbar} \sum_{j=-\infty}^{\infty} \delta(j - Bt/\pi\hbar) \tag{B.4.26}$$

Since the function is only non-zero when $Bt/\pi\hbar$ is an integer, the complex exponential will only ever be non-zero when $e^{itB/\hbar} = \pm 1$. Assuming that the delta functions will cancel at these points allows us to retrieve the following limiting case for this correlation function

$$\lim_{\beta\to 0}\langle \cos\hat{\varphi}\cos\hat{\varphi}(t)\rangle = \begin{cases} 1/2 & \text{if } Bt/\pi\hbar \text{ is even} \\ -1/2 & \text{if } Bt/\pi\hbar \text{ is odd} \\ 0 & \text{otherwise} \end{cases} \tag{B.4.27}$$

We now compute the high temperature limit of the Kubo-transformed correlation function

$$\lim_{\beta\to 0}\langle \cos\hat{\varphi}\cos\hat{\varphi}(t)\rangle_{(K)} = \frac{1}{2\delta(0)} e^{iBt/\hbar} \sum_{j=-\infty}^{\infty} e^{2iBjt/\hbar} \tag{B.4.28}$$

$$= \frac{1}{2\delta(0)} e^{iBt/\hbar} \sum_{j=-\infty}^{\infty} \delta(j - Bt/\pi\hbar) \tag{B.4.29}$$

and so the limit is identical to the regular correlation function

$$\lim_{\beta\to 0}\langle \cos\hat{\varphi}\cos\hat{\varphi}(t)\rangle_{(K)} = \begin{cases} 1/2 & \text{if } Bt/\pi\hbar \text{ is even} \\ -1/2 & \text{if } Bt/\pi\hbar \text{ is odd} \\ 0 & \text{otherwise} \end{cases} \tag{B.4.30}$$

We note that even in the high temperature limit the classical and quantum cases of the free particle on a ring are different, with the quantum version experiencing periodic recoherence. We have not ruled out that this result is a product of some error when taking the limit.

# Appendix C

# Projections

## C.1 Coherent state centroid density

Here we derive the centroid density when the projection is onto a coherent state of the QHO. Recall that the definition of the QHO coherent states is

$$|z\rangle := e^{-\frac{|z|^2}{2}} \sum_{n=0}^{\infty} \frac{z^n}{\sqrt{n!}} |n\rangle = e^{-\frac{|z|^2}{2}} e^{z\hat{a}^\dagger} |0\rangle \tag{C.1.1}$$

where $z$ is any complex number. We first split the operator exponential of the effective centroid Hamiltonian

$$\hat{H}' := \hat{H} - i\frac{\xi}{\beta}\hat{q} - i\frac{\eta}{\beta}\hat{p} \tag{C.1.2}$$

into a product of operator exponentials using the results from section C.3, specifically (C.3.4) where the operators are reordered with (C.3.44)

$$e^{-\beta\hbar\omega\left(\hat{N}+\frac{1}{2}\right)+i\nu^*\hat{a}+i\nu\hat{a}^\dagger} = e^{-|\nu|^2\frac{e^{-\beta\hbar\omega}+\beta\hbar\omega-1}{(\beta\hbar\omega)^2}} e^{i\nu\frac{e^{-\beta\hbar\omega}-1}{\beta\hbar\omega}\hat{a}^\dagger} e^{-\beta\hbar\omega\left(\hat{N}+\frac{1}{2}\right)} e^{i\nu\frac{e^{-\beta\hbar\omega}-1}{\beta\hbar\omega}\hat{a}} \tag{C.1.3}$$

where we have defined

$$\nu := \sqrt{\frac{\hbar}{2m\omega}}\,(\xi + im\omega\eta) \tag{C.1.4}$$

To work out the coherent state density we will need to use the fact that the coherent state is the right eigenvector for the annihilation operator, and hence the left eigenvector for the creation operator

$$\hat{a}\,|z\rangle = z\,|z\rangle \qquad \langle z|\,\hat{a}^\dagger = \langle z|\,z^* \qquad \langle z|\hat{N}|z\rangle = |z|^2 \equiv |\langle n|z\rangle|^2 \tag{C.1.5}$$

It is also useful to show that

$$\langle z|e^{\lambda\hat{N}}|z\rangle = e^{-|z|^2} \sum_{m,n=0}^{\infty} \frac{\alpha^n(\alpha^*)^m}{\sqrt{n!m!}} \langle m|e^{\lambda\hat{N}}|n\rangle \tag{C.1.6}$$

$$= e^{-|z|^2} \sum_{n=0}^{\infty} \frac{(|\alpha|^2 e^{\lambda})^n}{n!} \tag{C.1.7}$$

$$= \exp\Big(-|z|^2\left(1-e^{\lambda}\right)\Big) \tag{C.1.8}$$

The diagonal matrix elements of (C.1.3) in the coherent state representation can now be worked out

$$\langle z|e^{-\beta\hat{H}'}|z\rangle = e^{-|\nu|^2\frac{e^{-\beta\hbar\omega}+\beta\hbar\omega-1}{(\beta\hbar\omega)^2}}\langle z|e^{i\nu\frac{1-e^{-\beta\hbar\omega}}{\beta\hbar\omega}\hat{a}^\dagger}e^{-\beta\hbar\omega\left(\hat{N}+\frac{1}{2}\right)}e^{i\nu\frac{1-e^{-\beta\hbar\omega}}{\beta\hbar\omega}\hat{a}}|z\rangle \tag{C.1.9}$$

$$= e^{-\beta\hbar\omega/2}e^{-|\nu|^2\frac{e^{-\beta\hbar\omega}+\beta\hbar\omega-1}{(\beta\hbar\omega)^2}}e^{i\nu\frac{1-e^{-\beta\hbar\omega}}{\beta\hbar\omega}z^*}e^{i\nu\frac{1-e^{-\beta\hbar\omega}}{\beta\hbar\omega}z}\langle z|e^{-\beta\hbar\omega\hat{N}}|z\rangle \tag{C.1.10}$$

$$= e^{-\beta\hbar\omega/2}e^{-|\nu|^2\frac{e^{-\beta\hbar\omega}+\beta\hbar\omega-1}{(\beta\hbar\omega)^2}}e^{i\frac{1-e^{-\beta\hbar\omega}}{\beta\hbar\omega}(\nu z^*+\nu^* z)}e^{-|z|^2(1-e^{-\beta\hbar\omega})} \tag{C.1.11}$$

Reintroducing the original parameters, the matrix element is

$$\begin{aligned}\langle z|e^{-\beta\hat{H}'}|z\rangle =& e^{-\beta\hbar\omega/2}e^{-(1-e^{-\beta\hbar\omega})|z|^2}e^{-\left(\frac{\hbar}{2m\omega}\xi^2+\frac{m\omega\hbar}{2}\eta^2\right)\frac{e^{-\beta\hbar\omega}+\beta\hbar\omega-1}{(\beta\hbar\omega)^2}}\\ &\times e^{i\xi\sqrt{\frac{\hbar}{2m\omega}}\frac{1-e^{-\beta\hbar\omega}}{\beta\hbar\omega}(z+z^*)}e^{i\eta\sqrt{\frac{m\omega\hbar}{2}}\frac{1-e^{-\beta\hbar\omega}}{\beta\hbar\omega}i(z^*-z)}\end{aligned} \tag{C.1.12}$$

Ignoring the constant term $e^{-\beta\hbar\omega/2}e^{-(1-e^{-\beta\hbar\omega})|z|^2}$, we can now perform the Fourier integrals

$$\iint\hbar\frac{d\xi\,d\eta}{2\pi}e^{-\left(\frac{\hbar}{2m\omega}\xi^2+\frac{m\omega\hbar}{2}\eta^2\right)\frac{e^{-\beta\hbar\omega}+\beta\hbar\omega-1}{(\beta\hbar\omega)^2}}e^{-i\xi\left(x_c-\sqrt{\frac{\hbar}{2m\omega}}\frac{1-e^{-\beta\hbar\omega}}{\beta\hbar\omega}(z+z^*)\right)}e^{-i\eta\left(p_c-\sqrt{\frac{m\omega\hbar}{2}}\frac{1-e^{-\beta\hbar\omega}}{\beta\hbar\omega}i(z^*-z)\right)} \tag{C.1.13}$$

$$= \frac{(\beta\hbar\omega)^2}{e^{-\beta\hbar\omega}+\beta\hbar\omega-1}e^{-\frac{(\beta\hbar\omega)^2}{4(e^{-\beta\hbar\omega}+\beta\hbar\omega-1)}\left[\left(\sqrt{\frac{2m\omega}{\hbar}}x_c-\frac{1-e^{-\beta\hbar\omega}}{\beta\hbar\omega}(z+z^*)\right)^2+\left(\sqrt{\frac{2}{m\omega\hbar}}p_c-\frac{1-e^{-\beta\hbar\omega}}{\beta\hbar\omega}i(z^*-z)\right)^2\right]} \tag{C.1.14}$$

$$= \frac{(\beta\hbar\omega)^2}{e^{-\beta\hbar\omega}+\beta\hbar\omega-1}e^{-\frac{(\beta\hbar\omega)^2}{e^{-\beta\hbar\omega}+\beta\hbar\omega-1}\left[\left(\mathrm{Re}(a_c)-\frac{1-e^{-\beta\hbar\omega}}{\beta\hbar\omega}\mathrm{Re}(z)\right)^2+\left(\mathrm{Im}(a_c)-\frac{1-e^{-\beta\hbar\omega}}{\beta\hbar\omega}\mathrm{Im}(z)\right)^2\right]} \tag{C.1.15}$$

$$= \frac{(\beta\hbar\omega)^2}{e^{-\beta\hbar\omega}+\beta\hbar\omega-1}e^{-|z|^2\left(\frac{(1-e^{-\beta\hbar\omega})^2}{e^{-\beta\hbar\omega}+\beta\hbar\omega-1}\right)}e^{-\frac{(\beta\hbar\omega)^2}{e^{-\beta\hbar\omega}+\beta\hbar\omega-1}|a_c|^2}e^{\frac{\beta\hbar\omega(1-e^{-\beta\hbar\omega})}{e^{-\beta\hbar\omega}+\beta\hbar\omega-1}(za_c^*+z^*a_c)} \tag{C.1.16}$$

$$\tag{C.1.17}$$

where we have substituted the position and momentum centroid symbols for a complex ladder operator centroid symbol

$$a_c := \sqrt{\frac{m\omega}{2\hbar}}\left(q_c+\frac{i}{m\omega}p_c\right) \tag{C.1.18}$$

Subbing the constant term back into (C.1.16) we can simplify further and so retrieve an expression for the coherent state projected centroid density

$$\rho_c^{(z)}(a_c,a_c^*)$$

$$= \frac{(\beta\hbar\omega)^2e^{-\beta\hbar\omega/2}}{e^{-\beta\hbar\omega}+\beta\hbar\omega-1}e^{-(1-e^{-\beta\hbar\omega})|z|^2}e^{-|z|^2\left(\frac{(1-e^{-\beta\hbar\omega})^2}{e^{-\beta\hbar\omega}+\beta\hbar\omega-1}\right)}e^{-\frac{(\beta\hbar\omega)^2}{e^{-\beta\hbar\omega}+\beta\hbar\omega-1}|a_c|^2}e^{\frac{\beta\hbar\omega(1-e^{-\beta\hbar\omega})}{e^{-\beta\hbar\omega}+\beta\hbar\omega-1}(za_c^*+z^*a_c)} \tag{C.1.19}$$

$$= \frac{\beta\hbar\omega}{\sinh(\beta\hbar\omega/2)}\frac{1}{1+\alpha}\exp\left(-\frac{2}{1+\alpha}|z|^2\right)\exp\left(-\left(\beta\hbar\omega+\frac{2}{1+\alpha}\right)|a_c|^2\right)\exp\left(\frac{2}{1+\alpha}(za_c^*+z^*a_c)\right) \tag{C.1.20}$$

$$= \frac{\beta\hbar\omega}{\sinh(\beta\hbar\omega/2)}\frac{1}{1+\alpha}\exp\left(-\beta\hbar\omega|a_c|^2\right)\exp\left(-\frac{2}{1+\alpha}|z-a_c|^2\right) \tag{C.1.21}$$

We have introduced a new parameter $\alpha$ into our final results to better relate the results to those from [21] where it appears frequently to compactify the results obtained for the QHO

$$\alpha := \coth\left(\frac{\beta\hbar\omega}{2}\right) - \frac{2}{\beta\hbar\omega} \tag{C.1.22}$$

We can write this in the usual centroid symbols as

$$\begin{aligned}\rho_c^{(z)}(q_c,p_c) = &\frac{\beta\hbar\omega}{\sinh(\beta\hbar\omega/2)}\frac{1}{1+\alpha}\exp\left(-\frac{2}{1+\alpha}|z|^2\right)\exp\left(-\left(\beta\hbar\omega+\frac{2}{1+\alpha}\right)\left(\frac{m\omega}{2\hbar}q_c^2+\frac{1}{2m\omega\hbar}p_c^2\right)\right)\\ &\times\exp\left(\frac{2}{1+\alpha}\left(\sqrt{\frac{2m\omega}{\hbar}}\operatorname{Re}(z)q_c+\sqrt{\frac{2}{m\omega\hbar}}\operatorname{Im}(z)p_c\right)\right)\end{aligned} \tag{C.1.23}$$

where we can see that the distribution is a Gaussian centred at the amplitude of the coherent state and is entirely real and positive. Recalling that the coherent states form an over complete basis, the resolution of the identity is

$$\mathbb{1} = \frac{1}{\pi}\int d^2z\ |z\rangle\langle z|, \quad \text{where} \quad d^2z = d\operatorname{Re}(z)\, d\operatorname{Im}(z) \tag{C.1.24}$$

Integrating over all coherent state centroid densities gives us

$$\begin{aligned}&\frac{1}{\pi}\int d^2z\rho_c^{(z)}(q_c,p_c)\\ &= \frac{\beta\hbar\omega}{\pi\sinh(\beta\hbar\omega/2)}\frac{1}{1+\alpha}\left(\sqrt{\frac{\pi(1+\alpha)}{2}}\right)^2 e^{\frac{1+\alpha}{8}\left(\frac{2}{1+\alpha}\right)^2\left(\frac{2m\omega}{\hbar}q_c^2+\frac{2}{m\omega\hbar}p_c^2\right)}e^{-\left(\beta\hbar\omega+\frac{2}{1+\alpha}\right)\left(\frac{m\omega}{2\hbar}q_c^2+\frac{1}{2m\omega\hbar}p_c^2\right)}\end{aligned} \tag{C.1.25}$$

$$= \frac{\beta\hbar\omega}{2\sinh(\beta\hbar\omega/2)}\exp\left(-\beta\hbar\omega\left(\frac{m\omega}{2\hbar}q_c^2+\frac{1}{2m\omega\hbar}p_c^2\right)\right) \tag{C.1.26}$$

which is indeed to usual centroid distribution for the QHO.

## C.2 Number state representation centroid density

We will derive the number eigenstate representation of the Fourier transform of the centroid density

$$\rho_c^{(n,m)}(q_c,p_c) := \int_{-\infty}^{\infty}\int_{-\infty}^{\infty}\hbar\frac{d\xi\, d\eta}{2\pi}\langle n|e^{\beta\hat{H}'}|m\rangle \tag{C.2.1}$$

To do this we will use the diagonal elements of the coherent state representation, which was derived in the previous section and the fact that the number eigenstate representation of an arbitrary operator, $\hat{A}$, may be obtained from the coherent state representation via the following relation [39, pp. 102]

$$\langle n|\hat{A}|m\rangle = \frac{1}{\sqrt{n!m!}}\frac{\partial^n}{\partial z^{*n}}\frac{\partial^m}{\partial z^m}\left(e^{|z|^2}\langle z|\hat{A}|z\rangle\right)|_{z=0} \tag{C.2.2}$$

Subbing in the result from the previous section this then becomes

$$\rho_c^{(n,m)} = \frac{1}{\sqrt{n!m!}}\frac{\beta\hbar\omega}{\sinh(\beta\hbar\omega/2)}\frac{1}{1+\alpha}e^{-(\beta\hbar\omega+\frac{2}{1+\alpha})|a_c|^2}\frac{\partial^n}{\partial z^{*n}}\frac{\partial^m}{\partial z^m}\left(e^{-zz^*\left(-1+\frac{2}{1+\alpha}\right)}e^{\frac{2}{1+\alpha}(za_c^*+z^*a_c)}\right)\Bigg|_{z=0} \tag{C.2.3}$$

For temporary compactness when taking the derivatives, we define two intermediate constants

$$\mu = \frac{2}{1+\alpha} \qquad \lambda = -1 + \frac{2}{1+\alpha} = \frac{1-\alpha}{1+\alpha} \tag{C.2.4}$$

and the expression we differentiate becomes

$$\frac{\partial^n}{\partial z^{*n}} \frac{\partial^m}{\partial z^m} \left( e^{-zz^*\lambda} e^{\mu(za_c^* + z^* a_c)} \right) \Bigg|_{z=0} \tag{C.2.5}$$

We make a useful change of coordinates to retrieve

$$\lambda^{\frac{m+n}{2}} e^{\frac{\mu^2}{\lambda}|a_c|^2} \frac{\partial^n}{\partial \Xi^{*n}} \frac{\partial^m}{\partial \Xi^m} e^{-\Xi^*\Xi} \Bigg|_{\Xi = -\frac{\mu}{\sqrt{\lambda}} a_c} \quad \text{where} \quad \Xi = \sqrt{\lambda} z - \frac{\mu}{\sqrt{\lambda}} a_c \tag{C.2.6}$$

which we immediately replace with the 2D Laguerre polynomial, defined as follows [40]

$$L_{n,m}(z, z^*) = (-1)^{n+m} e^{zz^*} \frac{\partial^n}{\partial z^{*n}} \frac{\partial^m}{\partial z^m} e^{-zz^*} \tag{C.2.7}$$

$$= (-1)^m m!\, z^{n-m}\, L_m^{(n-m)}(zz^*) \tag{C.2.8}$$

$$= (-1)^n n!\, z^{*m-n}\, L_n^{(m-n)}(zz^*) \tag{C.2.9}$$

where $L_k^{(a)}(x)$ is the associated Laguerre polynomial. It follows that (C.2.6) may be written as

$$\begin{aligned} &(-1)^n m! \lambda^{\frac{m+n}{2}} e^{\frac{\mu^2}{\lambda}|a_c|^2} e^{-\Xi\Xi^*} \Xi^{n-m} L_m^{(n-m)}(\Xi\Xi^*) \Big|_{\Xi = -\frac{\mu}{\sqrt{\lambda}} a_c} \\ =&(-1)^n m! \lambda^{\frac{m+n}{2}} \left( -\frac{\mu}{\sqrt{\lambda}} a_c \right)^{n-m} L_m^{(n-m)}\left( \frac{\mu^2}{\lambda} |a_c|^2 \right) \end{aligned} \tag{C.2.10}$$

Replacing the two constants (C.2.3) now becomes

$$\rho_c^{(n,m)} = \sqrt{\frac{m!}{n!}} \frac{\beta\hbar\omega}{\sinh(\beta\hbar\omega/2)} \frac{(-1)^m}{1+\alpha} \left( \frac{1-\alpha}{1+\alpha} \right)^m \left( \frac{2}{1+\alpha} a_c \right)^{n-m} e^{-(\beta\hbar\omega + \frac{2}{1+\alpha})|a_c|^2} L_m^{(n-m)}\left( \frac{4}{1-\alpha^2} |a_c|^2 \right) \tag{C.2.11}$$

$$= \sqrt{\frac{n!}{m!}} \frac{\beta\hbar\omega}{\sinh(\beta\hbar\omega/2)} \frac{(-1)^n}{1+\alpha} \left( \frac{1-\alpha}{1+\alpha} \right)^n \left( \frac{2}{1+\alpha} a_c^* \right)^{m-n} e^{-(\beta\hbar\omega + \frac{2}{1+\alpha})|a_c|^2} L_n^{(m-n)}\left( \frac{4}{1-\alpha^2} |a_c|^2 \right) \tag{C.2.12}$$

In the case where we have some general projection represented in the number eigenstate basis as

$$\hat{\mathcal{P}} = \sum_{m,n=0}^{\infty} c_{m,n} \left| m \right\rangle \left\langle n \right| \tag{C.2.13}$$

then the associated state projected centroid density is

$$\rho_c(q_c, p_c) = \sum_{m,n=0}^{\infty} c_{m,n} \rho_c^{(n,m)}(q_c, p_c) \tag{C.2.14}$$

**Number eigenstate centroid projection**

In the case of projection onto a single number eigenstate the density reduces to

$$\rho_c^{(n)}(q_c,p_c)=\frac{\beta\hbar\omega}{\sinh(\beta\hbar\omega/2)}\frac{(-1)^n}{1+\alpha}\exp\!\left[-\left(\beta\hbar\omega+\frac{2}{1+\alpha}\right)|a_c|^2\right]\left(\frac{1-\alpha}{1+\alpha}\right)^n L_n\!\left(\frac{4}{1-\alpha^2}|a_c|^2\right) \tag{C.2.15}$$

Calculating the high temperature limit gives

$$\lim_{\beta\to 0}\rho_c^{(n)}(q_c,p_c)=(-1)^n\exp\!\left[-2\left(p_c^2\frac{1}{2m\omega\hbar}+q_c^2\frac{m\omega}{2\hbar}\right)\right]L_n\!\left[4\left(p_c^2\frac{1}{2m\omega\hbar}+q_c^2\frac{m\omega}{2\hbar}\right)\right] \tag{C.2.16}$$

and here we immediately notice the relation

$$\lim_{\beta\to 0}\rho_c^{(n)}(q_c,p_c)=2\pi\hbar W_n(q_c,p_c) \tag{C.2.17}$$

where $W_n(q_c,p_c)$ is the Wigner function for the $n^{\text{th}}$ eigenstate of the QHO. To determine the low temperature limit we note that the $\alpha$ parameter tends to 1 and so in this case all state projected centroid densities are 0 except for the ground state, which is simply a Gaussian

$$\lim_{\beta\to\infty}\rho_c^{(0)}=\exp\left[-\frac{1}{2\hbar}\left(m\omega q_c^2+\frac{1}{m\omega}p_c^2\right)\right] \tag{C.2.18}$$

Integration of this over the centroid phase space yields a partition function of 1 as is expected in this limit. Summation over all the state projected centroid densities should yield the expected density for the QHO. First we make use of the generating function for the Laguerre polynomials

$$\sum_{n=0}^{\infty}t^n L_n(x)=\frac{1}{1-t}e^{-\frac{tx}{1-t}} \tag{C.2.19}$$

We therefore have that $t=\dfrac{\alpha-1}{\alpha+1}$ so that $1-t=\dfrac{2}{\alpha+1}$. Using this we can write

$$\sum_{n=0}^{\infty}\rho_c^{(n)}(q_c,p_c)=\frac{\beta\hbar\omega}{\sinh(\beta\hbar\omega/2)}\frac{1}{1+\alpha}e^{-\left(\beta\hbar\omega+\frac{2}{1+\alpha}\right)|a_c|^2}\sum_{n=0}^{\infty}\left(\frac{\alpha-1}{\alpha+1}\right)^n L_n\!\left[\frac{4}{1-\alpha^2}|a_c|^2\right] \tag{C.2.20}$$

$$=\frac{\beta\hbar\omega}{\sinh(\beta\hbar\omega/2)}\frac{1}{1+\alpha}\left(\frac{\alpha+1}{2}\right)e^{-\left(\beta\hbar\omega+\frac{2}{1+\alpha}\right)|a_c|^2}e^{-\left(\frac{\alpha+1}{2}\right)\left(\frac{\alpha-1}{\alpha+1}\right)\left(\frac{4}{1-\alpha^2}|a_c|^2\right)} \tag{C.2.21}$$

$$=\frac{\beta\hbar\omega}{2\sinh(\beta\hbar\omega/2)}e^{-\beta\hbar\omega|a_c|^2} \tag{C.2.22}$$

which is indeed the canonical centroid density for the QHO.

## C.3 Splitting the operator exponential

When obtaining analytic results for the quantum harmonic oscillator, it is useful to have a more workable form of the operator exponential

$$e^{-\beta(\hat{p}^2/2m+m\omega^2\hat{q}^2/2)+i\xi\hat{q}+i\eta\hat{p}} \tag{C.3.1}$$

which we rewrite as

$$e^{-\beta\hbar\omega(\hat{N}+\frac{1}{2})+i\nu^*\hat{a}+i\nu\hat{a}^\dagger} \tag{C.3.2}$$

where we redefine the Fourier variables as

$$\nu := \sqrt{\frac{\hbar}{2m\omega}}\,(\xi + im\omega\eta) \tag{C.3.3}$$

Our goal is then to prove that the following equality is true

$$e^{-\beta\hbar\omega\hat{N}+i\nu^*\hat{a}+i\nu\hat{a}^\dagger} = e^{-|\nu|^2\frac{e^{-\beta\hbar\omega}+\beta\hbar\omega-1}{(\beta\hbar\omega)^2}} e^{-\beta\hbar\omega\hat{N}} e^{i\nu\frac{e^{\beta\hbar\omega}-1}{\beta\hbar\omega}\hat{a}^\dagger} e^{i\nu^*\frac{1-e^{-\beta\hbar\omega}}{\beta\hbar\omega}\hat{a}} \tag{C.3.4}$$

To accomplish this an expansion related to the Baker-Campbell-Hausdorf formula known as the Zassenhaus formula will be used. This states that given two objects $X$ and $Y$ which generate a Lie algebra $\mathcal{L}(X,Y)$, the exponential $e^{\lambda(X+Y)}$ may be decomposed as

$$e^{\lambda(X+Y)} = e^{\lambda X} e^{\lambda Y} \prod_{n=2}^{\infty} e^{\lambda^n C_n(X,Y)} \tag{C.3.5}$$

where $\lambda \in \mathbb{C}$ and $C_n(X,Y) \in \mathcal{L}(X,Y)$ is a homogeneous Lie polynomial in X and Y and of degree n. For clarity, a completely general form of (C.3.2) will be used so that we instead have to solve

$$e^{\lambda\hat{N}+q\hat{a}+r\hat{a}^\dagger} = e^{qr\frac{1+\lambda-e^\lambda}{\lambda^2}} e^{\lambda\hat{N}} e^{\frac{1-e^{-\lambda}}{\lambda}r\hat{a}^\dagger} e^{\frac{e^\lambda-1}{\lambda}q\hat{a}} \tag{C.3.6}$$

where $\lambda, q, r \in \mathbb{C}$. Using the QDO creation and annihilation operators as the base, a more convenient set of operators is defined

$$X := \hat{N} \qquad Y := \frac{q\hat{a}+r\hat{a}^\dagger}{\lambda} \qquad Z := \frac{-q\hat{a}+r\hat{a}^\dagger}{\lambda} \tag{C.3.7}$$

where despite the lack of "hats" the objects are understood to be operators. Recalling the known commutation relations for the QDO creation and annihilation operators

$$[\hat{N},\hat{a}] = -\hat{a} \qquad [\hat{N},\hat{a}^\dagger] = \hat{a}^\dagger \qquad [\hat{a},\hat{a}^\dagger] = 1 \tag{C.3.8}$$

and taking the Lie bracket $[\cdot,\cdot]$ to be the commutator, the Lie algebra generated by $X$ and $Y$ is therefore

$$[X,Y] = Z \qquad [X,Z] = Y \qquad [Y,Z] = \frac{2qr}{\lambda^2} := \kappa \tag{C.3.9}$$

The Lie polynomials in the Zassenhaus expansion for this group of operators are

$$C_{2m} = -\frac{1}{(2m)!}Z \qquad C_{2m+1} = \frac{1}{(2m+1)!}Y + \mu_{2m+1}\kappa \tag{C.3.10}$$

where $\mu_{2m+1}$ is a constant that is only recursively dependent on the coefficients for the operator terms in the Lie polynomials. To show that these statements are true we use the recursive definition for the Lie polynomials from [41]

$$C_{n+1} = \frac{1}{n+1} \sum_{(i_0,i_1,\ldots,i_n)\in\mathscr{I}_n} \frac{(-1)^{i_0+\cdots+i_n}}{i_0!i_1!\cdots i_n!} \mathrm{ad}_{C_n}^{i_n}\cdots\mathrm{ad}_{C_2}^{i_2}\mathrm{ad}_Y^{i_1}\mathrm{ad}_X^{i_0}Y \tag{C.3.11}$$

$\mathscr{I}_n$ is defined as the set of $(n+1)$-tuples of non-negative integers with the following properties

$$i_0 + i_1 + 2i_2 + \cdots + ni_n = n \tag{C.3.12}$$

$$i_0 + i_1 + 2i_2 + \cdots + ji_j \geq j+1 \quad \text{for } j = 0, \ldots, n-1 \tag{C.3.13}$$

$$i_m = 0 \quad \text{if } m > n/2 \tag{C.3.14}$$

Here $\text{ad}_A^n$ is referred to as the adjoint representation of the Lie algebra, which may be defined in terms of the Lie bracket as follows

$$\text{ad}_A^n B = [A, \text{ad}_A^{n-1} B] \qquad \text{ad}_A^1 B = [A, B] \qquad \text{ad}_A^0 B = B \qquad \text{ad}_{A+k}^n B = \text{ad}_A^n B \qquad \text{ad}_{kA}^n B = k^n \text{ad}_A^n B \tag{C.3.15}$$

where $A$ and $B$ are arbitrary operators, $n$ is a non-negative integer, and $k$ is a scalar. In our case these terms will simply generate a series of nested commutators. We will prove the statements (C.3.10) using strong induction with the recursive definition of the Lie polynomials (C.3.11). We first prove for the even and odd order Lie polynomial base cases, $n = 2, 3$. According to (C.3.10) these should be

$$C_2 = -\frac{1}{2} Z \qquad C_3 = \frac{1}{6} Y + \mu_3 \kappa \tag{C.3.16}$$

To show that (C.3.11) is consistent for the even base case, we first determine that the set of tuples is $\mathscr{I}_1 = \{(1, 0)\}$. We then have

$$C_2 = \frac{1}{2} \sum_{(i_0, i_1) \in \mathscr{I}_1} \frac{(-1)^{i_0 + i_1}}{i_0! i_1!} \text{ad}_Y^{i_1} \text{ad}_X^{i_0} Y \tag{C.3.17}$$

$$= -\frac{1}{2} \frac{1}{1!0!} \text{ad}_Y^0 \text{ad}_X^1 Y \tag{C.3.18}$$

$$= -\frac{1}{2} [X, Y] = -\frac{1}{2} Z \tag{C.3.19}$$

which is in agreement with the base case. Next for the odd base case, the set of tuples is $\mathscr{I}_2 = \{(2, 0, 0), (1, 1, 0)\}$. The Lie polynomial is then

$$C_3 = \frac{1}{3} \sum_{(i_0, i_1, i_2) \in \mathscr{I}_2} \frac{(-1)^{i_0 + i_1 + i_2}}{i_0! i_1! i_2!} \text{ad}_{C_2}^{i_2} \text{ad}_Y^{i_1} \text{ad}_X^{i_0} Y \tag{C.3.20}$$

$$= \frac{1}{3} \left( \frac{1}{2!0!0!} \text{ad}_{C_2}^0 \text{ad}_Y^0 \text{ad}_X^2 Y + \frac{1}{1!1!0!} \text{ad}_{C_2}^0 \text{ad}_Y^1 \text{ad}_X^1 Y \right) \tag{C.3.21}$$

$$= \frac{1}{3} \left( \frac{1}{2} \text{ad}_X^1 Z + \text{ad}_Y^1 Z \right) \tag{C.3.22}$$

$$= \frac{1}{6} Y + \frac{1}{3} \kappa \tag{C.3.23}$$

which is agreement with the base case, where it has been determined that $\mu_3 = 1/3$. Now that we know the base case is in agreement, we assume (C.3.10) works for all $C_k, k < n$ and must now prove it holds for the next greatest even integer $2m \geq n$ and odd integer $2l + 1 \geq n$. We begin with the even case. Using the properties (C.3.15) and the inductive hypothesis, the even order Lie polynomial may be written as

$$C_{2m} = \frac{1}{2m} \sum_{\mathscr{I}_{2m-1}} \frac{(-1)^{i_0 + \cdots i_{2m-1}}}{i_0! \cdots i_{2m-1}!} \text{ad}_{\frac{1}{(2m-1)!} Y}^{i_{2m-1}} \cdots \text{ad}_{-\frac{1}{2} Z}^{i_2} \text{ad}_Y^{i_1} \text{ad}_X^{i_0} Y \tag{C.3.24}$$

$$= \frac{1}{2m} \sum_{\mathscr{I}_{2m-1}} \frac{(-1)^{i_0 + \sum_{k=1}^m i_{2k-1}}}{i_0! \cdots i_{2m-1}!} \left( \prod_{k=1}^{2m-1} \left( \frac{1}{k!} \right)^{i_k} \right) \text{ad}_Y^{i_{2m-1}} \cdots \text{ad}_Z^{i_2} \text{ad}_Y^{i_1} \text{ad}_X^{i_0} Y \tag{C.3.25}$$

We now examine the two cases which can arise when $i_0$ is even or odd:

- If $i_0$ is odd then $\mathrm{ad}_X^{i_0} Y = Z$. In this case the only non-vanishing terms are those where $i_{2k} = 0, \forall\, 2k < 2m$ because the only terms which may appear in this Lie polynomial are proportional to $Z$ or $\kappa$ since we know that $\mathrm{ad}_Z^r Z = 0$ and $\mathrm{ad}_Z^r \kappa = 0$ for some non-negative integer $r$. The terms in the Lie polynomial with $i_0$ odd are then

$$\frac{1}{2m} \frac{(-1)^{i_0 + \sum_{k=1}^m i_{2k-1}}}{i_0! i_1! i_3! \cdots i_{2m-1}!} \left( \prod_{k=1}^m \left( \frac{1}{(2k-1)!} \right)^{i_{2k-1}} \right) \mathrm{ad}_Y^{\sum_{k=1}^m i_{2k-1}} Z \tag{C.3.26}$$

  There can be at most one non-zero commutator with $Y$ because $\mathrm{ad}_Y^0 Z = Z$ and $\mathrm{ad}_Y^1 Z = \kappa$ while $\mathrm{ad}_Y^r Z = 0$ for $r \geq 2$, so we have $\sum_{k=1}^m i_{2k-1} = \{0, 1\}$. If the sum is 1 then only one of the $i_{2k-1}$ terms would be non-zero and equal to unity. From (C.3.12) we require that $i_0 + (2k-1) = 2m - 1$, so this tuple is not possible since $2k-1$ and $i_0$ are both odd and cannot sum to an odd number. If the sum is 0, then only the $i_0$ term is non-zero and by (C.3.12) we must have that $i_0 = 2m-1$. Therefore, when $i_0$ is odd there is only one non-zero term

$$\frac{1}{2m} \frac{(-1)^{i_0 + 0}}{(2m-1)! 0! \cdots 0!} \left( \prod_{k=2}^m \left( \frac{1}{(2k-1)!} \right)^0 \right) \mathrm{ad}_Y^0 Z = -\frac{1}{2m!} Z \tag{C.3.27}$$

- If $i_0$ is even then $\mathrm{ad}_X^{i_0} Y = Y$. In this case the only non-vanishing terms are those with $i_{2k-1} = 0, \forall\, 2k-1 < 2m$ because the only terms which may appear in this Lie polynomial are proportional to $Y$ or $\kappa$ since we know that $\mathrm{ad}_Y^r Y = 0$ and $\mathrm{ad}_Y^r \kappa = 0$. The terms in the Lie polynomial with $i_0$ even are then

$$\frac{1}{2m} \frac{(-1)^{i_0}}{i_0! i_2! i_4! \cdots i_{2m-2}!} \left( \prod_{k=1}^{m-1} \left( \frac{1}{(2k)!} \right)^{i_{2k}} \right) \mathrm{ad}_Z^{\sum_{k=1}^{m-1} i_{2k}} Y \tag{C.3.28}$$

  At most only one commutator with $Z$ will be non-zero because $\mathrm{ad}_Z^0 Y = Y$ and $\mathrm{ad}_Z^1 Y = -\kappa$ while $\mathrm{ad}_Z^r Y = 0$ for $r \geq 2$, so we have $\sum_{k=1}^{m-1} i_{2k} = \{0, 1\}$. If the sum is 0 then $i_0 = 2m - 1$ which generates an invalid tuple since $i_0$ is even. If the sum is 1 then only one $i_{2k}$ is non-zero and it is equal to 1. However by (C.3.12) we must have $i_0 + k = 2m - 1$ which is again not possible since $i_0$ and $k$ are even. It follows that there are no non-zero terms in the Lie polynomial when $i_0$ is even.

The only non vanishing term in the Lie polynomial corresponds to the tuple where $i_0 = 2m - 1$ and all others are 0. The Lie polynomial $C_{2m}$ is therefore

$$C_{2m} = -\frac{1}{2m!} Z \tag{C.3.29}$$

and so we have proved (C.3.10) for the even order Lie polynomials so we now move to the odd case. Using the properties (C.3.15) and the inductive hypothesis, the odd order Lie polynomial may be written as

$$C_{2l+1} = \frac{1}{2l+1} \sum_{\mathscr{I}_{2l}} \frac{(-1)^{i_0 + \cdots i_{2l}}}{i_0! \cdots i_{2l}!} \mathrm{ad}_{-\frac{1}{2l!} Z}^{i_{2l}} \mathrm{ad}_{\frac{1}{(2l-1)!} Y}^{i_{2l-1}} \cdots \mathrm{ad}_{-\frac{1}{2} Z}^{i_2} \mathrm{ad}_Y^{i_1} \mathrm{ad}_X^{i_0} Y \tag{C.3.30}$$

$$= \frac{1}{2l+1} \sum_{\mathscr{I}_{2l}} \frac{(-1)^{i_0 + \sum_{k=1}^l i_{2k-1}}}{i_0! \cdots i_{2l}!} \left( \prod_{k=1}^{2l} \left( \frac{1}{k!} \right)^{i_k} \right) \mathrm{ad}_Z^{i_{2l}} \mathrm{ad}_Y^{i_{2l-1}} \cdots \mathrm{ad}_Z^{i_2} \mathrm{ad}_Y^{i_1} \mathrm{ad}_X^{i_0} Y \tag{C.3.31}$$

Again we examine the two cases which can arise when $i_0$ is even or odd:

- If $i_0$ is odd then $\mathrm{ad}_X^{i_0} Y = Z$. In this case the only non-vanishing terms are those where $i_{2k} = 0, \forall\, 2k < 2l-1$ because the only terms which may appear in this Lie polynomial are proportional to $Z$ or $\kappa$ since we know that $\mathrm{ad}_Z^r Z = 0$ and $\mathrm{ad}_Z^r \kappa = 0$. The terms in the Lie polynomial with $i_0$ odd are then

$$\frac{1}{2l+1}\frac{(-1)^{i_0+\sum_{k=1}^{l} i_{2k-1}}}{i_0! i_1! i_3! \cdots i_{2l-1}!}\left(\prod_{k=1}^{l}\left(\frac{1}{(2k-1)!}\right)^{i_{2k-1}}\right)\mathrm{ad}_Y^{\sum_{k=1}^{l} i_{2k-1}} Z \tag{C.3.32}$$

  At most only one commutator with $Y$ will be non-zero because $\mathrm{ad}_Y^0 Z = Z$ and $\mathrm{ad}_Y^1 Z = \kappa$ while $\mathrm{ad}_Y^r Z = 0$ for $r \geq 2$, so we have $\sum_{k=1}^{l} i_{2k-1} = \{0, 1\}$. If the sum is 0, then by (C.3.12) we have $i_0 = 2l$ but this contradicts the assumption that $i_0$ is odd so this is not a valid tuple. If the sum is 1 then one other term $i_{2k-1}$ will be equal to 1, and in this case we have $i_0 + (2k-1) = 2l$ which is possible since both $i_0$ and $2k-1$ are odd. In this case the only non-zero terms for odd $i_0$ are those which are proportional to $\kappa$ since we must have $i_{2k-1} = 1$. We must also recall that by (C.3.14) that $i_{2k-1} = 0$ if $(2k-1) > l$, so that the non-zero term in this case is

$$\frac{\kappa}{2l+1}\sum_{k=1}^{\lfloor \frac{l}{2} \rfloor}\frac{1}{(2l-2k+1)!(2k-1)!} \tag{C.3.33}$$

- If $i_0$ is even then $\mathrm{ad}_X^{i_0} Y = Y$. In this case the only non-vanishing terms are those where $i_{2k-1} = 0, \forall\, 2k-1 < 2l-1$ because the only terms which may appear in this Lie polynomial are proportional to $Y$ or $\kappa$ since we know that $\mathrm{ad}_Y^r Y = 0$ and $\mathrm{ad}_Y^r \kappa = 0$. The terms in the Lie polynomial with $i_0$ even are then

$$\frac{1}{2l+1}\frac{(-1)^{i_0}}{i_0! i_2! i_4! \cdots i_{2l}!}\left(\prod_{k=1}^{l}\left(\frac{1}{(2k)!}\right)^{i_{2k}}\right)\mathrm{ad}_Z^{\sum_{k=1}^{l} i_{2k}} Y \tag{C.3.34}$$

  At most only one commutator with $Z$ will be non-zero because $\mathrm{ad}_Z^0 Y = Y$ and $\mathrm{ad}_Z^1 Y = -\kappa$ while $\mathrm{ad}_Z^r Y = 0$ for $r \geq 2$, so we have $\sum_{k=1}^{l} i_{2k} = \{0, 1\}$. If the sum is 0, then by (C.3.12) we have $i_0 = 2l$ which is possible since $i_0$ is even making this a valid tuple. If the sum is 1 then one other term $i_{2k}$ will be equal to 1, and in this case we have $i_0 + 2k = 2l$ which is possible since both $i_0$ and $2k$ are even. There will therefore be one term proportional to $Y$ where $i_0 = 2l!$ and a number proportional to $\kappa$ where $i_0 = 2(l-k)$ and where according to (C.3.14) that $i_{2k} = 0$ if $2k > l$. The non-zero terms in this case are

$$\frac{1}{(2l+1)!}Y - \frac{\kappa}{2l+1}\sum_{k=1}^{\lceil \frac{l}{2} \rceil - 1}\frac{1}{(2l-2k)!(2k)!} \tag{C.3.35}$$

We can now combine the non-vanishing terms from above to retrieve $C_{2l+1}$

$$C_{2l+1} = \frac{1}{(2l+1)!}Y - \frac{\kappa}{2l+1}\sum_{k=1}^{\lceil \frac{l}{2} \rceil - 1}\frac{1}{(2l-2k)!(2k)!} + \frac{\kappa}{2l+1}\sum_{k=1}^{\lfloor \frac{l}{2} \rfloor}\frac{1}{(2l-2k+1)!(2k-1)!} \tag{C.3.36}$$

$$= \frac{1}{(2l+1)!}Y - \frac{\kappa}{2l+1}\sum_{k=1}^{l}\frac{(-1)^k}{(2l-k)!k!} \tag{C.3.37}$$

$$= \frac{1}{(2l+1)!}Y + \frac{\kappa}{2l+1}\left(\frac{(-1)^l(2l)! - 2(l!)^2}{2(l!)^2(2l)!}\right) \equiv \frac{1}{(2l+1)!}Y + \mu_{2l+1}\kappa \tag{C.3.38}$$

and so we have proved (C.3.10) for the odd order Lie polynomials. The formula for $\mu_{2l+1}$ is not dependent on previous terms so we cannot say that it is correct using induction. We now have the following formula for the operator exponential

$$e^{\lambda(X+Y)} = \exp\left(\kappa \sum_{k=1}^{\infty} \lambda^{2k+1} \mu_{2k+1}\right) e^{\lambda X} \prod_{m=0}^{\infty} \exp\left(\frac{\lambda^{2m+1}}{(2m+1)!} Y\right) \exp\left(-\frac{\lambda^{2m+2}}{(2m+2)!} Z\right) \tag{C.3.39}$$

which may be written using creation and annihilation operators again using the established definitions

$$e^{\lambda \hat{N} + q\hat{a} + r\hat{a}^\dagger} = e^{rq\Delta} e^{\lambda \hat{N}} \prod_{m=0}^{\infty} \exp\left(\frac{\lambda^{2m}}{(2m+1)!}(q\hat{a} + r\hat{a}^\dagger)\right) \exp\left(\frac{\lambda^{2m+1}}{(2m+2)!}(q\hat{a} - r\hat{a}^\dagger)\right) \tag{C.3.40}$$

where $\Delta$ is a proportionality constant

$$\Delta := 2 \sum_{k=1}^{\infty} \lambda^{2k-1} \mu_{2k+1} \tag{C.3.41}$$

We must now split the operators containing the creation and annihilation operator, moving all the creation operators to the right and all the annihilation operators to the left. To do this we use the Zassenhaus formula (C.3.5) again, though because of (C.3.8) only the second order Lie polynomial is non-zero

$$e^{q\hat{a} \pm r\hat{a}^\dagger} = e^{\pm r\hat{a}^\dagger} e^{q\hat{a}} e^{\pm rq/2} \tag{C.3.42}$$

We must also make use the following lemma of t he Baker-Campbell-Hausdorff formula

$$e^X e^Y = \exp\left(\sum_{k=0}^{\infty} \frac{1}{k!} \mathrm{ad}_X^k Y\right) e^X \tag{C.3.43}$$

to slide the operator exponentials past each other. For the operators under consideration here these are

$$e^{q\hat{a}} e^{r\hat{a}^\dagger} = e^{r\hat{a}^\dagger} e^{q\hat{a}} e^{qr} \qquad e^{\lambda \hat{N}} e^{q\hat{a}} = e^{qe^{-\lambda}\hat{a}} e^{\lambda \hat{N}} \qquad e^{\lambda \hat{N}} e^{r\hat{a}^\dagger} = e^{re^{\lambda}\hat{a}^\dagger} e^{\lambda \hat{N}} \tag{C.3.44}$$

Using these two formulas we can rewrite (C.3.40) as

$$\begin{aligned} &e^{\lambda \hat{N} + q\hat{a} + r\hat{a}^\dagger} \\ &= e^{rq\Delta} e^{rq\Omega} e^{\lambda \hat{N}} \prod_{m=0}^{\infty} \exp\left(\left(\frac{\lambda^{2m}}{(2m+1)!} - \frac{\lambda^{2m+1}}{(2m+2)!}\right) r\hat{a}^\dagger\right) \exp\left(\left(\frac{\lambda^{2m}}{(2m+1)!} + \frac{\lambda^{2m+1}}{(2m+2)!}\right) q\hat{a}\right) \end{aligned} \tag{C.3.45}$$

where we define the sum

$$\Omega := \frac{1}{2} \sum_{m=0}^{\infty} \left(\left(\frac{\lambda^{2m}}{(2m+1)!}\right)^2 - \left(\frac{\lambda^{2m+1}}{(2m+2)!}\right)^2 - 2\left(\frac{\lambda^{2m}}{(2m+1)!}\frac{\lambda^{2m+1}}{(2m+2)!}\right)\right) \tag{C.3.46}$$

to to compactify the result. We can now reorder all of the creation and annihilation operator exponentials; the infinite product in this case becomes

$$\prod_{m=0}^{\infty} \exp\left(\left(\frac{\lambda^{2m}}{(2m+1)!} - \frac{\lambda^{2m+1}}{(2m+2)!}\right) r\hat{a}^\dagger\right) \exp\left(\left(\frac{\lambda^{2m}}{(2m+1)!} + \frac{\lambda^{2m+1}}{(2m+2)!}\right) q\hat{a}\right) \tag{C.3.47}$$

$$= e^{rq\Xi} \left(\prod_{k=0}^{\infty} \exp\left((-1)^k \frac{\lambda^k}{(k+1)!} r\hat{a}^\dagger\right)\right) \left(\prod_{l=0}^{\infty} \exp\left(\frac{\lambda^l}{(l+1)!} q\hat{a}\right)\right) \tag{C.3.48}$$

$$= e^{rq\Xi} \exp\left(\frac{1-e^\lambda}{\lambda} r\hat{a}^\dagger\right) \exp\left(\frac{e^\lambda - 1}{\lambda} q\hat{a}\right) \tag{C.3.49}$$

where the constant $\Xi$ is double sum

$$\Xi := \sum_{k=0}^{\infty} \left(\frac{\lambda^{2k}}{(2k+1)!} + \frac{\lambda^{2k+1}}{(2k+2)!}\right) \sum_{m=k+1}^{\infty} \left(\frac{\lambda^{2m}}{(2m+1)!} - \frac{\lambda^{2m+1}}{(2m+2)!}\right) \tag{C.3.50}$$

$$\equiv \sum_{k=0}^{\infty} \left(\frac{\lambda^{2k}}{(2k+1)!} - \frac{\lambda^{2k+1}}{(2k+2)!}\right) \sum_{m=0}^{k-1} \left(\frac{\lambda^{2m}}{(2m+1)!} + \frac{\lambda^{2m+1}}{(2m+2)!}\right) \tag{C.3.51}$$

which is obtained by combining the constant terms which come from repeated use of the formula (C.3.44). We can now write

$$e^{\lambda\hat{N} + q\hat{a} + r\hat{a}^\dagger} = e^{rq(\Delta+\Omega+\Xi)} e^{\lambda\hat{N}} e^{\frac{1-e^\lambda}{\lambda} r\hat{a}^\dagger} e^{\frac{e^\lambda - 1}{\lambda} q\hat{a}} \tag{C.3.52}$$

The last step is to sum the constants we have collected so far

$$f(\lambda) := \Delta + \Omega + \Xi \tag{C.3.53}$$

though this is difficult to simplify by hand or with a computer algebra system. We instead approach this final step in a different manner by using the following result from Jang and Voth [21]

$$\rho_c(q_c, p_c) = \int_{-\infty}^{\infty} \int_{-\infty}^{\infty} \hbar \frac{d\xi d\eta}{2\pi} e^{-i\xi q_c} e^{-i\eta p_c} \mathrm{Tr}\left[e^{-\beta\hbar\omega(\hat{N}+1/2) + i\xi\hat{q} + i\eta\hat{p}}\right] \tag{C.3.54}$$

$$= \frac{\beta\hbar\omega}{2\sinh(\beta\hbar\omega/2)} e^{-\beta\hbar\omega\left(\frac{m\omega}{2\hbar} q_c^2 + \frac{1}{2m\omega\hbar} p_c^2\right)} \tag{C.3.55}$$

to find the value of the polynomial function $f(\lambda)$. Making the appropriate replacements, $\lambda = -\beta\hbar\omega$, $r = i\nu$, $q = i\nu^*$, we can evaluate the trace of (C.3.2)

$$\mathrm{Tr}\left[e^{-\beta\hbar\omega(\hat{N}+1/2) + i\nu^*\hat{a} + i\nu\hat{a}^\dagger}\right] = e^{-\beta\hbar\omega/2} e^{-|\nu|^2 f(\beta\hbar\omega)} \mathrm{Tr}\left[e^{-\beta\hbar\omega\hat{N}} e^{i\nu\frac{e^{\beta\hbar\omega}-1}{\beta\hbar\omega} a^\dagger} e^{i\nu^*\frac{1-e^{-\beta\hbar\omega}}{\beta\hbar\omega} a}\right] \tag{C.3.56}$$

Focusing purely on the operator portion we have

$$\mathrm{Tr}\left[e^{-\beta\hbar\omega\hat{N}}e^{i\nu\frac{e^{\beta\hbar\omega}-1}{\beta\hbar\omega}a^\dagger}e^{i\nu^*\frac{1-e^{-\beta\hbar\omega}}{\beta\hbar\omega}a}\right]=\sum_{n=0}^{\infty}\langle n|e^{-\beta\hbar\omega N}e^{i\nu\frac{e^{\beta\hbar\omega}-1}{\beta\hbar\omega}a^\dagger}e^{i\nu^*\frac{1-e^{-\beta\hbar\omega}}{\beta\hbar\omega}a}|n\rangle \tag{C.3.57}$$

$$=\sum_{n=0}^{\infty}e^{-\beta\hbar\omega n}\left(e^{-i\nu^*\frac{e^{\beta\hbar\omega}-1}{\beta\hbar\omega}a}|n\rangle\right)^\dagger\sum_{k=0}^{n}\frac{1}{k!}\left(i\nu^*\frac{1-e^{-\beta\hbar\omega}}{\beta\hbar\omega}\right)^k\sqrt{\frac{n!}{(n-k)!}}|n-k\rangle \tag{C.3.58}$$

$$=\sum_{n=0}^{\infty}e^{-\beta\hbar\omega n}\sum_{l=0}^{n}\sum_{k=0}^{n}\frac{1}{l!k!}\left(i\nu\frac{e^{\beta\hbar\omega}-1}{\beta\hbar\omega}\right)^l\left(i\nu^*\frac{1-e^{-\beta\hbar\omega}}{\beta\hbar\omega}\right)^k\sqrt{\frac{n!n!}{(n-l)!(n-k)!}}\delta_{n-l,n-k} \tag{C.3.59}$$

$$=\sum_{n=0}^{\infty}e^{-\beta\hbar\omega n}\sum_{k=0}^{n}\frac{n!}{(k!)^2(n-k)!}\left(-|\nu|^2\frac{e^{\beta\hbar\omega}-1}{\beta\hbar\omega}\cdot\frac{1-e^{-\beta\hbar\omega}}{\beta\hbar\omega}\right)^k \tag{C.3.60}$$

$$=\sum_{n=0}^{\infty}e^{-\beta\hbar\omega n}\sum_{k=0}^{n}\binom{n}{k}\frac{(-1)^k}{k!}\left(2|\nu|^2\frac{\cosh(\beta\hbar\omega)-1}{(\beta\hbar\omega)^2}\right)^k \tag{C.3.61}$$

$$=\sum_{n=0}^{\infty}e^{-\beta\hbar\omega n}L_n\left(2|\nu|^2\frac{\cosh(\beta\hbar\omega)-1}{(\beta\hbar\omega)^2}\right) \tag{C.3.62}$$

using the definition of the Laguerre polynomials. We can use the generating function for the Laguerre polynomials,

$$\sum_{n=0}^{\infty}t^nL_n(x)=\frac{1}{1-t}e^{-tx/(1-t)} \tag{C.3.63}$$

to write (C.3.62) as

$$e^{-\beta\hbar\omega/2}e^{-|\nu|^2f(\beta\hbar\omega)}\sum_{n=0}^{\infty}e^{-\beta\hbar\omega n}L_n\left(2|\nu|^2\frac{\cosh(\beta\hbar\omega)-1}{(\beta\hbar\omega)^2}\right) \tag{C.3.64}$$

$$=e^{-\beta\hbar\omega/2}e^{-|\nu|^2f(\beta\hbar\omega)}\frac{1}{1-e^{-\beta\hbar\omega}}\exp\left(-2|\nu|^2\frac{e^{-\beta\hbar\omega}}{1-e^{\beta\hbar\omega}}\frac{\cosh(\beta\hbar\omega)-1}{(\beta\hbar\omega)^2}\right) \tag{C.3.65}$$

$$=\frac{1}{2\sinh(\beta\hbar\omega/2)}\exp\left(-|\nu|^2\left(\frac{1-e^{-\beta\hbar\omega}}{(\beta\hbar\omega)^2}+f(\beta\hbar\omega)\right)\right) \tag{C.3.66}$$

Replacing $\nu$ with (C.3.3) we can solve the Fourier integrals to retrieve the centroid distribution

$$\frac{\hbar}{2\sinh(\beta\hbar\omega/2)}\int_{-\infty}^{\infty}\int_{-\infty}^{\infty}\frac{d\xi\,d\eta}{2\pi}e^{i\xi q_c}e^{i\eta p_c}\exp\left(-\left(\frac{\hbar}{2m\omega}\xi^2+\frac{m\omega\hbar}{2}\eta^2\right)\left(\frac{1-e^{-\beta\hbar\omega}}{(\beta\hbar\omega)^2}+f(\beta\hbar\omega)\right)\right) \tag{C.3.67}$$

$$=\frac{\hbar}{2\sinh(\beta\hbar\omega/2)}\left(\hbar^2\left(\frac{1-e^{-\beta\hbar\omega}}{(\beta\hbar\omega)^2}+f(\beta\hbar\omega)\right)^2\right)^{-1/2}\exp\left(-\frac{\left(\frac{2m\omega}{\hbar}q_c^2+\frac{2}{m\omega\hbar}p_c^2\right)}{4\left(\frac{1-e^{-\beta\hbar\omega}}{(\beta\hbar\omega)^2}+f(\beta\hbar\omega)\right)}\right) \tag{C.3.68}$$

$$=\frac{1}{2\sinh(\beta\hbar\omega/2)}\left(\frac{1-e^{-\beta\hbar\omega}}{(\beta\hbar\omega)^2}+f(\beta\hbar\omega)\right)^{-1}\exp\left(\frac{-1}{\frac{1-e^{-\beta\hbar\omega}}{(\beta\hbar\omega)^2}+f(\beta\hbar\omega)}\left(\frac{m\omega}{2\hbar}q_c^2+\frac{1}{2m\omega\hbar}p_c^2\right)\right) \tag{C.3.69}$$

Since (C.3.55) and (C.3.69) must be identical, we merely have to solve

$$\beta\hbar\omega = \left(\frac{1-e^{-\beta\hbar\omega}}{(\beta\hbar\omega)^2} + f(\beta\hbar\omega)\right)^{-1} \tag{C.3.70}$$

$$f(\beta\hbar\omega) = \frac{-1+e^{-\beta\hbar\omega}}{(\beta\hbar\omega)^2} + \frac{1}{\beta\hbar\omega} \tag{C.3.71}$$

$$f(\beta\hbar\omega) = \frac{e^{-\beta\hbar\omega}+\beta\hbar\omega-1}{(\beta\hbar\omega)^2} \tag{C.3.72}$$

We can now return to (C.3.2) expression and can finally write the final result

$$e^{-\beta\hbar\omega(N+\frac{1}{2})-i\nu^* a - i\nu a^\dagger} = e^{-|\nu|^2\frac{e^{-\beta\hbar\omega}+\beta\hbar\omega-1}{(\beta\hbar\omega)^2}} e^{-\beta\hbar\omega(N+\frac{1}{2})} e^{i\nu\frac{e^{\beta\hbar\omega}-1}{\beta\hbar\omega}a^\dagger} e^{i\nu^*\frac{1-e^{-\beta\hbar\omega}}{\beta\hbar\omega}a} \tag{C.3.73}$$

which may be generalized to

$$e^{\lambda\hat{N}+q\hat{a}+r\hat{a}^\dagger} = e^{qr\frac{1+\lambda-e^\lambda}{\lambda^2}} e^{\lambda\hat{N}} e^{\frac{1-e^{-\lambda}}{\lambda}r\hat{a}^\dagger} e^{\frac{e^\lambda-1}{\lambda}q\hat{a}} \tag{C.3.74}$$

and so we can state that (C.3.4) is absolutely true.

## C.4 Double Kubo transformed correlation function

The following derivation only holds for an operator which is linear combination of $\hat{q}$ and $\hat{p}$, i.e. $\hat{B} = A_0\hat{I} + B_1\hat{q} + B_2\hat{p}$, which by definition will have the centroid symbol $B_c = B_0 + B_1 q_c + B_2 p_c$. Since we are mostly interested in position or velocity autocorrelation functions, this restriction is not limiting. The correlation function of the centroid variables is then

$$\langle B_c A_c^{(\psi)}(t;q_c,p_c)\rangle = \frac{1}{Z_\psi}\int_{-\infty}^{\infty}\frac{dq_c\,dp_c}{2\pi\hbar}\rho_c^{(\psi)}(q_c,p_c)\,B_c\,A_c^{(\psi)}(t;q_c,p_c) \tag{C.4.1}$$

$$= \frac{1}{Z_\psi}\int_{-\infty}^{\infty}\frac{dq_c\,dp_c}{2\pi\hbar}\,B_c\int_{-\infty}^{\infty}\hbar\frac{d\xi\,d\eta}{2\pi}e^{-i\xi q_c}e^{-i\eta p_c} \times \mathrm{Tr}\left[\int_0^1 du\, e^{-(1-u)\beta\hat{H}'}\hat{\mathcal{P}}_\psi e^{-u\beta\hat{H}'}e^{it\hat{H}/\hbar}\hat{A}e^{-it\hat{H}/\hbar}\right] \tag{C.4.2}$$

where $\hat{H}'$ is defned by (C.1.2). For the $B_0$ term, the integrals over $q_c$ and $p_c$ can be immediately performed to yield delta functions $\sqrt{2\pi}\delta(\xi)$ and $\sqrt{2\pi}\delta(\eta)$, respectively. Performing the integrals over $\xi$ and $\eta$ reduces the effective centroid Hamiltonian to the system Hamiltonian, $\hat{H}' \to \hat{H}$. We therefore have

$$\frac{1}{Z_\psi}\int_{-\infty}^{\infty}\frac{dq_c\,dp_c}{2\pi}\,B_0\int_{-\infty}^{\infty}\hbar\frac{d\xi\,d\eta}{2\pi}e^{-i\xi q_c}e^{-i\eta p_c}\,\mathrm{Tr}\left[\int_0^1 du\, e^{-(1-u)\beta\hat{H}'}\hat{\mathcal{P}}_\psi e^{-u\beta\hat{H}'}e^{it\hat{H}/\hbar}\hat{A}e^{-it\hat{H}/\hbar}\right] \tag{C.4.3}$$

$$= \frac{1}{Z_\psi}B_0\mathrm{Tr}\left[\int_0^1 du\, e^{-(1-u)\beta\hat{H}}\hat{\mathcal{P}}_\psi e^{-u\beta\hat{H}}e^{it\hat{H}/\hbar}\hat{A}e^{-it\hat{H}/\hbar}\right] \tag{C.4.4}$$

$$= \frac{1}{Z_\psi}B_0\mathrm{Tr}\left[e^{-\beta\hat{H}}\int_0^1 du\,\hat{\mathcal{P}}_\psi(-iu\beta\hbar)\hat{A}(t)\right] \tag{C.4.5}$$

This is merely the correlation of the identity operator with $\hat{A}(t)$ where there projection operator has been Kubo transformed. Turning to the $q_c$ term, we can immediately perform the integral over $p_c$, which will be replaced by the delta function $\sqrt{2\pi}\delta(\eta)$. The integral over $\eta$ is then easily performed, the result being that the effective centroid Hamiltonian is simplified to only include the $\xi$ term. We are then left to evaluate

$$\langle q_c A_c^{(\psi)}(t;q_c,p_c)\rangle = \frac{1}{Z_\psi}\int_{-\infty}^{\infty}\frac{dq_c\,d\xi}{2\pi}\,e^{-i\xi q_c}q_c\,\mathrm{Tr}\bigg[\int_0^1 du\,e^{-(1-u)(\beta\hat{H}-i\xi\hat{q})}\hat{\mathcal{P}}_\psi e^{-u(\beta\hat{H}-i\xi\hat{q})}\hat{A}(t)\bigg] \tag{C.4.6}$$

We can now use the Fourier transform property

$$\int_{-\infty}^{\infty}\sqrt{2\pi}\,x^n\,e^{-i\omega x}dx = i^n\sqrt{2\pi}\delta^{(n)}(x) \tag{C.4.7}$$

and the following property of the distributional derivative of the delta function

$$\int_{-\infty}^{\infty}\delta'(x)f(x)dx = -\int_{-\infty}^{\infty}\delta(x)f'(x)dx \tag{C.4.8}$$

to evaluate the integrals over $q_c$ and $\xi$. Our correlation function may now be written

$$\langle q_c A_c^{(\psi)}(t;q_c,p_c)\rangle = -\frac{i}{Z_\psi}\int_{-\infty}^{\infty}d\xi\,\delta(\xi)\,\frac{\partial}{\partial\xi}\mathrm{Tr}\bigg[\int_0^1 du\,e^{-(1-u)(\beta\hat{H}-i\xi\hat{q})}\hat{\mathcal{P}}_\psi e^{-u(\beta\hat{H}-i\xi\hat{q})}\hat{A}(t)\bigg] \tag{C.4.9}$$

We must now make use of an operator derivative identity from Wilcox [38] to evaluate this derivative

$$\frac{\partial}{\partial\lambda}e^{-a\hat{L}} = -\int_0^a e^{-(a-u)\hat{L}}\,\frac{\partial\hat{L}}{\partial\lambda}\,e^{-u\hat{L}}du \tag{C.4.10}$$

and in conjuncture with the regular properties of derivatives, evaluate the derivative over $\xi$. Hence

$$\frac{\partial}{\partial\xi}e^{-(1-u)(\beta\hat{H}-i\xi\hat{q})} = -\int_0^{1-u}e^{-(1-u-v)(\beta\hat{H}-i\xi\hat{q})}\,\frac{\partial}{\partial\xi}(\beta\hat{H}-i\xi\hat{q})\,e^{-v(\beta\hat{H}-i\xi\hat{q})}dv \tag{C.4.11}$$

$$= i\int_0^{1-u}e^{-(1-u-v)(\beta\hat{H}+i\xi\hat{q})}\,\hat{q}\,e^{-v(\beta\hat{H}+i\xi\hat{q})}dv \tag{C.4.12}$$

and so

$$\frac{\partial}{\partial\xi}e^{-u(\beta\hat{H}-i\xi\hat{q})} = i\int_0^u e^{-(u-v)(\beta\hat{H}-i\xi\hat{q})}\,\hat{q}\,e^{-v(\beta\hat{H}-i\xi\hat{q})}dv \tag{C.4.13}$$

The integral over $\xi$ is easily performed; the resulting correlation function is then

$$\begin{aligned}\langle\hat{q}\hat{A}(t)\rangle_{(DK)}^{(\psi)} = \frac{1}{Z_\psi}\mathrm{Tr}\bigg[\int_0^1 du\int_0^{1-u}dv\,e^{-(1-u-v)\beta\hat{H}}\,\hat{q}\,e^{-v\beta\hat{H}}\hat{\mathcal{P}}_\psi e^{-u\beta\hat{H}}e^{it\hat{H}/\hbar}\hat{A}e^{-it\hat{H}/\hbar}\bigg]\\ + \frac{1}{Z_\psi}\mathrm{Tr}\bigg[\int_0^1 du\,e^{-(1-u)\beta\hat{H}}\hat{\mathcal{P}}_\psi\int_0^u dv\,e^{-(u-v)\beta\hat{H}}\,\hat{q}\,e^{-v\beta\hat{H}}e^{it\hat{H}/\hbar}\hat{A}e^{-it\hat{H}/\hbar}\bigg]\end{aligned} \tag{C.4.14}$$

The inclusion of the Kubo transform in the QDO means that the centroid correlation function is equal to the double Kubo (DK) transformed state projected quantum correlation function, i.e.

$$\langle q_c A_c^{(\psi)}(t;q_c,p_c)\rangle \equiv \langle\hat{q}\hat{A}(t)\rangle_{(DK)}^{(\psi)} \tag{C.4.15}$$

The expression for $\langle \hat{q}\,\hat{A}(t)\rangle^{(\psi)}_{(DK)}$ may be condensed using the standard Heisenberg notation for time evolution

$$\langle \hat{q}\hat{A}(t)\rangle^{(\psi)}_{(DK)} = \frac{1}{Z_\psi}\mathrm{Tr}\left[e^{-\beta\hat{H}}\int_0^1 du\left(\int_0^{1-u} dv\,\hat{q}(-iv\beta\hbar)\hat{\mathcal{P}}_\psi\hat{A}(t-iu\beta\hbar)\right.\right.$$
$$\left.\left.+\hat{\mathcal{P}}_\psi(-iu\beta\hbar)\int_0^u dv\,\hat{q}(-iv\beta\hbar)\hat{A}(t)\right)\right] \tag{C.4.16}$$

Redefining $u+v\to v$ in the first integral and changing the limits of integration to $(u,1)$ we arrive at the more familiar form

$$\langle \hat{q}\hat{A}(t)\rangle^{(\psi)}_{(DK)} = \frac{1}{Z_\psi}\mathrm{Tr}\left[e^{-\beta\hat{H}}\int_0^1 du\left(\int_u^1 dv\,\hat{q}(-iv\beta\hbar)\hat{\mathcal{P}}_\psi(-iu\beta\hbar)\hat{A}(t)\right.\right.$$
$$\left.\left.+\int_0^u dv\,\hat{\mathcal{P}}_\psi(-iu\beta\hbar)\hat{q}(-iv\beta\hbar)\hat{A}(t)\right)\right] \tag{C.4.17}$$

The steps for the correlation function involving $p_c$ follow in much the same manner and yield the similar relation

$$\langle p_c A^{(\psi)}_c(t;q_c,p_c)\rangle \equiv \langle \hat{p}\hat{A}(t)\rangle^{(\psi)}_{(DK)} \tag{C.4.18}$$

Returning briefly to the $B_0$ term, we note that

$$\frac{1}{Z_\psi}B_0\mathrm{Tr}\left[e^{-\beta\hat{H}}\int_0^1 du\,\hat{\mathcal{P}}_\psi(-iu\beta\hbar)\hat{A}(t)\right] \tag{C.4.19}$$
$$=\frac{1}{Z_\psi}B_0\mathrm{Tr}\left[e^{-\beta\hat{H}}\int_0^1 du\int_0^1 dv\,\hat{\mathcal{P}}_\psi(-iu\beta\hbar)\hat{A}(t)\right] \tag{C.4.20}$$
$$=\frac{1}{Z_\psi}B_0\mathrm{Tr}\left[e^{-\beta\hat{H}}\int_0^1 du\left(\int_u^1 dv\,\hat{\mathcal{P}}_\psi(-iu\beta\hbar)+\int_0^u dv\,\hat{\mathcal{P}}_\psi(-iu\beta\hbar)\right)\hat{A}(t)\right] \tag{C.4.21}$$
$$=\frac{1}{Z_\psi}B_0\mathrm{Tr}\left[e^{-\beta\hat{H}}\int_0^1 du\left(\int_u^1 dv\,\hat{I}(-iv\beta\hbar)\,\hat{\mathcal{P}}_\psi(-iu\beta\hbar)+\int_0^u dv\,\hat{\mathcal{P}}_\psi(-iu\beta\hbar)\,\hat{I}(-iv\beta\hbar)\right)\hat{A}(t)\right] \tag{C.4.22}$$

which is allowed since $\hat{I}(-iv\beta\hbar)=\hat{I}$. Combining the three double Kubo transforms gives us the desired result (valid only for operators of the form $\hat{B}=B_0\hat{I}+B_1\hat{q}+B_2\hat{p}$)

$$\langle B_c A^{(\psi)}_c(t;q_c,p_c)\rangle = \langle \hat{B}\hat{A}(t)\rangle^{(\psi)}_{(DK)} \tag{C.4.23}$$

or equivalently

$$\frac{1}{Z_\psi}\int_{-\infty}^{\infty}\frac{dq_c\,dp_c}{2\pi\hbar}\rho^{(\psi)}_c(q_c,p_c)\,B_c\,A^{(\psi)}_c(t;q_c,p_c)$$
$$=\frac{1}{Z_\psi}\mathrm{Tr}\left[e^{-\beta\hat{H}}\int_0^1 du\left(\int_u^1 dv\,\hat{B}(-iv\beta\hbar)\,\hat{\mathcal{P}}_\psi(-iu\beta\hbar)+\int_0^u dv\,\hat{\mathcal{P}}_\psi(-iu\beta\hbar)\,\hat{B}(-iv\beta\hbar)\right)\hat{A}(t)\right] \tag{C.4.24}$$

For computational purposes, it is convenient to change this expression from being evaluated using numerical integration involving matrices to simple nested sums; it is easiest to work in the basis of the eigenstates of the Hamiltonian. Inserting resolutions of the identity in the form of sums

over the outer product of the eigenstates between the exponentials of the Hamiltonians and the operators yields the expression

$$\begin{aligned}
&\langle \hat{A}\hat{B}(t)\rangle^{(\psi)}_{(DK)} \\
&= \frac{1}{Z_\psi}\sum_{k,l,m}\Bigg(e^{-\beta E_k}\int_0^1 du\left(\int_u^1 dv\, e^{v\beta(E_k-E_l)}e^{u\beta(E_l-E_m)}e^{it(E_m-E_k)/\hbar}\,\langle\chi_k|\hat{B}|\chi_l\rangle\langle\chi_l|\hat{\mathcal{P}}_\psi|\chi_m\rangle\langle\chi_m|\hat{A}|\chi_k\rangle\right. \\
&\qquad\left.+\int_0^u dv\, e^{u\beta(E_k-E_l)}e^{v\beta(E_l-E_m)}e^{it(E_m-E_k)/\hbar}\,\langle\chi_k|\hat{\mathcal{P}}_\psi|\chi_l\rangle\langle\chi_l|\hat{B}|\chi_m\rangle\langle\chi_m|\hat{A}|\chi_k\rangle\right)\Bigg)
\end{aligned} \tag{C.4.25}$$

The integrals are then performed

$$e^{-\beta E_k}\int_0^1 du\int_u^1 dv\, e^{v\beta(E_k-E_l)}e^{u\beta(E_l-E_m)} = \frac{1}{\beta(E_k-E_l)}\left(\frac{e^{-\beta E_m}-e^{-\beta E_l}}{\beta(E_l-E_m)}+\frac{e^{-\beta E_k}-e^{-\beta E_m}}{\beta(E_k-E_m)}\right) \tag{C.4.26}$$

$$e^{-\beta E_k}\int_0^1 du\int_0^u dv\, e^{u\beta(E_k-E_l)}e^{v\beta(E_l-E_m)} = \frac{1}{\beta(E_l-E_m)}\left(\frac{e^{-\beta E_k}-e^{-\beta E_m}}{\beta(E_m-E_k)}+\frac{e^{-\beta E_k}-e^{-\beta E_m}}{\beta(E_k-E_m)}\right) \tag{C.4.27}$$

The double Kubo transformed correlation function is then

$$\begin{aligned}
&\langle \hat{B}\hat{A}(t)\rangle^{(\psi)}_{(DK)} \\
&= \frac{1}{Z_\psi}\sum_{k,l,m}\left(\frac{1}{\beta(E_k-E_l)}\left(\frac{e^{-\beta E_m}-e^{-\beta E_l}}{\beta(E_l-E_m)}+\frac{e^{-\beta E_k}-e^{-\beta E_m}}{\beta(E_k-E_m)}\right)\langle\chi_k|\hat{B}|\chi_l\rangle\langle\chi_l|\hat{\mathcal{P}}_\psi|\chi_m\rangle\langle\chi_m|\hat{A}(t)|\chi_k\rangle\right. \\
&\qquad\left.+\frac{1}{\beta(E_l-E_m)}\left(\frac{e^{-\beta E_k}-e^{-\beta E_m}}{\beta(E_m-E_k)}+\frac{e^{-\beta E_k}-e^{-\beta E_l}}{\beta(E_k-E_l)}\right)\langle\chi_k|\hat{\mathcal{P}}_\psi|\chi_l\rangle\langle\chi_l|\hat{B}|\chi_m\rangle\langle\chi_m|\hat{A}(t)|\chi_k\rangle\right)
\end{aligned} \tag{C.4.28}$$

Since the indices are arbitrary in the sums we can swap the indices $k \leftrightarrow m$ in the first term of the sum; the correlation function is now

$$\begin{aligned}
\langle \hat{B}\hat{A}(t)\rangle^{(\psi)}_{(DK)} = \frac{1}{Z_\psi}\sum_{k,l,m}\Bigg[&\frac{1}{\beta(E_l-E_m)}\left(\frac{e^{-\beta E_k}-e^{-\beta E_m}}{\beta(E_m-E_k)}+\frac{e^{-\beta E_k}-e^{-\beta E_l}}{\beta(E_k-E_l)}\right) \\
&\times\Big(\langle\chi_m|\hat{B}|\chi_l\rangle\,\langle\chi_l|\hat{\mathcal{P}}_\psi|\chi_k\rangle\,\langle\chi_k|\hat{A}(t)|\chi_m\rangle \\
&+\langle\chi_k|\hat{\mathcal{P}}_\psi|\chi_l\rangle\,\langle\chi_l|\hat{B}|\chi_m\rangle\,\langle\chi_m|\hat{A}(t)|\chi_k\rangle\Big)\Bigg]
\end{aligned} \tag{C.4.29}$$

Under the assumption that $\hat{\mathcal{P}}_\psi, \hat{B}$ and $\hat{A}(t)$ are Hermitian operators we can write

$$\langle\chi_m|\hat{B}|\chi_l\rangle\,\langle\chi_l|\hat{\mathcal{P}}_\psi|\chi_k\rangle\,\langle\chi_k|\hat{A}(t)|\chi_m\rangle = \langle\chi_k|\hat{\mathcal{P}}_\psi|\chi_l\rangle\,\langle\chi_k|\hat{B}|\chi_m\rangle\,\langle\chi_m|\hat{A}(t)|\chi_k\rangle \tag{C.4.30}$$

The more compact form is therefore

$$\begin{aligned}
\langle \hat{B}\hat{A}(t)\rangle^{(\psi)}_{(DK)} = \frac{2}{Z_\psi}\sum_{k,l,m}&\frac{1}{\beta(E_l-E_m)}\left(\frac{e^{-\beta E_k}-e^{-\beta E_m}}{\beta(E_m-E_k)}+\frac{e^{-\beta E_k}-e^{-\beta E_l}}{\beta(E_k-E_l)}\right) \\
&\times\langle\chi_k|\hat{\mathcal{P}}_\psi|\chi_l\rangle\,\langle\chi_l|\hat{B}|\chi_m\rangle\,\langle\chi_m|\hat{A}(t)|\chi_k\rangle
\end{aligned} \tag{C.4.31}$$

Using this result we can then compactly write the double Kubo transform as a single double integral

$$\langle \hat{B}\hat{A}(t)\rangle^{(\psi)}_{(DK)} = \frac{2}{Z_\psi}\mathrm{Tr}\left[e^{-\beta\hat{H}}\int_0^1 du\int_u^1 dv\,\hat{B}(-iv\beta\hbar)\,\hat{\mathcal{P}}_\psi(-iu\beta\hbar)\hat{A}(t)\right] \tag{C.4.32}$$

$$= \frac{2}{Z_\psi}\mathrm{Tr}\left[e^{-\beta\hat{H}}\int_0^1 du\int_0^u dv\,\hat{\mathcal{P}}_\psi(-iu\beta\hbar)\,\hat{B}(-iv\beta\hbar)\hat{A}(t)\right] \tag{C.4.33}$$

If we consider the case where the projection is the identity operator the double Kubo transform will reduce to a single Kubo transform, corresponding to the canonical ensemble

$$\langle \hat{B}\hat{A}(t)\rangle^{(\mathcal{I})}_{(DK)} = \mathrm{Tr}\left[e^{-\beta\hat{H}}\int_0^1 du\left(\int_u^1 dv\,\hat{B}(-iv\beta\hbar)\hat{\mathcal{I}}(-iu\beta\hbar)\hat{A}(t)+\int_0^u dv\,\hat{\mathcal{I}}(-iu\beta\hbar)\hat{B}(-iv\beta\hbar)\hat{A}(t)\right)\right] \tag{C.4.34}$$

$$= \mathrm{Tr}\left[e^{-\beta\hat{H}}\int_0^1 du\left(\int_u^1 dv\,\hat{B}(-iv\beta\hbar)\hat{A}(t)+\int_0^u dv\,\hat{B}(-iv\beta\hbar)\hat{A}(t)\right)\right] \tag{C.4.35}$$

$$= \mathrm{Tr}\left[e^{-\beta\hat{H}}\int_0^1 dv\,\hat{B}(-iv\beta\hbar)\hat{A}(t)\right] \tag{C.4.36}$$

$$= \langle \hat{B}\hat{A}(t)\rangle_{(K)} \tag{C.4.37}$$

If we have a set of eigenvectors which forms a basis for the Hilbert space, $\{|\psi_n\rangle\}$ with associated normalization constants $\{Z_{\psi_n}\}$ for their microcanonical ensembles, then the sum of all double Kubo transform correlation functions renormalized by $Z_{\psi_n}/Z$ therefore recovers the single Kubo transform correlation function for the canonical ensemble.

## C.5 Undoing the double Kubo transform

### C.5.1 Eigenstate projection

The double Kubo transformed correlation function between two arbitrary operators can be undone in the case that the projection is a sum of individual projection operators onto eigenstates of the Hamiltonian

$$\hat{\mathcal{P}} = \sum p_n\,|\chi_n\rangle\,\langle\chi_n| \equiv \sum p_n\hat{\mathcal{P}}_n \tag{C.5.1}$$

Here we just study the case of one eigenstate; the general case can be retrieved by taking a linear combination of the results. We recall the correlation function for the microcanonical ensemble in question is

$$\langle \hat{B}\hat{A}(t)\rangle^{(\psi)} := \frac{1}{Z_\psi}\mathrm{Tr}\left[\hat{\mathcal{P}}_\psi e^{-\beta\hat{H}}\hat{B}\hat{A}(t)\right] \tag{C.5.2}$$

$$= \frac{1}{Z_\psi}\sum_{k,l,m} e^{-\beta E_k}\,\langle\chi_k|\hat{\mathcal{P}}_\psi|\chi_l\rangle\,\langle\chi_l|\hat{B}|\chi_m\rangle\,\langle\chi_m|\hat{A}|\chi_k\rangle\,e^{it(E_m-E_k)/\hbar} \tag{C.5.3}$$

In the case of an eigenstate projection this may be further simplified

$$\langle \hat{B}\hat{A}(t)\rangle^{(n)} = \frac{1}{Z_n}\sum_{k,l,m} e^{-\beta E_k}\,\langle\chi_k|\chi_n\rangle\,\langle\chi_n|\chi_l\rangle\,\langle\chi_l|\hat{B}|\chi_m\rangle\,\langle\chi_m|\hat{A}|\chi_k\rangle\,e^{it(E_m-E_k)/\hbar} \tag{C.5.4}$$

$$= e^{\beta E_n}\sum_{k,l,m} e^{-\beta E_k}\delta_{k,n}\delta_{n,l}\,\langle\chi_l|\hat{B}|\chi_m\rangle\,\langle\chi_m|\hat{A}|\chi_k\rangle\,e^{it(E_m-E_k)/\hbar} \tag{C.5.5}$$

$$= \sum_m \langle\chi_n|\hat{B}|\chi_m\rangle\,\langle\chi_m|\hat{A}|\chi_n\rangle\,e^{it(E_m-E_n)/\hbar} \tag{C.5.6}$$

The Fourier transform of the eigenstate projected correlation function is therefore

$$\mathcal{F}\{\langle \hat{B}\hat{A}(t)\rangle^{(n)}\}(\omega) = \sum_m \langle\chi_n|\hat{B}|\chi_m\rangle\,\langle\chi_m|\hat{A}|\chi_n\rangle\,\delta\left(\omega - \frac{E_m-E_n}{\hbar}\right) \tag{C.5.7}$$

Now turning to the double Kubo transform correlation function, we use the sum version (C.4.31) already derived, and sub in our projection operator

$$\langle \hat{B}\hat{A}(t)\rangle^{(\psi)}_{(DK)}$$

$$= \frac{2}{Z_n}\sum_{k,l,m}\frac{1}{\beta(E_l-E_m)}\left(\frac{e^{-\beta E_k}-e^{-\beta E_m}}{\beta(E_m-E_k)} + \frac{e^{-\beta E_k}-e^{-\beta E_l}}{\beta(E_k-E_l)}\right)\delta_{k,n}\delta_{n,l}\,\langle\chi_l|\hat{B}|\chi_m\rangle\langle\chi_m|\hat{A}(t)|\chi_k\rangle \tag{C.5.8}$$

$$= 2\,e^{\beta E_n}\sum_m \frac{1}{\beta(E_n-E_m)}\left(\frac{e^{-\beta E_n}-e^{-\beta E_m}}{\beta(E_m-E_n)} - e^{-\beta E_n}\right)\langle\chi_n|\hat{B}|\chi_m\rangle\langle\chi_m|\hat{A}|\chi_n\rangle\,e^{it(E_m-E_n)/\hbar} \tag{C.5.9}$$

$$= 2\sum_m \frac{e^{-\beta(E_m-E_n)}-1+\beta(E_m-E_n)}{(\beta(E_m-E_n))^2}\,\langle\chi_n|\hat{B}|\chi_m\rangle\langle\chi_m|\hat{A}|\chi_n\rangle\,e^{it(E_m-E_n)/\hbar} \tag{C.5.10}$$

We know perform the Fourier transform on this object

$$\mathcal{F}\{\langle \hat{B}\hat{A}(t)\rangle^{(n)}_{(DK)}\}(\omega)$$

$$= 2\sum_m \frac{e^{-\beta(E_m-E_n)}+\beta(E_m-E_n)-1}{(\beta(E_m-E_n))^2}\,\langle\chi_n|\hat{B}|\chi_m\rangle\langle\chi_m|\hat{A}|\chi_n\rangle\,\delta\left(\omega-\frac{E_m-E_n}{\hbar}\right) \tag{C.5.11}$$

$$= 2\frac{e^{-\beta\hbar\omega}+\beta\hbar\omega-1}{(\beta\hbar\omega)^2}\sum_m \langle\chi_n|\hat{B}|\chi_m\rangle\langle\chi_m|\hat{A}|\chi_n\rangle\,\delta\left(\omega-\frac{E_m-E_n}{\hbar}\right) \tag{C.5.12}$$

We notice that the sum in the Fourier transform of both correlation functions are identical and so they differ by a common frequency factor

$$\mathcal{F}\{\langle \hat{B}\hat{A}(t)\rangle^{(n)}\}(\omega) = \frac{(\beta\hbar\omega)^2}{2(e^{-\beta\hbar\omega}+\beta\hbar\omega-1)}\mathcal{F}\{\langle \hat{B}\hat{A}(t)\rangle^{(n)}_{(DK)}\}(\omega) \tag{C.5.13}$$

Undoing the Fourier transform, a direct relation may be established between the microcanonical correlation function for an eigenstate and its double Kubo transformed version

$$\langle \hat{B}\hat{A}(t)\rangle^{(n)} = \int_{-\infty}^{\infty} d\omega e^{i\omega t}\frac{(\beta\hbar\omega)^2}{2(e^{-\beta\hbar\omega}+\beta\hbar\omega-1)}\int_{-\infty}^{\infty} dt' e^{-i\omega t}\langle \hat{B}\hat{A}(t)\rangle^{(n)}_{(DK)} \tag{C.5.14}$$

### C.5.2 General state projection

We now check to see under what conditions the double Kubo transform correlation function can be undone when the projection operator is an arbitrary pure state; from there the formalism can be extended to cover any mixed state. In the basis of the Hamiltonian's eigenstates the pure state projection operator can be written as

$$\hat{P}_\psi = \sum_{x,y} c_x^* c_y \left|\chi_x\right\rangle \left\langle\chi_y\right| = \sum_x \left|c_x\right|^2 \left|\chi_x\right\rangle \left\langle\chi_x\right| + \frac{1}{2}\sum_{x\neq y} c_x^* c_y \left|\chi_x\right\rangle \left\langle\chi_y\right| + c_y^* c_x \left|\chi_y\right\rangle \left\langle\chi_x\right| \tag{C.5.15}$$

which will have diagonal elements which can be connected to the normal projected correlation function as detailed in the previous section. We recall that the frequency factor connecting the Fourier transforms of the correlation functions was

$$\frac{(\beta\hbar\omega)^2}{2(e^{-\beta\hbar\omega} + \beta\hbar\omega - 1)} \tag{C.5.16}$$

and for consistency purposes it is desirable that the constant be the same for the off-diagonal elements as well. In deriving any additional restrictions on the possible operators, we will examine the off-diagonal elements of the projection operator when constructed in the Hamiltonian eigenstate basis

$$\hat{P}_\psi = \alpha_{x,y} \left|\chi_x\right\rangle \left\langle\chi_y\right| + \alpha_{x,y}^* \left|\chi_y\right\rangle \left\langle\chi_x\right| \tag{C.5.17}$$

where summation over all possible $x$ and $y$ is implied. Starting with equation (C.5.3) the regular correlation function is

$$\langle \hat{B}\hat{A}(t)\rangle^{(\psi)} = \frac{1}{Z_\psi}\sum_{k,l,m} e^{-\beta E_k}(\alpha\delta_{k,x}\delta_{y,l} + \alpha^*\delta_{k,y}\delta_{x,l}) \left\langle\chi_l|\hat{B}|\chi_m\right\rangle \left\langle\chi_m|\hat{A}|\chi_k\right\rangle e^{it(E_m - E_x)/\hbar} \tag{C.5.18}$$

$$= \frac{1}{Z_\psi}\sum_m \Big(\alpha e^{-\beta E_x} \left\langle\chi_y|\hat{B}|\chi_m\right\rangle \left\langle\chi_m|\hat{A}|\chi_x\right\rangle e^{it(E_m - E_x)/\hbar} + \alpha^* e^{-\beta E_y} \left\langle\chi_x|\hat{B}|\chi_m\right\rangle \left\langle\chi_m|\hat{A}|\chi_y\right\rangle e^{it(E_m - E_y)/\hbar}\Big) \tag{C.5.19}$$

and the corresponding double Kubo transformed correlation function can be obtained from equation (C.4.31)

$$\begin{aligned}
&\langle \hat{B}\hat{A}(t)\rangle_{(DK)}^{(\psi)} \\
&= \frac{2}{Z_\psi}\sum_m \left[\frac{\alpha}{\beta(E_y - E_m)}\left(\frac{e^{-\beta E_x} - e^{-\beta E_m}}{\beta(E_m - E_x)} + \frac{e^{-\beta E_x} - e^{-\beta E_y}}{\beta(E_x - E_y)}\right)\left\langle\chi_y|\hat{B}|\chi_m\right\rangle\left\langle\chi_m|\hat{A}|\chi_x\right\rangle e^{it(E_m - E_x)/\hbar}\right. \\
&\qquad \left. + \frac{\alpha^*}{\beta(E_x - E_m)}\left(\frac{e^{-\beta E_y} - e^{-\beta E_m}}{\beta(E_m - E_y)} + \frac{e^{-\beta E_y} - e^{-\beta E_x}}{\beta(E_y - E_x)}\right)\left\langle\chi_x|\hat{B}|\chi_m\right\rangle\left\langle\chi_m|\hat{A}|\chi_y\right\rangle e^{it(E_m - E_y)/\hbar}\right]
\end{aligned} \tag{C.5.20}$$

From here we will define

$$\mathcal{G}(\chi_x, \chi_y) = \left\langle\chi_x|\hat{B}|\chi_m\right\rangle \left\langle\chi_m|\hat{A}|\chi_y\right\rangle \tag{C.5.21}$$

in order to compactify the notation. The goal now is so show, given a completely general projection operator, if any restrictions must be placed on the operators $\hat{A}$ and $\hat{B}$ such that (C.5.14) is always

satisfied. We begin by using the Fourier transformed versions of the correlation functions

$$\begin{aligned}
&2\frac{e^{-\beta\hbar\omega}+\beta\hbar\omega-1}{(\beta\hbar\omega)^2}\mathcal{F}\{\langle\hat{B}\hat{A}(t)\rangle^{(\psi)}\}(\omega)\\
&=\frac{1}{Z_\psi}\sum_m\left[2\alpha\frac{e^{-\beta E_m}+(\beta(E_m-E_x)-1)e^{-\beta E_x}}{\beta^2(E_m-E_x)^2}\,\mathcal{G}(\chi_y,\chi_x)\,\delta\!\left(\omega-\frac{E_m-E_x}{\hbar}\right)\right.\\
&\qquad\left.+2\alpha^*\frac{e^{-\beta E_m}+(\beta(E_m-E_y)-1)e^{-\beta E_y}}{\beta^2(E_m-E_y)^2}\,\mathcal{G}(\chi_x,\chi_y)\,\delta\!\left(\omega-\frac{E_m-E_y}{\hbar}\right)\right]
\end{aligned}\tag{C.5.22}$$

The Fourier transform of the double Kubo transform correlation function is then

$$\begin{aligned}
&\mathcal{F}\{\langle\hat{B}\hat{A}(t)\rangle^{(\psi)}_{(DK)}\}(\omega)\\
&=\frac{2}{Z_\psi}\sum_m\left[\frac{\alpha}{\beta(E_y-E_m)}\left(\frac{e^{-\beta E_x}-e^{-\beta E_m}}{\beta(E_m-E_x)}+\frac{e^{-\beta E_x}-e^{-\beta E_y}}{\beta(E_x-E_y)}\right)\,\mathcal{G}(\chi_y,\chi_x)\,\delta\!\left(\omega-\frac{E_m-E_x}{\hbar}\right)\right.\\
&\qquad\left.+\frac{\alpha^*}{\beta(E_x-E_m)}\left(\frac{e^{-\beta E_y}-e^{-\beta E_m}}{\beta(E_m-E_y)}+\frac{e^{-\beta E_y}-e^{-\beta E_x}}{\beta(E_y-E_x)}\right)\,\mathcal{G}(\chi_x,\chi_y)\,\delta\!\left(\omega-\frac{E_m-E_y}{\hbar}\right)\right]
\end{aligned}\tag{C.5.23}$$

The peaks in this spectrum will only overlap in the case where the eigenenergy differences $E_m-E_x$ and $E_{m'}-E_y$ are equal. Since we are assuming that the states are not the same when $E_m=E_{m'}$ this can only arise when the eigenenergies are degenerate, but this contradicts the assumption that the projection operator is totally general. In the case that $E_m\neq E_{m'}$ then the energy differences must be the same but this is only guaranteed to happen for the QHO where the eigenenergies are evenly spaced. Our goal is then to check that the amplitude of each individual peak in frequency space is related to the amplitudes from the double Kubo transform correlation function via the same frequency factor, and the final result follows from taking a linear combination. We must therefore match terms in the Fourier transforms, choosing an arbitrary peak at $E_m-E_x$

$$\frac{1}{\beta(E_y-E_m)}\left(\frac{e^{-\beta E_x}-e^{-\beta E_m}}{\beta(E_m-E_x)}+\frac{e^{-\beta E_x}-e^{-\beta E_y}}{\beta(E_x-E_y)}\right)=\frac{e^{-\beta E_m}+(\beta(E_m-E_x)-1)e^{-\beta E_x}}{\beta^2(E_m-E_x)^2}\tag{C.5.24}$$

which can be rearranged to give

$$\begin{aligned}
0=&e^{-\beta E_x}((E_m-E_x)^2-(E_y-E_x)^2-\beta(E_m-E_x)(E_m-E_y)(E_y-E_x))\\
&+e^{-\beta E_m}(E_y-E_x)^2-e^{-\beta E_y}(E_m-E_x)^2
\end{aligned}\tag{C.5.25}$$

This equation is only solvable in the case where $E_m=E_x$, $E_m=E_y$, or $E_x=E_y$, and so in general we require that one of our observables is simply the identity, otherwise the frequency factors are dependent on the eigenenergies. We can conclude that it is not always possible to make a direct connection to the regular correlation function without knowledge of the eigenvalues of the system.

# References


[1] R. P. Feynman and A. R. Hibbs, *Quantum mechanics and path integrals: Emended edition*, Courier Dover Publications, 2012.

[2] J. Cao and G. A. Voth, *J. Chem. Phys.* **100**, 5093 (1994).

[3] J. Cao and G. A. Voth, *J. Chem. Phys.* **100**, 5106 (1994).

[4] J. Cao and G. A. Voth, *J. Chem. Phys.* **101**, 6157 (1994).

[5] J. Cao and G. A. Voth, *J. Chem. Phys.* **101**, 6168 (1994).

[6] S. Jang and G. A. Voth, *J. Chem. Phys.* **111**, 2371 (1999).

[7] T. D. Hone, P. J. Rossky, and G. A. Voth, *J. Chem. Phys.* **124**, 154103 (2006).

[8] S. Habershon, D. E. Manolopoulos, T. E. Markland, and T. F. Miller III, *Annu. Rev. Phys. Chem.* **64**, 387 (2013).

[9] A. Pérez, M. E. Tuckerman, and M. H. Müser, *J. Chem. Phys.* **130**, 184105 (2009).

[10] R. Zwanzig, *Annu. Rev. Phys. Chem.* **16**, 67 (1965).

[11] S. Jang, A. V. Sinitskiy, and G. A. Voth, *J. Chem. Phys.* **140**, 154103 (2014).

[12] Y. Yonetani and K. Kinugawa, *J. Chem. Phys.* **119**, 9651 (2003).

[13] N. Blinov and P.-N. Roy, *J. Chem. Phys.* **120**, 3759 (2004).

[14] T. D. Hone and G. A. Voth, *J. Chem. Phys.* **121**, 6412 (2004).

[15] F. Paesani, S. S. Xantheas, and G. A. Voth, *J. Phys. Chem. B* **113**, 13118 (2009).

[16] F. Paesani and G. A. Voth, *J. Chem. Phys.* **132**, 014105 (2010).

[17] I. R. Craig and D. E. Manolopoulos, *J. Chem. Phys.* **122**, 084106 (2005).

[18] I. R. Craig and D. E. Manolopoulos, *J. Chem. Phys.* **123**, 034102 (2005).

[19] N. Boekelheide, R. Salomón-Ferrer, and T. F. Miller, *Proc. Natl. Acad. Sci. U.S.A.* **108**, 16159 (2011).

[20] A. Arthurs, Path integrals in polar coordinates, in *Proc. R. Soc. A*, Volume 313, pp. 445–452, The Royal Society, 1969.

[21] S. Jang and G. A. Voth, *J. Chem. Phys.* **111**, 2357 (1999).

[22] R. Hernandez, J. Cao, and G. A. Voth, *J. Chem. Phys.* **103**, 5018 (1995).

[23] D. R. Reichman, P.-N. Roy, S. Jang, and G. A. Voth, *J. Chem. Phys.* **113**, 919 (2000).

[24] L. H. de la Peña and P. Kusalik, *Mol. Phys.* **102**, 927 (2004).

[25] W. Louisell, *Phys. Lett.* **7**, 60 (1963).

[26] P. Carruthers and M. M. Nieto, *Rev. Mod. Phys.* **40**, 411 (1968).

[27] K. Kowalski and J. Rembieliński, *Phys. Lett. A* **293**, 109 (2002).

[28] K. Kowalski, J. Rembielinski, and L. Papaloucas, *J. Phys. A* **29**, 4149 (1996).

[29] P. A. Dirac, *Lectures on quantum mechanics*, Courier Corporation, 2013.

[30] M. Henneaux and C. Teitelboim, *Quantization of gauge systems*, Princeton university press, 1992.

[31] A. Scardicchio, *Phys. Lett. A* **300**, 7 (2002).

[32] D. H. Bailey and P. N. Swarztrauber, *SIAM J. Sci. Comput.* **15**, 1105 (1994).

[33] S. Wolf and E. Curotto, *J. Chem. Phys.* **137**, 014109 (2012).

[34] S. Wolf and E. Curotto, *J. Chem. Phys.* **141**, 024116 (2014).

[35] K. Kowalski and J. Rembielinski, *J. Phys. A* **33**, 6035 (2000).

[36] N. Blinov and P.-N. Roy, *J. Chem. Phys.* **115**, 7822 (2001).

[37] Y. Huh and P.-N. Roy, *J. Chem. Phys.* **125**, 164103 (2006).

[38] R. Wilcox, *J. Math. Phys.* **8**, 962 (1967).

[39] C. Gardiner and P. Zoller, *Quantum noise: a handbook of Markovian and non-Markovian quantum stochastic methods with applications to quantum optics*, Volume 56, Springer Science & Business Media, 2004.

[40] A. Wünsche, *J. Comput. Appl. Math.* **133**, 665 (2001).

[41] F. Casas, A. Murua, and M. Nadinic, *Comput. Phys. Commun.* **183**, 2386 (2012).